WHP Cruise Summary Information

WOCE section designation	A01EW (leg 3), A02 (leg 2)
Expedition designation (EXPOCODE)	06MT30_2-3
Chief Scientist(s) and their affiliation	Peter Koltermann, BSH, Jens Meincke, IfMHH
Dates	1994.10.12 – 1994.11.12, 1994.11.15 – 1994.12.22
Ship	METEOR
Ports of call	Las Palmas, Hamburg to St. John's, Hamburg
Number of stations	53 (leg 2), 63 (leg 3)
Geographic boundaries of the stations	
Leg 2	49°14.10''N 48°45.00''W 10°39.60''W 41°59.60''N
Leg 3	60°33.90''N 54°29.50''W 14°15.40''W 51°35.10''N
Floats and drifters deployed	6 Floats (leg 3)
Moorings deployed or recovered	3 (leg 2); 1 (leg 3)
Contributing Authors (In order of appearance)	W. Balzer, O. Pfannkuche, H. Thiel, B.v. Bodungen, U. Brockmann, M. Andreae, K.P. Koltermann, J. Duinker, L. Mintrop, W. Roether, J. Meincke, R. Bayer, A. Sy, M. Rhein, B. Schneider, G.M. Raisbeck, R. Davis, B. Owens, I. Büns, A. Pfeifer, A. Deeken, H. Dierssen, S. Otto, H. Wellmann, G. Uher, O. Flöck, G. Schebeske, V. Ulshöfer, A.N Antia, W. Erasmi, R.S. Lampitt, T. Kumbier, G. Lehnert, K. Poremba, K. Jeskulke, T. Soltwedel, K.C. Soetje, V. Terechtchenkov, P. Wöckel, M. Stolley, H. Johannsen, F. Malien, A. Putzka, K. Bulsiewicz, C. Rüth, H. Rose, B. Kromer, M. Born, D. Kirkwood, I. Horn, R. Kramer, F. Oestereich, D.S. Kirkwood, E. Gier, F. Müller, P. Heil, A. Schaub, C. Atwood, A. Krötzinger, S. Schweinsberg, A.v. Hippel, C. Senet, H. Thomas, R. Prado-Fiedler

Meteor Cruise M30

JGOFS, OMEX and WOCE
in the North Atlantic 1994

Cruise No 30

7 September - 22 December 1994

Las Palmas - Hamburg - St John's - Hamburg

WHP Cruise and Data Information

Instructions: Click on items below to locate primary reference(s) or use navigation tools above.

TABLE OF CONTENTS

ABSTRACT
ZUSAMMENFASSUNG

1 RESEARCH OBJECTIVES
Leg M30/1: Las Palmas – Hamburg
OMEX Ocean Margin Exchange
Legs M30/2-3: Hamburg – St. John's – Hamburg
WOCE World Ocean Circulation Experiment
JGOFS Joint Global Ocean Flux Study

2 PARTICIPANTS
2.1 Leg M30/1
2.2 Leg M30/2
2.3 Leg M30/3
2.4 Participating Institutions

3 RESEARCH PROGRAMMES
3.1 OMEX Programmes:
3.1.1 Organic Matter Degradation, Denitrification and Trace Metal Diagenesis
3.1.2 Carbon Mineralization by the Benthic Community
3.1.3 Vertical Particle Flux at the Continental Margin
3.1.4 Phase Transfer of Organic Compounds During Shelf Edge Passage
3.1.5 Flux of Trace Gases at the Boundary Between Ocean and Atmosphere
3.2 WOCE Programmes:
3.2.1 Determination of the Meridional Transports of Heat, Salt and Freshwater at 48˚N in the North Atlantic along the WHP section A2
3.2.2 Nutrients Measurements for the Fine Resolution of Oceanic Water Masses on the Meteor Cruise M30/2 (section WHP-A2) in the North Atlantic
3.2.3 CFCs on the section WHP-A2
3.2.4 Mooring Recovery on sections WHP-A2 and WHP-A1
3.2.5 Tritium/Helium and ^{14}C-Sampling along WHP-sections A2 and A1
3.2.6 WOCE North Atlantic Overturning Rate Determination (WOCE-NORD, WHP section A1)
3.2.7 CFCs on the section WHP-A1
3.3 JGOFS – Programmes:
3.3.1 The Control Function of the Carbonate-System in the Oceanic CO_2 uptake, WHP-A2

3.3.2 The Ocean as a CO_2 Sink: Complimentary Studies of the Baltic Sea and the North Atlantic, WHP-A1
3.4 Individual Projects
3.4.1 ^{129}I from Nuclear Fuel Processing as an Oceanographic Tracer
3.4.2 Profiling ALACE Floats to Determine the Development of the Stratification in the Labrador Sea Over Two Years

4 NARRATIVE OF THE CRUISE
4.1 Leg M30/1 (Chief Scientist-O. Pfannkuche)
4.2 Leg M30/2 (Chief Scientist-K.P. Koltermann)
4.3 Leg M30/3 (Chief Scientist-J. Meincke)

5 OPERATIONAL DETAILS AND PRELIMINARY RESULTS
5.1 OMEX Programmes:
5.1.1 Biochemistry
- Phase Transfer of Organic Compounds During Shelf Edge Passage
- Organic Matter Degradation, Denitrification and Trace Metal Diagenesis
- Dissolved Organic Carbon
- Pore Water Chemistry
- Benthis Denitrification and Bioirrigation

5.1.2 Air Chemistry
- Exchange of Reduced Sulphur Compounds Between Ocean and Atmosphere

5.1.3 Sedimentology
- Particle Flux and *in situ* Marine Aggregate Studies at the Continental Margin
- Particle Flux
- Marine Snow Studies
- CTD – work

5.1.4 Benthic Biology
- Benthic Microbiology
- Carbon Mineralization by the Benthic Community

5.2 WOCE Programmes:
5.2.1 Physical and Chemical Oceanography on Leg M30/2
- Determination of the Meridional Transports of Heat, Salt and Freshwater at 48˚N in the North Atlantic Along the WHP section A2
- Nutrients Measurements for Fine Resolution of Oceanic Water Masses on the Meteor Cruise M30/2 (section WHP-A2) in the North Atlantic
- CFCs on the WHP section A2
- Tritium/Helium and ^{14}C-Sampling Along WHP-sections A2 and A1

5.2.2 Mooring Recovery on WHP-A2 and WHP-A1
5.2.3 Physical, Chemical and Tracer Oceanography on Leg M30/3
- Hydrographic Measurements on WHP-A1
  Nutrients Along WHP-A1
- Spreading of Newly Formed Labrador Sea Water

- Thermosalinograph, XBT and XCTD Measurements
  - XBT Sections
  - XCTD Field Test
- Sample Oxygen Measurements on WHP-A1
- Nutrient Measurements on WHP-A1
- Tracer Studies on WHP-A1
  - Tracer Oceanography: Tritium/Helium and Radiocarbon
  - Tracer Oceanography: CFCs

5.3 JGOFS Programmes:
5.3.1 The Control Function of the Carbonate-System in the Oceanic CO_2 uptake, WHP-A2
5.3.2 The Ocean as a CO_2 Sink: Complimentary Studies of the Baltic Sea and the North Atlantic, WHP-A1
5.4 Individual Programmes:
5.4.1 ^{129}I from Nuclear Fuel Processing as an Oceanographic Tracer
5.4.2 ALACE Float Deployments

6 SHIP'S METEOROLOGICAL STATION
6.1 Leg M30/1
6.2 Leg M30/2
6.3 Leg M30/3

7 LISTS
7.1 List of Stations
7.1.1 Lists of Sampling Stations M30/1
7.1.2 Station List Leg M30/2 Section WHP-A2
- Summary of Sub-Sampling Schemes, Hydrographic Stations on M30/2
- Summary of Daily Station Activities M30/2

7.1.3 Station List Leg M30/3 Section A1W
- Station List Leg M30/3 Section A1E

7.2 List of Moored Instruments
7.2.1 Leg M30/1 Sediment Trap Mooring Positions
7.2.2 Leg M30/2 Current Meter Mooring Positions
7.2.3 Leg M30/3 Current Meter Mooring Positions
7.3 List of Figures

8 CONCLUDING REMARKS
9 REFERENCES
10 NOTES

ABSTRACT

The Meteor Cruise M30 focused on the North Atlantic components of the global research programmes Joint Ocean Flux Study JGOFS, the World Ocean Circulation Experiment WOCE and the European programme Ocean Margin EXchange OMEX.

On the first leg, the exchange processes between the oceanic continental margins and the open ocean were addressed. A special emphasis has been put in this programme on the interfaces sediment/ocean and ocean/atmosphere. The Celtic shelf edge was chosen as the regional focus for this multidisciplinary research work.

The second and third leg used the unique opportunity to determine the modification and partitioning of the North Atlantic water masses in a fully enclosed region between 48° and 61°N. This programme is part of a longer-lasting effort to observe long-term changes of the meridional transports of heat, salt and fresh-water on time scales relevant to climate change. The WOCE component of ca. 10 weeks field-work will be used to describe in space the quasi-synoptic evolution of the hydrographic situation of the "overturning cell" of the global thermohaline circulation in the North Atlantic Ocean. Previous assessments as part of the WOCE Hydrographic Programme WHP on the section WHP-A1E in 1991 by FS Meteor, of AR7E in September 1992 with FS Valdivia (WOCE-NORD) and of WHP-AR19 in summer 1993 with FS Gauss already showed dramatic changes in water mass properties and the depth of individual water mass layers compared to work done during the International Geophysical Year IGY in 1957 and other in 1962 and 1982. These changes in intermediate and deep water masses associate directly with the annual winter sections worked in the Labrador Sea by Canadian colleagues since 1988 and this new assessment promises to describe in much greater details the linkage between local forcing and the large-scale reaction of the North Atlantic circulation.

ZUSAMMENFASSUNG

Die Meteor - Reise 30 war den nordatlantischen Komponenten der globalen Forschungsprogramme Joint Global Ocean Flux Study JGOFS und World Ocean Circulation Experiment WOCE und dem europäischen Programm Ocean Margin EXchange OMEX gewidmet.

Im ersten Fahrtabschnitt (M30/1) standen die Austauschprozesse zwischen den ozeanischen Kontinentalrändern und dem offenen Ozean im Mittelpunkt. Dabei wurde ein besonderes Gewicht auf die Grenzflächen Sediment/Wasser und Ozean/Atmosphäre gelegt. Als regionaler Schwerpunkt für diese umfangreichen multidisziplinären Untersuchungen wurde der keltische Schelfrand gewählt.

Der zweite und dritte Fahrtabschnitt (M30/2 und M30/3) boten die erstmalige Möglichkeit, die Modifikation der nordatlantischen Wassermassen und ihre daran beteiligten jeweiligen Anteile in einem abgeschlossenen Gebiet zwischen 48°N und 61°N eindeutig zu bestimmen. Diese Arbeiten führen die Beobachtung der langzeitigen klimarelevanten Schwankungen von meridionalen Wärme-, Salz- und Süßwassertransporten der letzten Jahre fort. Dabei gewährleistete das WOCE-Feldprogramm von ca. 10 Wochen erstmalig eine räumlich abgeschlossene quasi-synoptische

Erfassung des hydrographischen Zustandes der "overturning cell" der globalen thermohalinen Zirkulation im Nordatlantik. Die bisherigen Aufnahmen im Rahmen des WOCE Hydrographic Programme WHP von WHP-A1E im Jahre 1991 mit FS "Meteor" bzw. von AR7E im September 1992 mit FS "Valdivia" (WOCE-NORD) und WHP-AR19 im Sommer 1993 mit FS "Gauss" haben bereits drastische Veränderungen in den Eigenschaften der Wassermassen und der Tiefe der individuellen Schichten der Wassermassen im Vergleich zu den früheren Aufnahmen während des Internationalen Geophysikalischen Jahr 1957 und in den Jahren 1962 und 1982 ergeben. Die erneute Erfassung der intermediären und tiefen Zirkulation insbesondere im Zusammenhang mit den jährlichen winterlichen Aufnahmen der Labrador-See durch kanadische Kollegen seit 1988 verbessert die Beschreibung der sich abzeichnenden Beziehung zwischen dem örtlichen "forcing" und der großräumigen Reaktion des nördlichen Atlantiks.

1 RESEARCH OBJECTIVES

Leg M30/1: Las Palmas – Hamburg
OMEX Ocean Margin Exchange

On the first leg of METEOR cruise 30 the exchange processes of carbon and "green house" gases between the western European shelf edge and the open ocean were studied within the frame of an interdisciplinary European Union Programme "Ocean Margin Exchange" (OMEX). Station work concentrated on a transect from the outer Celtic Sea (Great Sole Bank) across the Goban Spur into the Porcupine Seabight covering a depth range from 220 m to 4800 m (Fig. 1). Special emphasis was put on the interfaces sediment/ocean and ocean/atmosphere.

Legs M30/2 and M30/3: Hamburg – St. John's – Hamburg
WOCE World Ocean Circulation Experiment

This German contribution to the international WOCE Programme as part of the World Climate Research Programme WCRP focused on the Northern North Atlantic in late autumn. Here we find significant changes in the water mass characteristics such as temperature, salinity and the contents of dissolved oxygen caused by the highly variable meteorological forcing on annual and interannual time scales. These changes affect the contribution of the North Atlantic to the global thermohaline circulation in the form of the North Atlantic Deep Water and its signatures. It, in the end, will affect the meridional transports of heat, salinity and freshwater.

For a highly resolved description of the water masses that are modified by these processes besides measurements of temperature and salinity, the concentrations of dissolved oxygen content, nutrients and a sequence of transient tracers such as CFCs, carbon ^{14}C, helium ^{3}He and ^{4}He and tritium ^{3}H was analysed from water samples. Using the characteristic input functions into the ocean, the relevant modification processes and their regions will be better resolved.

Since the scientific programme for both cruise legs M30/2 and M30/3 is essentially identical and only most of the participating groups changed, for both legs a joint programme description is given below.

The German contributions to WOCE and JGOFS have been funded by the Federal Ministry for Research and Technology (BMFT).

JGOFS Joint Global Ocean Flux Study

In co-operation with JGOFS, all WOCE WHP-sections are to be sampled for dissolved and particular CO_2 to better quantify the ocean's role as a reservoir in the global carbon system. Sections A2 at 48°N and A1 at ca. 57°N have been sampled in this context. The data are being made available to the appropriate data centres.

2 PARTICIPANTS

2.1 Leg M30/1

Name	Speciality	Institution
Pfannkuche, Olaf, Dr., Chief Scientist	Benthic Biology	GEOMAR
Antia, Avan, Dr.	Planktology	IfMK
Balzer, Wolfgang Prof. Dr.	Marine Chemistry	UBMCh
Bassek, Dieter	Weather Technician	DWD/SWA
Behrens, Katrin	Benthic Biology	IHF
Bosse, Kai	Benthic Biology	IHF
Büns, Ilse	Biochemistry	UHIBL
Deeken, Aloys	Marine Chemistry	UBMCh
Dierßen, Holger	Marine Chemistry	UBMCh
Dölle, Martina	Benthic Biology	IHF
Erasmi, Wolfgang	Hydrography	IfMK
Flöck, Otmar	Biogeochemistry	MPICh
Götz, Sabine	Benthic Biology	IHF
Jeskulke, Karen	Benthic Biology	IfMK
Kahl, G.	Meteorology	DWD/SWA
Kumbier, Thomas	Electronics	IfMK
Lampitt, Richard Dr.	Planktology	IOSDL
Lehnert, Gerhard	Planktology	IOW
Nuppenau, Volker	Electronics	IHF
Otto, Sabine	Marine Chemistry	UBMCh
Pfeiffer, Alexander	Biochemistry	UHIBL
Poremba, Knut, Dr.	Benthic Biology	IfMK
Schebeske, Günther	Biogeochemistry	MPICh
Soltwedel, Thomas Dr.	Benthic Biology	IHF
Uher, Günther	Biogeochemistry	MPICh
Ulshöver, Veit	Biogeochemistry	MPICh
Wellmann, Hartwig	Marine Chemistry	UBMCh
Witte, Ursula Dr.	Benthic Biology	IHF

2.2 Leg M30/2

Name	Speciality	Institution
Dr. Koltermann, Klaus Peter, Chief Scientist	Phys. Oceanography	BSH
Wöckel, Peter	CTD-support	BSH
Soetje, Kai C	CTD-Computing	BSH
Mauritz, Heiko	CTD-computing	BSH
Stolley, Martin	Hydro watch	BSH
Frohse, Alex	Salinometer	BSH
Berger, Ralf	CTD-support	IfMK
Dr. Terechtchenkov, Vladimir	Hydro watch	BSH/PPS
Hatten, Helge	Hydro watch	IfMHH
Outzen, Olaf	Hydro watch	IfMHH
Löwe; Peter	Hydro watch	BSH
Giese, Holger	Hydro/moorings	BSH
Dr. Mintrop, Ludger	Chemistry/CO_2	IfMK
Körtzinger, Arne	Chemistry/CO_2	IfMK
Johannsen, Helge	Chemistry/nutrients	IfMK
Malien, Frank	Chemistry/nutrients	IfMK
Schweinsberg, Susanne	Chemistry/CO_2	IfMK
Senet, Christian	Chemistry/CO_2	IfMK
von Hippel, Annette	Chemistry/CO_2	IfMK
Atwood, Chris	Chemistry/CO_2	SIO
Bulsiewicz, Klaus	CFCs	IUP-B
Rose, Henning	CFCs	IUP-B
Rüth, Christine	CFCs	IUP-B
Dr. Bayer, Reinhold	Tracer	IUP-HD
Dr. Kromer, Bernd	Tracer	IUP-HD
Dr. Born, Matthias	Tracer	IUP-HD
Rübel, André	Tracer	IUP-HD
Kühr, Sabine	Tracer	IUP-HD
Dr. Röd, Erhard	Ship's Meteorologist	SWA
Lambert, Hans-Peter	Weather Technician	SWA

2.3 Leg M30/3

Name	Speciality	Institution
Dr. Meincke, Jens, Chief Scientist	Phys Oceanography	IfMHH
Dr. Sy, Alexander	Hydrography	BSH
Bersch, Manfred	Hydro watch	IfMHH
Paul, Uwe	Hydro watch	BSH
Dr. Lazier, John	Hydro watch	BIO
Gerdes, Jürgen	Hydro watch	IfMHH
Haak, Helmuth	Hydro watch	IfMHH
Bock, Jan	Hydro watch	IfMHH
Dombrowski, Uwe	CTD-support	IfMK
Verch, Norbert	Salinometer	IfMHH
Mauritz, Heiko	CTD-computing	BSH
Gottschalk, Ilse	CTD-computing	BSH
Kramer, Rita	O2	BSH
Horn, Ines	O2	BSH
Oestereich, Frank	O2/nutrients	BSH
Kirkland, Donald	Nutrients	MAFF
Dr. Schneider, Bernd	CO2	IOW
Thomas, Helmut	CO2	IOW
Prado-Fiedler, Ronaldo	CO2	IOW
Dr. Bayer, Reinhold	Tracer	IUP-HD
Dr. Born, Matthias	Tracer	IUP-HD
Müller, Franziska	Tracer	IUP-HD
Gier, Eva-Maria	Tracer	IUP-HD
Dr. Rhein, Monika	CFCs	IfMK
Haie, Petra	CFCs	IfMK
Badewien, Thomas	CFCs	IfMK
Dr Röd, Erhard	Ship's Meteorologist	SWA
Lambert, Hans-Peter	Weather Technician	SWA

2.4 Participating Institutions

BIO Bedford Institute of Oceanography, P.O.B. 1006, Dartmouth, N.S., B2Y 4A2, Canada

BSH Bundesamt für Seeschiffahrt u. Hydrographie, Bernhard-Nocht-Str. 78, 20597 Hamburg, Germany

CSNSM Centre des Spectrométrie Nucléaire et de Spectrométrie de Masse (IN2P3-CRNS), Bâtiment 108, 91405 CAMPUS ORSAY, France

DWD Deutscher Wetterdienst, Seewetteramt, Bernhard - Nocht - Str. 76, 29359 Hamburg, Germany

Geomar	Forschungszentrum für marine Geowissenschaften der Christian-Albrechts-Universität zu Kiel, Wischhofstr. 1-3, 24148 Kiel, Germany
IfMHH	Institut für Meereskunde der Universität Hamburg, Troplowitzstr. 7, 22529 Hamburg, Germany
IfMK	Institut für Meereskunde an der Universität Kiel, Düsternbrooker Weg 20, 24105 Kiel, Germany
IHF	Institut für Hydrobiologie und Fischereiwissenschaft, Universität Hamburg, Zeiseweg 9, 22765 Hamburg, Germany
IOSDL	Institute of Oceanographic Sciences, Deacon Laboratory, Wormley, Godalming, Surrey GU8 5UB, United Kingdom *now:* Southampton Oceanography Centre, Empress Dock, Southampton, Hampshire, SO14 3ZH, United Kingdom
IOW	Institut für Ostseeforschung, Seestr. 15, 18119 Rostock-Warnemünde, Germany
IUP-B	Universität Bremen, Fachbereich 1, Institut für Umweltphysik, Abt. Tracer - Ozeanographie, Bibliotheksstrasse, 28359 Bremen, Germany
IUP-HD	Institut für Umweltphysik der Universität Heidelberg, Im Neuenheimer Feld 366, 69120 Heidelberg, Germany
MAFF	Ministry of Agriculture, Food and Fisheries, Fisheries Laboratory, Lowestoft, Suffolk NR33 0HT, United Kingdom
MPICh	Max-Planck-Institut für Chemie, Abt. Biogeochemie, Postfach 3060, 55020 Mainz, Germany
UBMCh	FB-2 Meereschemie, Universität Bremen, Postfach 330440, 28334 Bremen, Germany
UHIBL	Institut für Biochemie, Universität Hamburg, Martin-Luther-King Pl. 6, 20146 Hamburg, Germany
IORAS/PPS	P.P. Shirshov Institute of Oceanology, 23 Krasikova str., Moscow 117851, Russia
SIO	Scripps Institution of Oceanography, University of California, San Diego, La Jolla, CA 92093, USA
WHOI	Woods Hole Oceanographic Institution, Woods Hole, Ma 02543, USA

3 RESEARCH PROGRAMMES

3.1 OMEX Programmes

The OMEX project is funded by the European Union within the frame-work of MAST II ("Targeted Projects"). The various multinational and interdisciplinary programmes focus on the exchange processes of carbon and a variety of gases - which occur to be relevant to climatic changes - between European shelf areas, the adjacent continental margin and open ocean. Special emphasis is paid on exchange processes at the sediment/water and ocean/atmosphere interfaces. The Celtic Margin at the Goban Spur (Fig. 1), where leg M30/1 took place, was chosen as a regional focus of the OMEX project for the time span 1993-1995. The cruise M30/1 was part of a series of cruises of various European research vessels organized to gain a seasonal coverage of the sampling stations on the Goban Spur Transect. It was intended to investigate a typical autumn situation for the different processes.

3.1.1 Organic Matter Degradation, Denitrification and Trace Metal Diagenesis
(UBMCh, W. Balzer)

For the understanding of the major controls over release fluxes from margin sediments a detailed investigation of early diagenetic processes acting within the sediments is necessary. Therefore, extensive work on pore water chemistry and on solid sediment phases at transects across the continental margin was conducted. The integrated rate of organic matter remineralization in near-surface sediments will quantified by modelling the pore water profiles obtained during M27. In dependence on both the diagenetic redox milieu and the input terms, the benthic reactions and fluxes of selected trace metals were investigated to assess the significance of margin processes for the trace metal chemistry of the ocean. By analysing the trace metal content in trapped particles, in suspended material, in sediments and in pore waters we will contribute to finding relationships between vertical/lateral sedimentation fluxes, benthic release fluxes and burial rates of chemically differing elements. A special study deals with sedimentary denitrification in continental margin sediments.

3.1.2 Carbon Mineralization by the Benthic Community
(GEOMAR, O. Pfannkuche; IHF, H. Thiel)

Rates of remineralization of organic carbon in the benthal are controlled by all transport processes in the water column. Parametrization of benthic processes is necessary to determine what portion of the sedimenting carbon is remineralized and what portion is accumulating in the sediments. The understanding of the biological, chemical and physical processes involved and their quantitative determination is vital for balancing carbon fluxes in the sediment. For the assessment of the role of benthic organisms for carbon cycling it is necessary to determine benthic community respiration, biomass production and benthic activity. Present knowledge obtained from deep-sea investigations of the temperate Atlantic Ocean suggests that benthic respiration, activity and biomass production is subject to strong seasonal variations which correlate with carbon input by sedimentation. The largest part of benthic carbon removal is by organism respiration, its seasonal range being 80-90%. The determination of in-situ benthic oxygen respiration rates by use of "bottom landers" is therefore of central significance for balancing the carbon fluxes. Since most of the biotic oxygen

consumption is performed by micro-organisms, it is necessary to determine the part played by micro-organisms in community respiration and biomass production. The main objective of this project is the quantification of biological mediated carbon fluxes through the sediment measuring benthic oxygen consumption rates, metabolic activity and biomass production on a seasonal scale.

3.1.3 Vertical Particle Flux at the Continental Margin
(IfMK, B. v. Bodungen)

The overall goal is the investigation of the seasonal pattern of particle sedimentation from the epipelagic zone to the sea floor and its dependence on the water depth at transects from the shelf edge to the abyssal plain. It is intended to identify the quality and relative significance of the different source materials. Therefore, the particle flux at different water depths were determined with high temporal resolution by using sediment traps. In the sedimenting material the following components and parameters have been determined: carrier phases, $^{15}N/^{14}N$ isotopic ratios, pigments, stable carbon isotopes, and trace elements. Light and electron microscopy was used to identify individual particles. In relation to the particulate fluxes of carbon and nitrogen as measured with traps, DOC- and DON-measurements of water samples serve to assess the significance of dissolved organic components for the cycling of carbon and nitrogen.

3.1.4 Phase Transfer of Organic Compounds During Shelf Edge Passage
(UHIBL, Uwe Brockmann)

At the shelf edge, nutrient rich water masses are injected into the euphotic zone due to upwelling processes. Here, inorganic components are rapidly transformed into particulate organic material, a part of which sediments to the sea floor where it is subject to remineralization. The spatial distribution of these processes depends to a large extent on advective processes at the shelf edge. Provided that currents are directed consistently to the shelf edge, the succession of individual processes can be traced by analysing the distribution of nutrients as well as the distribution of the dissolved and particulate organic components. Because the different nutrient elements are remineralized at different rates, gross inferences on the state of the biological development may be drawn from measured element ratios in both the dissolved nutrients and in the dissolved/particulate organic substances. These investigations are closely related to hydrographic studies and to an ecosystem analysis at the shelf edge of the selected region.

3.1.5 Flux of Trace Gases at the Boundary Between Ocean and Atmosphere
(MPICh, M. Andreae)

In collaboration with other European research groups the biogeochemical processes were investigated that are involved in the production and emission of trace gases being selected according to their relevance for climate and atmospheric chemistry. In continuation of measurements during the METEOR cruise M21/2 the photochemical production of carbonyl sulphide (COS) in the ocean and its exchange flux between ocean and atmosphere was determined. COS is produced from certain dissolved organic compounds and may be emitted to the atmosphere. Due to its long life time of more than one year, COS may reach the stratosphere where it forms the main source of the sulphate layer which influences both the ozone layer and the incoming solar radiation. Of particular significance in this context is the seasonal and spatial

variability of the ocean as a source of COS. During M27/1 a photochemical/kinetic model was tested and now improved that considers light dependent production of COS, hydrolysis of COS and its exchange at the ocean/atmosphere interface as well as vertical mixing in the ocean.

3.2 WOCE Programmes:

3.2.1 Determination of the Meridional Transports of Heat, Salt and Freshwater at 48˚N in the North Atlantic along the WHP section A2

(BSH, K.P. Koltermann)

The meridional transports of heat, freshwater and salt in the Atlantic Ocean and their seasonal and interannual changes are determined for the 90s across the latitude of the global maximum freshwater transport at ca. 50°N in the Atlantic Ocean. These results are compared with previous measurements in the 50s and 80s. This "time series" is augmented with Russian data along 48°N that have been collected at quarterly intervals between 1975 and 1987 down to a depth of 2000 m. This will result in a climatology of the changes in the surface and intermediate layers and will improve the estimate of the seasonal cycle. Comparisons with results from eddy-resolving modelling efforts are separately pursued.

These estimates will provide the variance of these integral parameters, and finally lead to a history of their development since the IGY in 1957. This section elucidates the interaction of the thermohaline North Atlantic circulation with the wind-driven one at intermediate and great depths. Furthermore we expect a better formulation of the coupling between these changes and the changes in the "forcing fields", particularly the fluxes of latent and sensible heat, evaporation and precipitation E-P and wind stress from operational atmospheric models (ECMWF, NMC) at the surface. The WOCE-NORD project will in addition document estimates of the temperature distribution and heat content at ca. 50°N for the top kilometre on time scales of months from its VOS subprogramme to establish their seasonal cycle. In co-operation, we will attempt to complement the circulation estimates of the convective area north of 48°N with the estimates from this section.

Working this section in the summer of 1993 with FS Gauss has shown the Labrador Sea Water temperatures some 0.4°C below its historical characteristic temperature, and deeper in the water column by some 700 m. This fits in with observations from the early 90s along 60°N and 24°30'N and indicates a rapid reaction of the intermediate circulation of the northern North Atlantic to changes in the forcing in the Labrador Sea. We expect to get some first estimates on how changes in the heat, salt and freshwater transports of the boundary currents of the North Atlantic continue into the ocean interior, and what likely impact this will have on the coupled ocean-atmosphere system.

3.2.2 Nutrients Measurements for the Fine Resolution of Oceanic Water Masses on the Meteor Cruise M30/2 (section WHP-A2) in the North Atlantic

(IfMK, J. Duinker, L. Mintrop)

The concentrations of nutrients PO_4, NO_3, NO_2, NH_4, $Si(OH)_4$ from 1692 samples and the content of dissolved oxygen O_2 from 1737 water samples have been determined on board according to the WHP Standards. For quality assurance purposes additional samples were taken as duplicates or replicates. All data were processed on board, subjected to detailed consistency and quality checks and compared to existing data sets from this region. An annotated data file was produced at the end of the cruise, containing all relevant information and documentation on methodology and the quality of the data.

3.2.3 CFCs on the section WHP-A2

(IUP-B, W. Roether)

On all stations of the WOCE WHP section A2 water samples from all depths were analysed for CFCs. Some 1100 measurements of F11, F12, F113 and CCl_4 have been processed. These data will be used to determine mixing rates and apparent ages of the water masses in the North Atlantic. Sampling and interpretation will be done in close co-operation with all groups involved.

For running the CFC analyses onboard

(1) 1062 samples for CFC have been collected and analysed for F11, F12, F113, CCl_4. All analyses have been evaluated preliminarily at sea.
(2) In addition 77 ^{3}He-samples have been collected (classical method) for inter comparisons with the Heidelberg group.

All samples were collected with the standard rosette system. The CFC-samples were drawn on large glass syringes. During sampling, contamination with helium and CFCs was to be avoided or controlled. The sampling strategy on the section followed the WOCE recommendations. Except for shallower areas each station was sampled at up to 36 levels. The vertical resolution had a higher priority than the horizontal one for the case the throughput of the CFC-system was limited. The deep boundary currents, particularly in the western part of the section, were of special interest.

3.2.4 Mooring Recovery on sections WHP-A2 and WHP-A1

(BSH, K.P. Koltermann and IfMHH, J. Meincke)

On the Gauss cruise 226 an array of three mooring was deployed west of the Mid-Atlantic Ridge an section WHP-A2 in the summer of 1993 to measure the vertical and horizontal extend of a deep high salinity boundary current and its temporal changes. Previous attempts to recover these mooring had failed as there seem to are problems with the acoustic releasers. On this cruise another attempt for recovery was planned, depending on the prevailing weather situation and time availability.

On WHP-A1 the mooring D2 was deployed to measure the vertical structure of the depth controlled current. Several attempts to recover the mooring acoustically had failed. On the leg M30/3 another attempt to recover the mooring by dredging was not successful. Further attempts to dredge for other moorings on this section had to be abandoned for weather reasons.

3.2.5 Tritium/Helium and ^{14}C-Sampling along WHP-sections A2 and A1
(IUP-HD, R. Bayer)

The zonal section along 48°N (WHP-A2) was sampled for the first time for a detailed analysis of helium, tritium and ^{14}C signals.

Comparing the 1972 GEOSECS data in the Northwestern Atlantic with the TTO/NAS data in 1980-81 has shown a prominent invasion of the transient tracer signals from the surface into the deep waters. An additional survey of these tracer fields in 1994 (WHP-A2) gives further indications on how much and how fast this invasion has proceeded. This will help to parameterize the renewal rates for the individual deep basins. Clear horizontal gradients of higher tracer signals in the West are seen. The deep western boundary currents with the most recent and youngest waters are clearly evident, showing similar features as on the A1 section sampled in 1991. A detailed survey of these gradients along the sections and the meridional connection of the tracer signals in the Deep Western Boundary Currents are of particular interest.

On WHP-A2 474 helium and tritium samples have been collected. In addition 311 helium samples have been taken to test a sea-going extraction facility. Of the 51 stations sampled a denser coverage was attempted for the western boundary currents, but had to be aborted due to bad weather but succeeded across the Mid Atlantic Ridge, with an even station distribution along the rest of the section.

In parallel to the large volume ^{14}C-sampling we sampled for AMS-^{14}C-analyses. The large volume samplers are used at the relevant stations in two casts: the shallow cast was followed by the CTD-rosette cast for small volume samples to give time for the ^{14}C-extraction and the subsequent preparation of the large volume samplers for the deep cast for ^{14}C. As experienced in recent years in our polar work a complete ^{14}C station was worked in about 5 hours (ca. 20 LVS samples at 4000 m water depth). For the 48°N section 8 LVS stations with 204 LVS samples and 60 samples for AMS-^{14}C have been worked.

Sampling on WHP-A1 (West and East) followed for the Eastern part largely the 1991 strategy and results. Some 400 helium and tritium samples were analysed ashore. We used the seagoing extraction facility with great success. Similar to the sampling strategy on the previous leg on A2, sampling focused on the basin boundaries with ca. 25 stations in total. We tried to resolve the temporal and seasonal variability of the tracer signatures in order to compare them with existing data from the European Polar Seas and work done further south within the frame-work of WOCE. This also applies for the work in the Labrador Sea on A1 West. Here we had planned ca. 100 samples for helium and tritium, and 3 stations for LVS-^{14}C work but succeeded only in working 2 stations due to bad weather.

3.2.6 WOCE North Atlantic Overturning Rate Determination (WOCE-NORD, WHP section A1)

(IfMHH, J. Meincke and BSH, A. Sy)

The meridional transports of heat and matter in the North Atlantic are quantified through a section connecting Ireland and South Greenland. This section runs south of the region where the atmospheric forcing transforms the water advected to high latitudes such that it will sink to intermediate and greater depths and spreads further south, forming the source water masses of the North Atlantic Deep Water. This "overturning" process is regarded as the main driving mechanism for the global thermohaline circulation. Quantifying both input and output in the North Atlantic overturning system will help to improve modelling the role of the ocean in the climate system.

Leg M30/3 is part of the WOCE-NORD project, running over six years. To extend the data basis needed to calculate the transport rates involved in the overturning process, sections have been repeated seasonally between Ireland and South Greenland. A combination of current measurements from the ship in motion, long-term moorings of current meters and surface topographies from altimeter data are being used. This leg M30/3 was the third repeat of the WOCE hydrographic section A1E/AR7E. Extending this time the work to the western part A1W together with the work on A2 improves the transport estimates using inverse modelling.

Along a section through the Labrador Sea Basin (A1W) from Hamilton Bank to South Greenland and continuing on a section from South Greenland to Ireland (A1E) we observed the fields of the classical hydrographic parameters pressure, temperature, salinity, content of dissolved oxygen and nutrients (NO_3, NO_2, PO_4, SiO_3). The work along A1E was, except for weather "gaps", an identical repeat of the work on Meteor cruise M18 (September 1991). The work programme followed the strategy used during the previous leg M30/2 and all instruments and procedures were continued. Only for nutrients and oxygen work other groups joined in St. John's employing their own slightly modified procedures. All data, particular the CTD data, were processed on board, except for applying post-cruise laboratory calibrations to the pressure and temperature sensors.

3.2.7 CFCs on the section WHP-A1

(IfMK, M. Rhein)

On the third leg of M30 we determined the tracer characteristics of the water masses that have spilt over the ridge system between Greenland and Iceland (DSOW) and between Iceland and the Shetlands (ISOW). After leaving the ridges these denser masses sink to the bottom and entrain ambient water masses. The extent of the mixing and the changes of the water mass characteristics after leaving the ridges are also a focus of these investigations. The data will be used to improve the parameterisation of the Deep Water formation process north of the ridge system and to derive at better mean spreading velocities for individual water mass components. Other tracer and oceanographic data will be used as well. Besides the overflow water masses we also sampled the newly formed deep water from the Labrador Sea, both at the exit of the Labrador Sea and along its spreading paths in the Irminger Sea and the North-Eastern Atlantic.

On all stations of the WOCE section WHP-A1 water samples from all depths were analysed for CFCs. Some 1800 measurements of F11, F12, F113 and CCl_4 have been processed. These data will be used to determine mixing rates and apparent ages of the water masses in the North Atlantic. Sampling and interpretation will be done in close co-operation with all groups involved.

3.3 JGOFS- Programme

3.3.1 The Control Function of the Carbonate-System in the Oceanic CO_2 Uptake, WHP-A2

(IfMK, J. Duinker, L. Mintrop)

Measuring pCO_2, total carbonate and alkalinity we investigated the CO_2 exchange between ocean and atmosphere in a regional and seasonal resolution to contribute to a global budget. In parallel these data will be used together with measurements of the $\delta^{13}C$-signal to follow the spreading of the anthropogenic CO_2-signal in the ocean.

We used on the WHP section A2, M30/2 the experience of our previous WOCE cruise Meteor M22/5 along 30°S (WHP-A10).

(1) <u>Sampling</u>

- Sampling for alkalinity and total carbonate ca. once every 24 h (i.e. every third or fourth CTD station in parallel with the tracer sampling),
- sampling for ^{13}C-measurements in total on 23 stations (359 samples),
- surface sampling from the clean sea water system along the cruise track every 30 to 60nm.

(2) <u>Measurements</u>

- direct measurements on board of alkalinity and total carbonate,
- in parallel we used a continuous system to measure the CO_2 partial pressure.

3.3.2 The Ocean as a CO_2 Sink: Complimentary Studies of the Baltic Sea and the North Atlantic, WHP-A1

(IOW, B. Schneider)

Measuring the parameters pCO_2, total carbonate and alkalinity we will, in combination with oxygen and nutrients data describe the CO_2 exchange between the ocean and the atmosphere in the North Atlantic in early winter. The results from the WHP section A1 of leg M30/3 are compared with similar measurements in the Baltic Sea to differentiate between the CO_2 systems of two ecologically different marine environments.

(1) Continuous measurements of the CO_2 partial pressure along the entire ship's track from St. John's into the North Sea (M30/3).

(2) Measurements of total carbonate on water samples of the WOCE stations along the sections A1W and A1E. We processed ca. 40 samples/d.

3.4 Individual Projects

3.4.1 ^{129}I from Nuclear Fuel Processing as an Oceanographic Tracer
(CSCSM-CNRS, G. M. Raisbeck)

On the two legs M30/2 and M30/3 water samples were taken to determine the ^{129}I concentration. This nuclide originates from the nuclear fuel reprocessing system and has shown some interesting facets used as an additional oceanographic tracer. Previous work in the North Atlantic has as yet not been satisfactory to provide an adequate signal/noise ratio to assess its information content in oceanographic applications.

^{129}I measurements, using AMS techniques, have been taken from seaweed and seawater along the European coasts and waters. From the ^{129}I/^{127}I ratios we have been able to demonstrate spreading pattern from this man-made tracer. First examples from the North Atlantic show that ^{129}I can be used to differentiate sources other then those associated with tracers already used in oceanography. With samples from this cruise on WHP-A2 and WHP-A1 we would like to develop an estimate of the dynamic range this signal has in the full-depth ocean and evaluate if the information contained in these data is useful to describe water masses, their fate and behaviour.

3.4.2 Profiling ALACE floats to determine the development of the stratification in the Labrador Sea over two years
(SIO, R.Davis and WHOI, B.Owens)

On the leg M30/3 six ALACE (Autonomous Lagrangian Circulation Explorer) floats for two US-American groups (SIO/WHOI) were deployed in the Labrador Sea to determine the velocity field at a pre-selected depth level of 1500dbar over more than two years. These floats surface at regular weekly intervals to radio their position and data from their drift and ascend and descend phases to a satellite. This provides information besides the float track-derived velocities, on the evolution of the profiles of temperature and salinity with time.

For two years we will follow the evolution of the Labrador Sea stratification for the top kilometre with profiling ALACE floats (P-ALACE). They are deployed across the Labrador Sea gyre and part of the boundary current regime and surface at weekly intervals to report profiles of temperature (5 floats) and temperature and salinity (one float) via satellite. The tracks will give a first glance at the velocity field of the gyre and its changes. We will use this information for planning a convection experiment in 1996. Some other ALACE floats with RAFOS transducers will be deployed to test the effective sound ranges with the existing Newfoundland Basin array. Experience from the Arctic has shown that we have to consider reduced ranges in this region. The results are needed to design a RAFOS array for work from 1996 onwards.

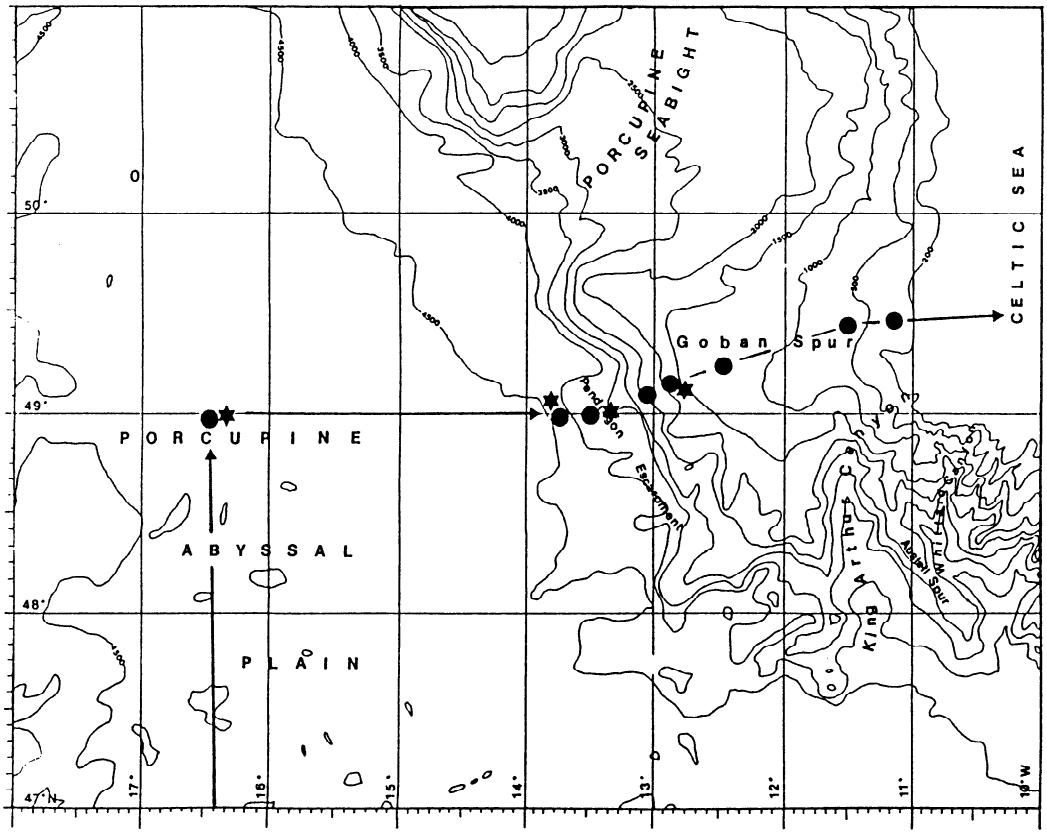

Fig. (1) Track and Station map of Meteor leg M30/1

* moorings, • benthic station, → cruise track

4 NARRATIVE OF THE CRUISE

4.1 Leg M30/1

(Chief Scientist O. Pfannkuche)

FS Meteor left Las Palmas on the evening of Sept. 6, 1994 heading north for the first station at 49°N, 16°30'W on the Porcupine Abyssal Plain. En route the ship stopped 3 times in international waters on the Iberian Abyssal Plain in order to test a new version of the multiple corer and the CTD/Rosette system. On Sept. 12 at 0400h we started to work at the first station at the Porcupine Abyssal Plain. After water sampling and CTD profiling the sediment trap mooring of the Institute of Oceanographic Sciences, UK, which was deployed in spring 1994, was successfully retrieved. A series of multiple corer samples followed. In the afternoon the refitted sediment trap mooring was deployed again and Meteor headed east for the next station at the bottom of the continental rise. Besides sediment and water sampling a new sediment trap mooring (OMEX IV) was deployed. From now on sampling stations followed the contours of the continental slope (Fig. 1) from the Pendragon Escarpment (water depth 3600 m) up to the Great Sole Bank (water depth 220 m). Station work on the Pendragon Escarpment had to be interrupted on Sept. 13 until the afternoon of Sept. 14 as a storm (8-9 Bft) prevented the use of any sampling gear. On all slope stations sampling followed the same routine: sediment

samples with box grab and multiple corers, water samples with Go-Flow bottles, a Niskin bottle rosette sampler and a marine snow catcher (only one haul), and CTD profiling. Two more sediment trap moorings of the OMEX project were successfully retrieved and re-deployed after refitting. OMEX III at 3670 m on the Pendragon Escarpment on Sept. 15 and OMEX II at 1418 m on the upper slope on Sept. 16. A free vehicle grab respirometer (bottom lander) was moored on the Pendragon Escarpment for two days (Sept. 13 - 15). At 1700h on Sept. 17 station work was finished on the outer Great Sole Bank and METEOR headed back to Germany. The cruise M30/1 ended at 0800h on Sept. 21, in the port of Bremen.

4.2 Leg M30/2

(Chief Scientist K.P. Koltermann)

FS Meteor left its berth in Hamburg after a routine shipyard refit in thick fog on Oct 12, 1994 at 0900. After a smooth transit with increasing visibility, the first station (#436) for testing all equipment was worked on Oct. 15, 1994 from 1232 UTC on 48°09.9'N, 11°44.9'W on 3420 m depth in international waters. On Oct 16, the first station of the trans-Atlantic transect was begun at 0444 UTC on 49°14.1'N, 10°39.9'W and a depth of 153 m. The first autumnal gales caught up with us already the next day, where winds of S10-11 Bft stopped station work. Weather-related breaks were used to find the optimum combination of rosette, underwater command module and CTD. Several attempts to dodge the weather and use lower wind speed periods where unsuccessful, so that we could only return to the planned station in the morning of Oct 20, 1994. Work progressed until the evening of the next day, when the ship again had to weather winds from the West with 10-11 Bft.

The next week saw better progress westward. On Oct 27 an attempt to dredge for the mooring K1 west of the Mid-Atlantic Ridge was not successful, although the mooring had responded to acoustic signals. Moorings K2 and K3 were acoustically located but did not release. No dredging attempts were made. Increasing winds prohibited station work afterwards until Oct 29, although that station had to be interrupted again for heavy winds. This stop-and-go station work continued until Nov 8. Station spacing had to be adjusted to allow for distance made west during gales and time lost. Time had also to be used either to return to a planned station position when the position had been overrun or heave to at a new position and wait for the weather to calm down. While work was stopped at times by heavy weather east of the Mid-Atlantic Ridge, work was only possible in the "weather windows" between a succession of depressions west of the ridge. In the westernmost part of the section up onto the Grand Banks the number of stations had to be reduced severely as time was running out when the extra-tropical storm "Florence" hit the area. This decision was made easier as the CCS Hudson had worked that part only days earlier during recovery of an extended mooring array. The last two stations of the section could be worked as planned, and in transit an extensive set of deep XBT casts will provide the essential continuity between stations. Work was finished on Nov 10, 1994 at 0059 UTC and the ship made for St John's, Nfld where she arrived on Nov 12, 1994 at 0600. A total of 53 stations with 82 rosette casts was worked instead of the planned 82 stations (Fig. 2).

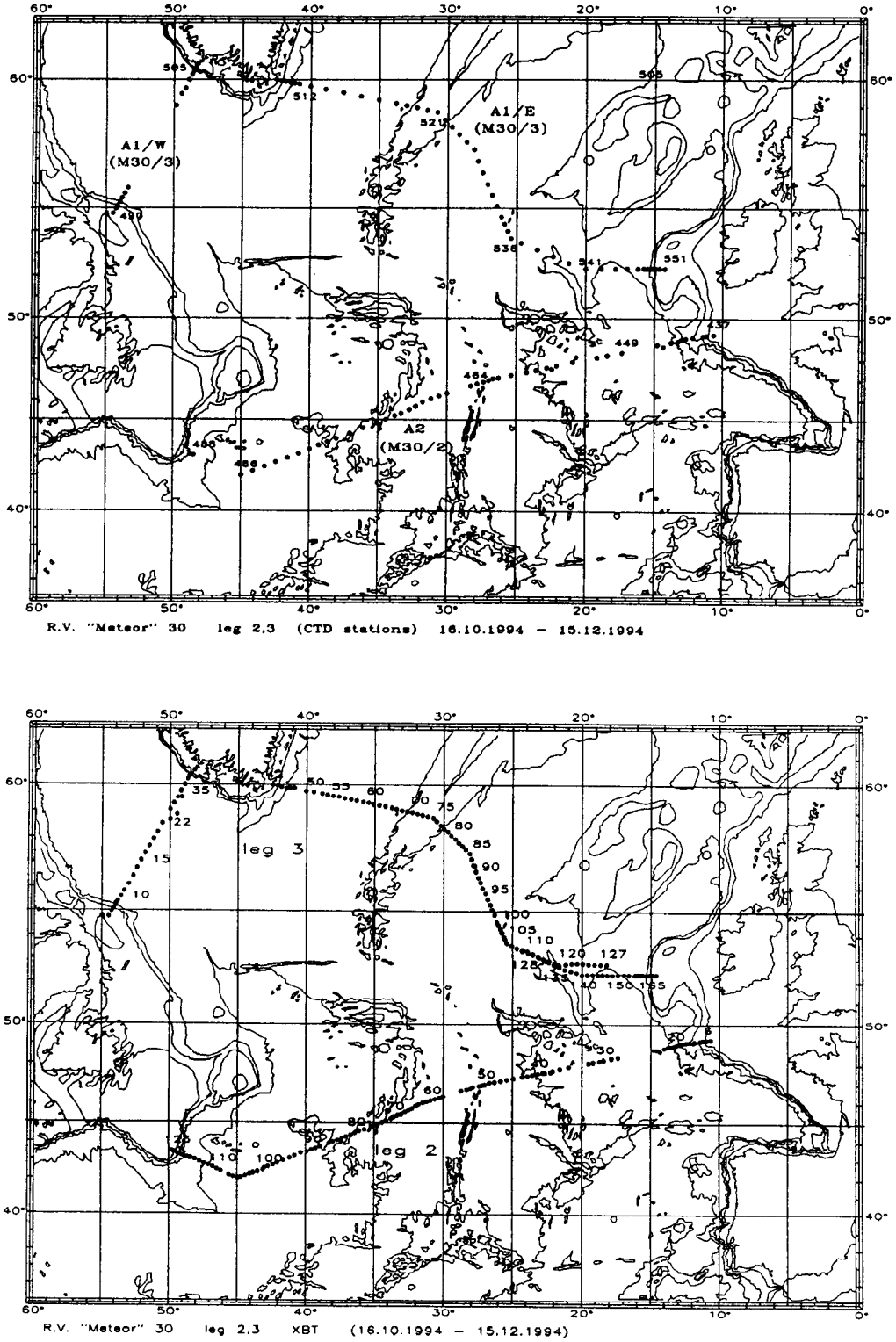

Fig. (2) Track and station maps of Meteor legs M30/2 (WHP-A2) and M30/3 (WHP-A1). Top panel: hydrographic stations and numbers, bottom: XBT stations and numbers

4.3 Leg M30/3

(Chief Scientist J. Meincke)

Following three days in port for exchanging the scientific party, setting up the laboratory installations, hand-over meeting with the previous party and visits between the ship and local scientific institutions at the St. John's Memorial University and the Northeast Fisheries Center, the ship left St John's on Nov 15, 1994 at 1400. A test-station for the CTD-Rosette systems was carried out en route to the starting position for the Labrador Sea section WOCE A1W on Hamilton Bank. Station work only began on Nov 18, at 0600 since a NW-gale stopped any progress for 20 hrs during Nov 16/17. Stations 490 to 496 over the Canadian continental slope were completed on Nov 19, 1200 when the weather forecast strongly recommended to leave the Canadian side and change over to the Greenland side of the Labrador Sea as fast as possible. During the transit four P-ALACE (Profiling Autonomous Lagrangian Circulation Explorers) were deployed and 2000 m XBTs were launched every 20 nm. The following two days were dominated by strong winds at temperatures around the freezing point, only one station (497) could be completed. From Nov 22 onwards regular station work resumed, starting in the convective regime of the Labrador Sea and crossing the boundary current regime towards the Greenland shelf (stations 498 -505). Again the weather forecast determined to finish activities in the Labrador Sea and take up the WOCE line A1E from east of Kap Farvel to Ireland. Therefore we had to leave the section A1W uncompleted in its central part and sailed around Kap Farvel.

Station work resumed on Nov 24 at 2200 on the eastern Greenland shelf (stat 506) down the slope into the Irminger Basin, but had to be interrupted following station 511 for Nov 26 and 27 because of a severe gale. However, we experienced a full week of moderate winds and seas and completed stations 512 - 537 until Dec 4, 1994. This phase included 12 hours on Dec 2 of unsuccessful dredging for the current meter mooring D2 which had been deployed in 1992. Three previous recovery attempts in 1993 and 1994 had already failed.

The next phase of severe winds and seas started on Dec 5 in the area 53°N, 24°W. On Dec 6 we experienced the highest wind speeds (100 kts) and highest seas (12 m) during this cruise. On Dec 9 a continuation of these conditions until at least Dec 14 became evident from the long- and medium-range numerical weather predictions. We decided to give up to complete of this WOCE section and return to Hamburg. At 2000 the ship started to head east, launching XBTs every 15nm and XCTDs every 30nm. However, on the morning of Dec 10 the numerical forecasts changed radically and predicted the development of a high pressure ridge over the operation area to stabilize for a few days from Dec 12 onwards. This chance was to be taken, the ship turned around and indeed from Dec 12 to Dec 15 0600 the WOCE section was completed in fine weather conditions (stations 538 - 551).

Since a few series of intense atmospheric depressions was announced to move into the operations area for Dec 16, the original plans to dredge for further moorings with release malfunction were given up. The ship made for Hamburg were it docked on Dec 19, 1994 at 0100 LT.

5 OPERATIONAL DETAILS AND PRELIMINARY RESULTS

5.1. OMEX Programmes

5.1.1 Biochemistry

- **Phase Transfer of Organic Compounds During Shelf Edge Passage**
  (UHIBI, I. Büns, A. Pfeifer and U. Brockmann)

Within the biogeochemical transfer and transformation processes in the area across the shelf edge, nutrients and organic compounds are key parameters. During the cruise, water samples were taken from defined depths at fixed stations on a west-east profile along the Goban Spur. The samples were filtrated and conserved for a later analysis, since besides oxygen titration, pH and photometric measurements, no chemical analysis could be done on board. Sampling should be done with a multi-bottle-rosette (24), connected to a CTD probe (Oceanography, Kiel). A test-run at station 423 was successful. Unfortunately, this was the only station, where multi-bottle-rosette and probe worked properly! We have to thank Prof. Balzer for the use of their GO-Flow rosette as a temporary replacement for the multi-bottle-rosette at some stations! Furthermore, they took care that another multi-bottle-rosette (University Bremen), which was stored on board, could be used later.

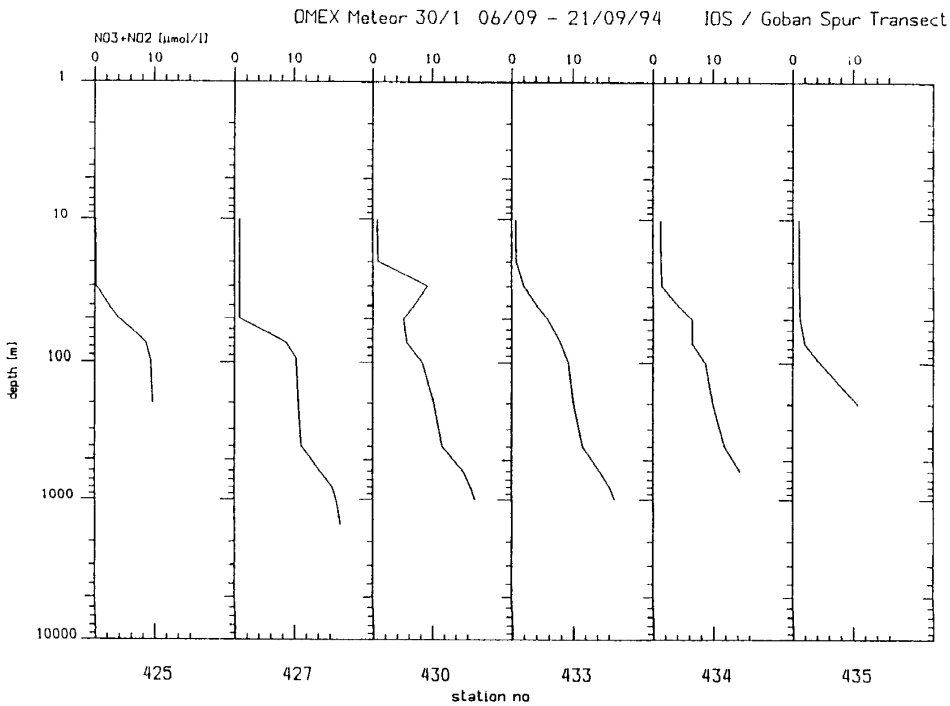

Fig. (3a) Nitrate (including nitrite) profiles. This diagram is dominated by the variations of nitrate. In general, there was a strong gradient (0.1 - 9.5 mol/l), increasing with depth, already in the euphotic zone. At station 430 a peak was observed in 30 m depths.

At station 425/IOS (depths > 4800 m), when multi-bottle-rosette and CTD totally failed, only 5 samples with the GO-Flows down to 200 m could be taken.

Station 426/OMEX IV: multi-bottle-rosette and CTD still did not work; because of lack of time the GO-Flows couldn't be used.

At station 427/OMEX III the CTD probe was run separately; the multi-bottle-rosette still refused to work properly. As there was no time for a separate sampling, we got part of the samples of Prof. Balzer, but the total volume that we actually needed for the filtration was not available.

Station 428/F: another trial, to run the multi-bottle-rosette from Bremen together with the CTD failed. We got samples from the GO-Flows, but as the interval between sampling and the time where we got our subsamples was too long, we couldn't use them.

At the station 430/OMEX II the CTD probe and the multi-bottle-rosette were run separately. Finally, success!

At the stations 433/B 1, 434/OMEX 1 and 435/A sampling now was successful.

Methods:

A vacuum filtration was run with controlled 0.2 bar at 9 filtration stands. Depending on the concentration of suspended matter, volumes from 750ml to 1750ml were filtrated over Whatman GF/C filters for the determination of CHN, part. P, part. CH and dry weight. An additional filtration stand was used for volumes up to 5 l for each filter for the determination of lipids. All filters were stored frozen at -17°C. The filtrate was fixed with mercury-(II)-chloride (0.01% w/v) and stored in glass and polyethylene bottles in a cooling chamber for a later analysis of nitrate, nitrite, phosphate, silicate and ammonium. A wet-chemical oxidation method was used to prepare samples for determination of total dissolved nitrogen and phosphorus. Immediately after sampling, measurements of turbidity (Turner nephelometer), pH (WTW pH 91) and fluorescence (Turner fluorometer and 1 Hz fluorometer) were conducted. Oxygen was determined by Winkler titration with a Metrohm titration stand.

First results:

The following diagrams (Fig. 3a-c) show nutrient-depth profiles for the sequence of stations from west to east. The profiles consist of raw data, not yet controlled. In general, the profiles show high nutrient concentrations within the deep water masses and low values due to nutrient consumption in the euphotic zone in the mixed layer.

- **Organic Matter Degradation, Denitrification and Trace Metal Diagenesis.**
- **Dissolved and Particulate Trace Elements**
  (UBMCh, W.Balzer, A.Deeken, H.Dierssen)

Within the OMEX-project on trace element cycling at the Celtic margin it is our task to determine the fluxes and reactions near the sediment/water interface. In order to gain a link to water column processes, the distribution of dissolved trace elements in the pore water and solid sediments has to be compared with their concentration in the water column and its suspended particulate material (SPM). During M30/1 the main objectives were to investigate for a summer situation whether dissolved Al and suspended particles (eventually resuspended from the sediments) are injected from the margin into the open ocean and whether they affect the trace element chemistry of the open ocean. Two particulate phases were sampled using different techniques: (i) the SPM filtered by using in-situ pumps is supposed to consist of slowly sinking biogenic and terrestrial detritus exhibiting a large surface area for sorptive processes, (ii) the sediment representing the ultimate result of all water column processes and early diagenetic modifications near the sediment/water interface.

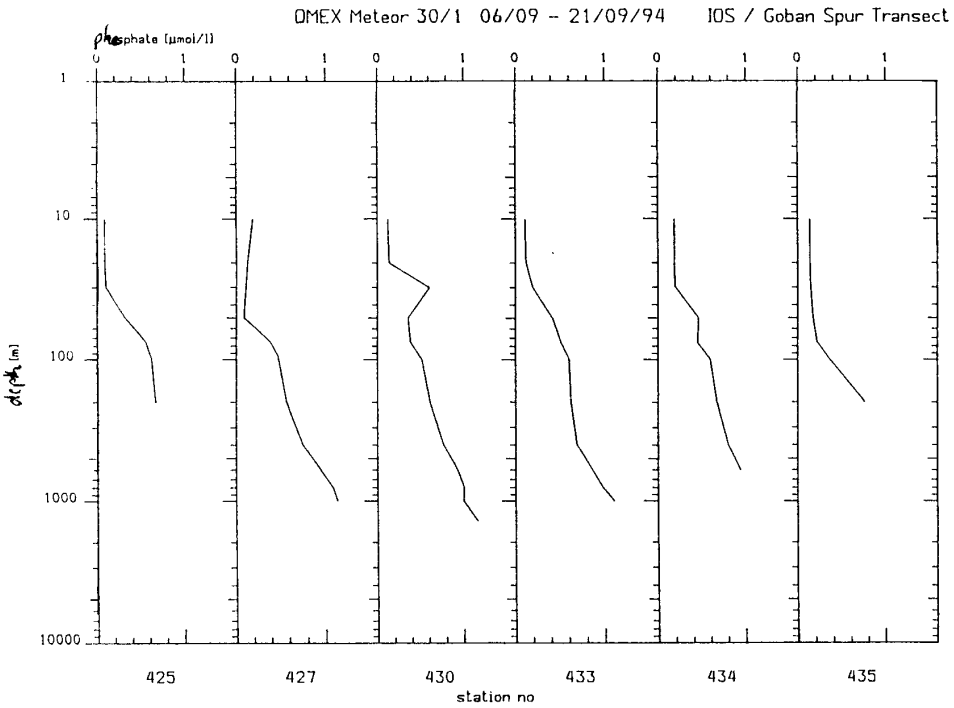

Fig. (3b) Phosphate profiles. Starting in the euphotic zone, similar strong gradients with increasing depths down to 1000 m characterized the profiles (0.1 - 1 mol/l). Again a peak (0.6 mol/l) occurred at 30 m depth at station 430.

Due to the low concentration of SPM below the mixed layer, large volumes of sea water were filtered for trace element determinations in SPM. Between 250L and 550L sea water were filtered through acid cleaned 293 mm Nuclepore filter using in-situ pumps. To reduce contamination risks a non-metallic wire was used and all handling of the filters was performed under a clean bench within a clean room container. Because in-situ pumping is very time-

consuming pumps were combined with bottle casts whenever possible. Due to limited ship time only 7 filters were obtained from the Goban Spur transect at depths between 50 m and 1450 m. Another 3 filters were disrupted during deployment. At all stations where in-situ-pumps were deployed and especially where sediment trap moorings were positioned, casts of GoFlo bottles were taken to analyse the vertical distribution of Al and eventually other trace metals in the water column. For the trace metal studies precautions had to be taken against the risks of contamination: before use the GoFlo bottles were acid cleaned thoroughly, at station the bottles were attached to a non-metallic wire, during handling on deck both opening ends were covered with plastic bags, all manipulations after sub-sampling were performed under a clean bench. During the cruise Al from 6 stations was measured on board using a fluorometric technique. The vertical and horizontal distribution will be compared with results from the particle analysis.

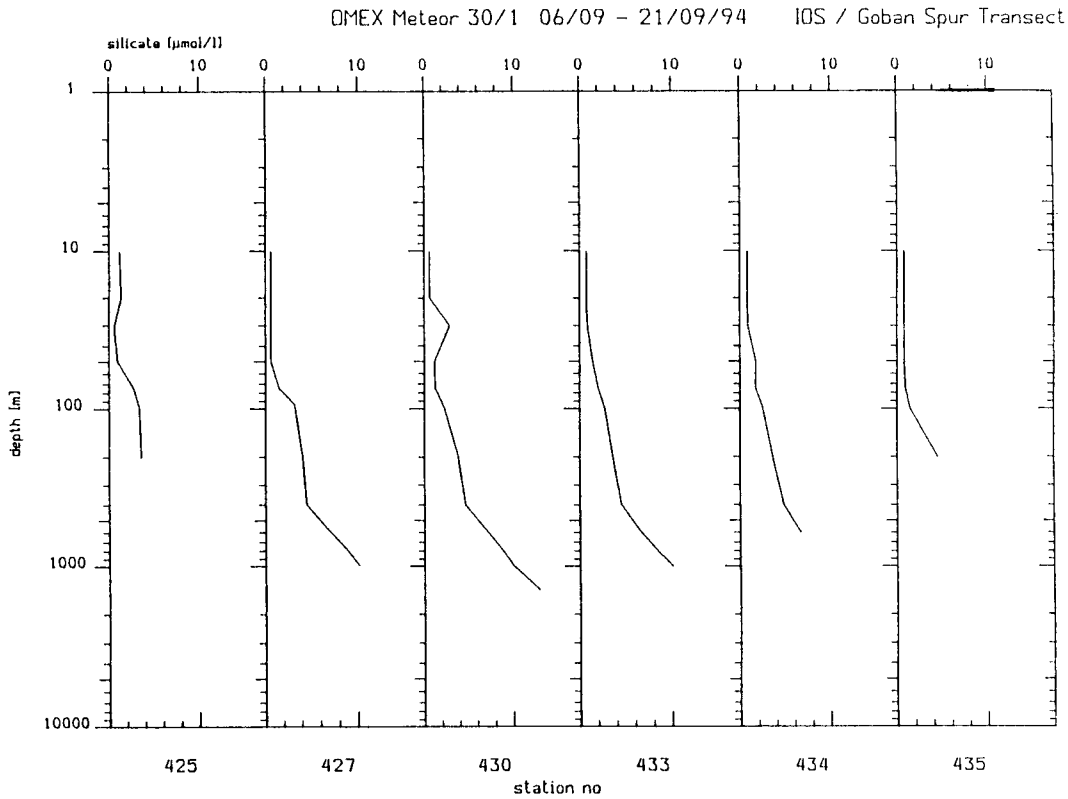

Fig. (3c) Silicate profiles. The silicate gradients in the euphotic zone started at 0.5 mol/l. In depths below 500 m the gradients were comparable to those of nitrate and phosphate. Again a small peak could be seen at 30 m depth at station 430.

Solid sediments and pore water samples for the determination of dissolved trace metals were taken at 7 stations along the Goban Spur transect (see below). On board ship the pore water samples were preserved after filtration and acidification; preconcentration and the separation from the salt matrix will be performed at the home laboratory.

- **Dissolved Organic Carbon**
  (UBMCh, S.Otto, W.Balzer)

In order to investigate dissolved organic carbon (DOC) in the water column across the continental margin, samples from seven CTD-rosettes or GoFlo casts were taken at the Goban Spur transect. At each position the whole water column was sampled. It is very critical in the determination of DOC to avoid contamination of the samples. Therefore, great care was taken from the first step of sampling throughout the whole work-up procedure: samples from the rosette were taken in pre-cleaned glass bottles, immediately filtered through pre-combusted GF/F filters and finally acidified and sealed in brown glass ampoules. All samples were stored at +4°C until analysis. The DOC determinations were performed by the High-Temperature-Catalytic-Oxidation (HTCO).

In addition to the investigation of DOC in the water column, sediments taken at 6 stations with a multi-corer were sampled to determine DOC in pore waters. After squeezing the sediment in a cold room, the pore water was analysed for DOC and for total inorganic carbon (TIC). While TIC at the deeper stations was always close to 2 mmol/L it was much higher at the shallow stations showing a maximum of 5.6 mmol/L. DOC in the pore water varied between 0.8 and 2.6 mmol/L, again having higher concentrations at the shallower stations.

- **Pore Water Chemistry**
  (UBMCh, W.Balzer, A.Deeken, H.Wellmann)

The OMEX-project was established to contribute towards the understanding of the cycling of nitrogen, carbon and trace metals at continental margins where benthic processes are expected to play a significant role for the chemistry of the whole ocean. Necessary for the understanding of the major controls over release fluxes from boundary sediments is a detailed investigation of early diagenetic processes acting within the sediments. It was therefore planned to conduct extensive work on pore water chemistry and on solid sediment phases at the Goban Spur transect across the Celtic margin. From the sediments taken at 7 stations (#425, #426, #427, #428, #430, #433, #434) by a multicorer, the pore water was squeezed or centrifuged under in-situ temperature conditions (cool room). Nitrate as the pore water constituent providing most information about the diagenetic milieu, showed systematic variations in the profiles over the transect. All nitrate pore water profile showed sub-oxic conditions typical for hemipelagic sediments of the North Atlantic ocean but there was also a significant contribution of sulphate reduction to organic matter degradation at the stations shallower than 1500 m. The rates of carbon combustion by oxygen and nitrate, respectively, were assessed by use of a model for steady-state diagenesis of organic matter. The rates for organic carbon degradation by oxygen decreased systematically with water depth with one exception: station #430 at 1500 m showed an extremely high rate which is consistent with benthic lander results obtained by Dutch colleagues.

- **Benthic Denitrification and Bioirrigation**
  (UBMCh, W.Balzer, A.Deeken, H.Wellmann)

For the estimation of denitrification rates two independent methods were applied: (i) the evaluation of the rate from the modelling of the pore water nitrate distribution, and (ii) the direct determination according to the "acetylene-block" incubation method. The pore water nitrate profiles can be used simultaneously to estimate integrated rates of denitrification, for the reaction being first order with respect to nitrate. Denitrification was detectable but weak in the depth range from 5300 m to 3665 m but became much more intensive when the shallower region (1500 m to 670 m) was approached.

The determination of denitrification rates by C_2H_2-block incubation comprises the following steps: (i) sub-sampling a box-corer with several acrylic glass tubes, (ii) injection of acetylene into the pore water of the whole sediment column of the sub-cores to block the further reduction of the intermittently formed N_2O to dinitrogen, (iii) sectioning of the sub-cores after appropriate incubation times, (iv) equilibration of the sediment sections with the gas phase in small closed jars after stopping the reactions with KOH, and (v) head-space analysis of the N_2O concentration in the gas phase by GC-ECD.

Only 4 sediment stations (#428, #430 (OMEX II), #433 and #434 (OMEX I)) were selected for this lengthy procedure. For each station 6 sub-cores were used: 2 sub-cores for an average N_2O-profile, 2 sub-cores for an average 1-day-incubation and 2 sub-cores for an average 2-day-incubation. There was no N_2O-production at station #428. The other 3 shallower stations showed intensive N_2O-production close to the surface with maximum rates at the depth range 2-4 cm in all cases. When comparing these rates with the denitrification rates obtained from pore water modelling two features deserve special attention: (i) considering the widely differing boundary conditions, assumptions, etc. of the two methods, the agreement within a factor of 3 is remarkable, (ii) there might be a difference in the process that is measured by the two methods: the pore water profile might correspond more to the long-term steady-state situation while the incubation might respond to seasonal effects more directly.

The N_2O profiles in the pore-water (without incubation; from which release rates were calculated) showed highest concentrations near the sediment surface in all cores investigated. N_2O release, however, is significant only in sediments of the upper continental margin again having a relative maximum at 1530 m as suggested by the relative heights of the rates obtained from incubation. The relative heights of the N_2O release rates can be estimated directly from a comparison of the profiles. The absolute rates can only be calculated when the modelling of the tracer incubation experiments for the calculation of bio-irrigation rates is finished - which is presently underway.

Especially in the shallower parts of the continental margin, the release fluxes from the sediment surface might be enhanced by the bio-irrigating action of (bioturbating) macrofauna organisms. To estimate the enhancement over molecular diffusion, tracer experiments were performed by applying a tracer in the overlying water and incubation of the sediment core at in-situ temperature. After 2-4 days the core was cut into slices and the tracer concentration was determined in the pore water. By numerical modelling (using a "quasi-diffusional"

coefficient) the transport of the tracer into the sediment column can be followed and the best-fitting coefficient can be evaluated.

5.1.2 Air Chemistry

- **Exchange of Reduced Sulphur Compounds Between Ocean and Atmosphere**
  (MPICh, G. Uher, O. Flöck, G. Schebeske, V.Ulshöfer)

The biogeochemical processes, which are controlling the production of carbonyl sulphide (COS) and dimethyl sulphide (DMS) in surface seawater as well as their emission to the atmosphere were the focus of the biogeochemical investigations by our group. These studies were accompanied by measurements of chlorophyll concentration, absorbance and fluorescence of dissolved organic matter on one hand, and of the atmospheric concentrations of condensation nuclei, black carbon, and radon (^{222}Rn) on the other hand. In the following sections some preliminary results are presented.

- *COS in surface seawater and atmosphere*
  *(*V. Ulshöfer)

COS is formed photochemically in surface seawater and is believed to be the main source of the stratospheric sulphate layer during periods of low volcanic activity. This sulphate layer affects the Earth's radiation balance as well as stratospheric ozone levels. Emission from the oceans is one of the main sources in the global budget of COS. In this budget, however, exists an imbalance between sources and sinks which partly may be due to large uncertainties in the quantification of single sources and sinks. For a better assessment of the oceanic source, we investigated the diurnal and seasonal cycle of COS in the Northeast Atlantic. Atmospheric and dissolved COS was determined using a semi-continuous seawater equilibration system with cryogenic preconcentration, gas chromatographic separation and flame photometric detection. Ambient air was drawn through a Teflon tube from the top of the ship's mast to the analytical system. Air was analysed directly and after equilibration with seawater (for the determination of dissolved COS in seawater). Water from approx. 7 m depth was supplied continuously to the equilibrator by a non-contaminating pumping system. This pumping system consisted of a Teflon membrane pump (all wetted parts polyvinylidene fluoride) and a polyvinyl chloride tube mounted inside a hollow stainless steel shaft which was submerged beneath the keel through the ship's "moon pool". The fully automated system allowed the hourly analysis of atmospheric and dissolved COS. The saturation ratio of COS in surface waters with respect to its atmospheric concentration was calculated:

$$SR = [COS]_{equilibrated\ air} / [COS]_{ambient\ air}$$

During the entire cruise leg dissolved COS was supersaturated in surface waters with respect to its ambient atmospheric concentration and a diurnal cycle with maxima in the afternoon and minima before sunrise was observed. The results from the former Meteor cruise legs M27/1 (January 1994, OMEX area) and M21/2 (April/May 1992, BIOTRANS area at 47°N, 20°W) are in contrast to these findings. The winter data (M 27/1) showed persistent undersaturation and no diurnal cycle of dissolved COS, probably due to low light intensity and hence low

photochemical production during daytime. The spring data from the BIOTRANS area (M 21/2) showed undersaturation as well as supersaturation and no net flux to the atmosphere could be found within the experimental uncertainty. The results from these three cruise legs cover three seasons (winter, spring, and summer) and show a pronounced seasonal variability of the sea surface COS concentration. This set of data will be used to estimate an annual cycle of dissolved COS in the Northeast Atlantic, based on meteorological and oceanographic data. Moreover a kinetic model for the diurnal cycle of dissolved COS will be applied that considers light dependent and light independent COS production, hydrolysis, and gas exchange across the air-sea interface. Consequences with respect to estimations of the global marine emissions of COS will be addressed.

- *Depth profiles of dissolved COS and photochemical incubation studies*
  (O. Flöck)

Depth profiles of dissolved COS were taken using non-contaminating, gas tight GoFlo water samplers. The water samples were pressure filtered (GF/F Whatman filters, preheated at 400 C for 2h), transferred into volume-calibrated glass flasks (approx. 300 ml) and stored in the dark at 4 C for not longer than 6 hours. Photochemical incubation studies were performed using surface seawater obtained from our non-contaminating seawater pumping system. The water was GF/F filtered, filled into glass flasks and exposed to sunlight for ca. 10 hours. The samples (including dark controls) were held at sea surface temperature during the irradiations. COS was determined by gas stripping of seawater, followed by cryogenic trapping, gas chromatographic separation, and flame photometric detection. All results were corrected for sample losses due to hydrolysis.

At ten stations the vertical distributions of dissolved COS were recorded. These data included high resolution profiles within the upper 100 m and profiles down to depths of 2000 m. Generally the vertical profiles showed maxima at the sea surface and an approximately exponential decay to a certain background level beneath the mixed layer (about 50 m during the cruise). Although the COS concentration in deeper waters was very low, some transport or non-photochemical production mechanisms are required to maintain this background level and compensate losses due to hydrolysis. In addition to the station work, time series of COS photoproduction were obtained from ten sunlight irradiations of surface seawater. These time series together with our continuously recorded UV-light intensities will enable us to determine COS photoproduction constants. Our complete data set which includes atmospheric mixing ratios, sea surface concentrations, depth profiles, and COS photoproduction constants, will be used to test one-dimensional transport models for the prediction of surface concentrations and global marine emissions of COS. We will be able to investigate the influence of downward mixing of dissolved COS out of the zone of photochemical formation on the sea surface concentration and hence on the sea-to-air flux of this climatically relevant trace gas.

- *Sea surface concentrations of dissolved DMS*
  (G. Uher)

DMS is formed mainly by the enzymatic cleavage of dimethylsulfonium propionate (DMS) which is a metabolic product of marine phytoplankton. Former work showed that the concentration of dissolved DMS is controlled by a complicated interplay of algal speciation and trophic interactions. Air-sea exchange processes result in the emission of dissolved DMS into the atmosphere where it is oxidized mostly to aerosol sulphate. These aerosol particles act as cloud condensation nuclei (CCN), and thereby influence the reflectivity and stability of clouds. Thus the Earth's radiation balance is sensitive to the CCN number concentration which in turn might be sensitive to changes in phytoplankton biomass. Global estimations of marine DMS emissions still suffer from the insufficient knowledge about its regional and seasonal distribution all over the oceans. The emission of DMS is largely controlled by its sea surface concentration and wind speed. During this cruise leg we performed measurements of sea surface DMS with high time resolution to improve our data base with respect to regional distribution, patchiness, and seasonality of DMS in surface waters.

DMS was determined using a semi-continuous seawater purge and trap system with cryogenic preconcentration, gas chromatographic separation and flame photometric detection. Seawater was sampled using our non-contaminating pumping system. The newly developed automated analytical system hourly sampled seawater which then was filtered (GF/F Whatman filters) and analyzed for dissolved DMS. The concentrations ranged from 1 nmol l-1 up to 12 nmol l-1 with an average of 2.8 nmol l-1 for the entire data set. During the transect from the Canary Islands to the Celtic Sea margin, the DMS concentrations increased slowly from 1.5 nmol l-1 to about 3 nmol l-1, but no pronounced gradient across the shelf edge could be observed. This is not surprising, however, since we could neither find any pronounced increase in chlorophyll (indicator of phytoplankton biomass) nor in absorbance or fluorescence of dissolved organic matter which were used to classify the water masses of the different biogeographic regions (e.g. coastal&shelf, open ocean). On the shelf region, dissolved DMS showed maxima up to 12 nmol l-1 which were associated with areas of high chlorophyll concentration. Our attempts to find consistent relationships between chlorophyll and dissolved organic matter on one hand and sea surface DMS on the other did not result in simple correlations. Nevertheless, we will continue in carefully looking for relations between DMS and chlorophyll within distinct oceanic regions to further investigate the possibility of using satellite imagery as a tool for extrapolating and predicting DMS concentrations.

Based on our time series of dissolved DMS we will estimate sea-to-air fluxes of DMS. These fluxes then will be compared to the number concentrations of condensation nuclei (CN, Aitken nuclei). Our black carbon and radon (^{222}Rn) data will help us to distinguish between marine and continental air masses. Hence we will be able to look for relationships between CN and the precursor compound DMS within the marine boundary layer.

- *Chlorophyll and dissolved organic matter in surface seawater*
  (G.Schebeske, V. Ulshöfer)

In addition to the defemination of sulphur compounds, chlorophyll along with absorbance and fluorescence of seawater was recorded. We intended to use chlorophyll as an indicator of phytoplankton biomass and furthermore absorbance and fluorescence of dissolved organic matter as tracers to determine the degree of mixing between different water masses as well as their optical and photochemical properties. Surface seawater from our non-contaminating pumping system was sampled approximately every 4 hours. The samples were stored in detergent washed polyethylene bottles at 4˚C in the dark, generally for not longer than 10 hours. 250 ml were filtered (GF/F Whatman filters, preheated at 400˚C for 2h). The filters were homogenised and extracted with acetone/water (90/10) at room temperature. Then the solution was filtered again to remove the glass fibres, filled up to a standard volume with acetone/water, and analyzed fluorometrically (Ex 425±20 nm, Em 665±20 nm) using a Shimadzu RF1501 spectrofluorometer equipped with a 10 mm quartz cell. The instrument was calibrated before and after the cruise using a solution of chlorophyll a (Sigma Chemie) in acetone/water.Both absorbance and fluorescence was measured on filtered seawater (GF/F Whatman filters, preheated at 400 C for 2h). The spectral absorbance was recorded from 250 nm to 700 nm using a Shimadzu UV160A spectrophotometer and 100 mm quartz cells. Milli-Q water was used as a reference. The absorbance data have been normalized to compensate for the instrument's drift by subtracting the reading at 690 to 700 nm. Fluorescence emission spectra., 325 nm, and 340 nm as excitation wavelengths and an emission wavelength scan in the range of excitation wavelength plus 15 nm up to 600 nm. The spectral response of Milli-Q water was subtracted and the fluorescence intensities then were expressed in quinine sulphate units (the maximum intensity of 1 mg l-1 quinine sulphate dihydrate in 0.105 M HClO4 at the excitation wavelength used was defined as 1 quinine sulphate unit). Preliminary results show absorption coefficients a(350 nm) lower than 0.1 m-1 for the transect from the Canary islands to the celtic sea margin and no significant increase across the shelf edge could be observed. (a(350 nm) here is defined as the decadic absorption coefficient and normalized to one meter optical pathlength. Thus Lambert Beer's law is written: A = a*l (A=absorbance, l=optical pathlength)). On the shelf area slightly higher absorption coefficients a(350 nm) of about 0.15 m-1 were found. The results from the fluorescence measurements in general showed the same trend.

(1) *Condensation nuclei (CN, Aitken nuclei), black carbon, and radon (^{222}Rn) within the marine boundary layer*
(G. Schebeske, V. Ulshöfer)

The atmospheric concentrations of condensation nuclei, black carbon, and radon were used as tracers to distinguish between marine and continental air masses. The sampling inlets for the continuous aerosol analysers (CN, black carbon, and ^{222}Rn) were located on a beam extending into the air flow just above the flying bridge (ca. 30 m above sea surface) where the ship's air chemistry laboratory is located. Tubing lengths between inlet and instruments were less than 5 m. For CN sampling electrically conductive tubing was used. The sampling inlet for black carbon was automatically interrupted by a Weathertronics sampler controller if the relative wind direction was more than 120 off the bow to avoid the sampling of stack

emissions. CN concentrations were determined with a TSI model 3020 condensation nucleus counter. Black carbon was measured with an aethalometer (Magee Scientific). Both CN and black carbon were recorded continuously and integrated over 5 min periods. ^{222}Rn was recorded continuously via the decay products ^{214}Po and ^{218}Po using an APIA monitor. The counts were integrated over 2 hour periods.

Acknowledgements

We thank Karl Pegler, Ralf Lendt, and Harald Rätzer for letting us use their stainless steel sampling inlet. Thanks are due to Alexander Pfeiffer and Ilse Büns for helping us with their pH-data.

5.1.3 Sedimentology

- **Particle Flux and *in situ* Marine Aggregate Studies at the Continental Margin**
  (IfMK, A.N. Antia, W. Erasmi; IOSDL, R.S.Lampitt; T. Kumbier; IOW, G. Lehnert)

- **Particle Flux**

Particle flux studies within the OMEX programme focus on addressing the transport of material on the shelf-slope regions of the Goban Spur, with an emphasis on exchange of material between these regions and the adjacent open ocean. The positions of moorings with sediment traps, current meters and transmissometers have been chosen to quantify both particle flux out of the euphotic zone and winter mixed layer as well as to determine mid-water transport at the slope edge on the Pendragon Escarpment, at which position particles from the continental margin may be expected to be exported to the adjoining abyssal basin and the transport of dissolved nutrients onto the slope would take place. During METEOR 30/1 these moorings were successfully recovered and re-deployed and yielded a near-complete set of sediment trap samples and current meter data for the previous 9 months of deployment (Jan - Sept 1994). For the deployment period July 1993 - Jan 1994 (autumn/winter), currents at the position OMEX 2 were seen to flow along the bottom contours in a northerly direction, i.e. along - slope, whereas at the Pedragon Escarpment off -slope water transport was registered, accompanied by an increase in particle concentrations in the sediment traps at intermediate depths as compared to that directly beneath the winter mixed layer. The data obtained during M 30/1 show a different picture for the spring and summer. Fig. 4 (a - e) shows current meter data from the moorings OMEX 2 and OMEX 3 at the different depths. Data are presented as 24-hour running means to smooth out tidal oscillations which are present in all data, though with decreasing amplitude with increasing distance from the shelf. At OMEX 2 a change in current direction from predominantly northwest-flowing (~300° magn.) to south-easterly currents during March and again during May is apparent. Mean current speed decreases from 11.75 cm/sec at 620 m to 9.41 cm/sec at 1070 m over the 9-month deployment. Although few data of this kind exist for the Goban Spur, such a reversal of shelf currents during the summer months has been documented by Pingree & LeCann (1989) in an adjacent region. This reversal in current direction has implications on the source area of particulate material intercepted in the sediment traps. Southwesterly currents would carry material from the region of the shelf break, characterised by high chlorophyll concentrations, to the trap positions. Another feature that is

evident from the data is the occurrence of warmer water during the winter months, as has been found in the Bay of Biscay region (Pingree & LeCann 1990). A transmissometer mounted on the vane of the current meter at 1070 water depth at OMEX 2 (data uncalibrated; jump at day 120 due to readjustment), show short events of increased water turbulence; the correlation of such variations in the suspended pool with particulate sedimentation is, however, tenuous at best. Results of sediment trap sample analyses will be available in the coming year; a *rough* idea of seasonality in bulk flux can be seen, however, from Fig. 5 (a and b); clear here is the increase in sedimentation during late April following spring phytoplankton growth.

At the OMEX 3 site on the Pedragon Escarpment, current direction fluctuates frequently during spring and summer. Residual currents flow eastward at 580 m, and south-westwards at 1450 and 3280 m during this deployment period. Average current speeds during this deployment period again decrease with depth, from 10.4 cm/sec at 580 m to 6.8 cm/sec and 4.4 cm/sec at 1450 and 3280 m respectively. However at all depths events of on - slope water flow are seen, providing valuable information on the cross-slope exchange of nutrients to the productive shelf and slope regions. The general impression of bulk sedimentation at OMEX 3 shows a marked increase in sedimentation with depth in the lower two traps (Fig. 5 c, d), as was seen at this site during the prior period of deployment (July 1993 - Jan 1994). The qualitative nature of this material, which we take as evidence of export of slope material to the abyssal plain, will be better described upon analyses of trap samples. Of particular interest in the context of OMEX is determination of the fate of this material leaving the slope environment and its deposition in the Porcupine Abyssal Plain, where conditions for the subsequent long-term burial of organic matter differ from those of the benthos in the slope and shelf environments. To be able to better elucidate and quantify this export of slope material to the deep sea bed, an additional mooring was deployed in 4485 m water depth off the Pedragon Escarpment in co-operation with colleagues at NIOZ (Texel, The Netherlands) (Mooring OMEX 4, 48°59.51'N; 13°44.06'W). This mooring contains a single sediment trap (at 4015 m depth) and current meter (at 3995 m), which, on the basis of previous data available from this site, are above the region of near-bottom resuspension.

Table 5.1.1 : OMEX Sediment trap moorings currently in deployment.

Mooring	Latitude	Longitude	Water Depth	Depth (m)	Instrument
OMEX 2	49°11.20'N	12°49.18'W	1445 m	595	Sed. trap
				618	RCM
				1052	Sed. trap
				1076	RCM+Trans.
OMEX 3	49°05.00'N	13°25.80'W	3650 m	556	Sed. trap
				580	RCM
				1465	Sed. trap
				1489	RCM+Trans
				3260	Sed. trap
				3284	RCM+Trans
OMEX 4	48°59.51'N	13°44.06'W	4485 m	4015	Sed. trap
				3995	RCM+Trans

A list of OMEX moorings presently in deployment is given in Table 5.1.1. These moorings will be recovered and redeployed from board the RSS DISCOVERY in September 1995.

The OMEX sediment trap mooring line naturally extends onto the Porcupine Abyssal Plain. Sediment traps have been deployed by the Institute of Oceanographic Sciences (UK.) at "Station H" (40°N, 16.5°W) since April 1992 with a view to determining long-term trends in particle flux at an oceanic site removed from the influence of the continental shelf and slope. Traps have in general been at depths of 100, 3400 and 4500 m above bottom (water depth 4600 m) with an array of current meters and camera systems to examine temporal trends in marine snow concentration. The latest deployment had been from RSS DARWIN in April 1994. During METEOR 30/1 this was recovered, refurbished and redeployed within 11 hours. From the recovered traps, apart from one on which the mechanism failed halfway through its cycle, all functioned well and have provided a good collection of samples. These will be analysed in a variety of ways to give information about the composition of the material, and the flux of organic carbon, nitrogen, pigments, radionuclides and various organic markers.

- **Marine Snow Studies**

Marine snow is loosely defined as inanimate particles of diameter greater than 0.5 mm. They are thought to be the principal vehicles by which material sinks through the water column. Such studies therefore are of considerable importance in developing our understanding of material flux. The distribution of these fragile particles is best determined using photographic techniques such as the Marine Snow Profiler. This instrument is attached to the CTD and photographs about 40 l of water every 15 seconds using orthogonal illumination from a deep-sea flash light. Up to 400 frames can be taken.

During Meteor M30/1 seven deployments of the MSP were successfully made and the resulting images will be examined on an image analyser to determine the abundance, size and volume concentration of these particles.

In order to make further studies on marine snow particles they must be collected. This was achieved during Meteor 30/1 using the specially designed marine snow catcher or "Snatcher". This is a messenger operated 100 l closing water bottle designed to minimise damage to the marine snow particles. After standing on deck for at least 2 hours, the upper 95 l is drained off and the lower portion of the Snatcher disconnected along with 5 l of water. The particles can then be recovered from the base plate using a pipette. During this cruise, after some initial compatibility problems, the Snatchers were successfully deployed on two occasions to depths of 30 and 50 m.

Table 5.1.2: MSP Deployments:

Depl. #	Sta #	Date	Time(h)	Cast depth (m)	Water depth(m)	Long.°N	Lat. °W
89	427	14.09.94	18:55	500	3668	49.09	13.41
88	428	15.09.94	00:02	500	3668	49.15	13.09
87	429	15.09.94	18:03	500	3643	49.08	13.41
86	430	16.09.94	02:31	500	1524	49.18	12.85
85	433	16.09.94	23:31	500	1148	49.24	12.50
84	434	17.09.94	06:59	500	672	49.42	11.54
89	435	17.09.94	13:55	200	211	49.47	11.15

- **CTD - work**

CTD profiles, with registrations of conductivity, temperature, pressure, fluorescence and oxygen, were taken at a number of stations along the transect followed during M 30/1. Unfortunately, malfunction of the release mechanism of the rosette prevented water samples being taken during these deployments. CTD drops were thus mainly confined to the upper 500 m of the water column where a marine snow profiler, attached to the CTD frame, registered snow concentrations with a fine vertical resolution.

5.1.4 Benthic Biology

- **Benthic Microbiology**
  (IfMK, K. Poremba, K. Jeskulke)

Microbiological investigations involved the determination of abundance and activity of bacteria in the sediment. Sediment samples were taken with a multicorer. The samples were immediately transferred into a cooled laboratory avoiding artefacts due to temperature shifts of the samples.

The measurements included the fixation of subsamples with formaldehyde and later counting of bacterial cells (in the home laboratory), and the measurement of extracellular hydrolytic activity using 5 different fluorogenic analog substrates for protease, esterase, chitinase, and beta-glucosidase. Esterase activity represents a value of overall microbial activity, while the other enzyme rates enables the detection of different types of microbial degraders.

Several stations of a transect over the continental shelf margin of Goban Spur were visited during leg M 30/1. The sampling was focused on sites deeper than 2000m, because extensive sampling between 200 and 2000 m had already been made on a former cruise with RV VALDIVA in July 1993 (VA 137). The experiments conducted on VA 137 had shown that the activity of hydrolytic enzymes in sediment decline with water depth. Cleavage rates of relatively easy degradable substances declined faster than degradation rates of more refractory molecules, which gave evidence for a close relationship between biological activity and quality of organic matter at the sea floor, and supported the theory of pelagic-benthic coupling in the sea. The measurements of M30/1 should elongate the transect of the previous measurements, because the sampling season of VA 137 and M30/1 was similar, so that only small seasonal impact could be expected.

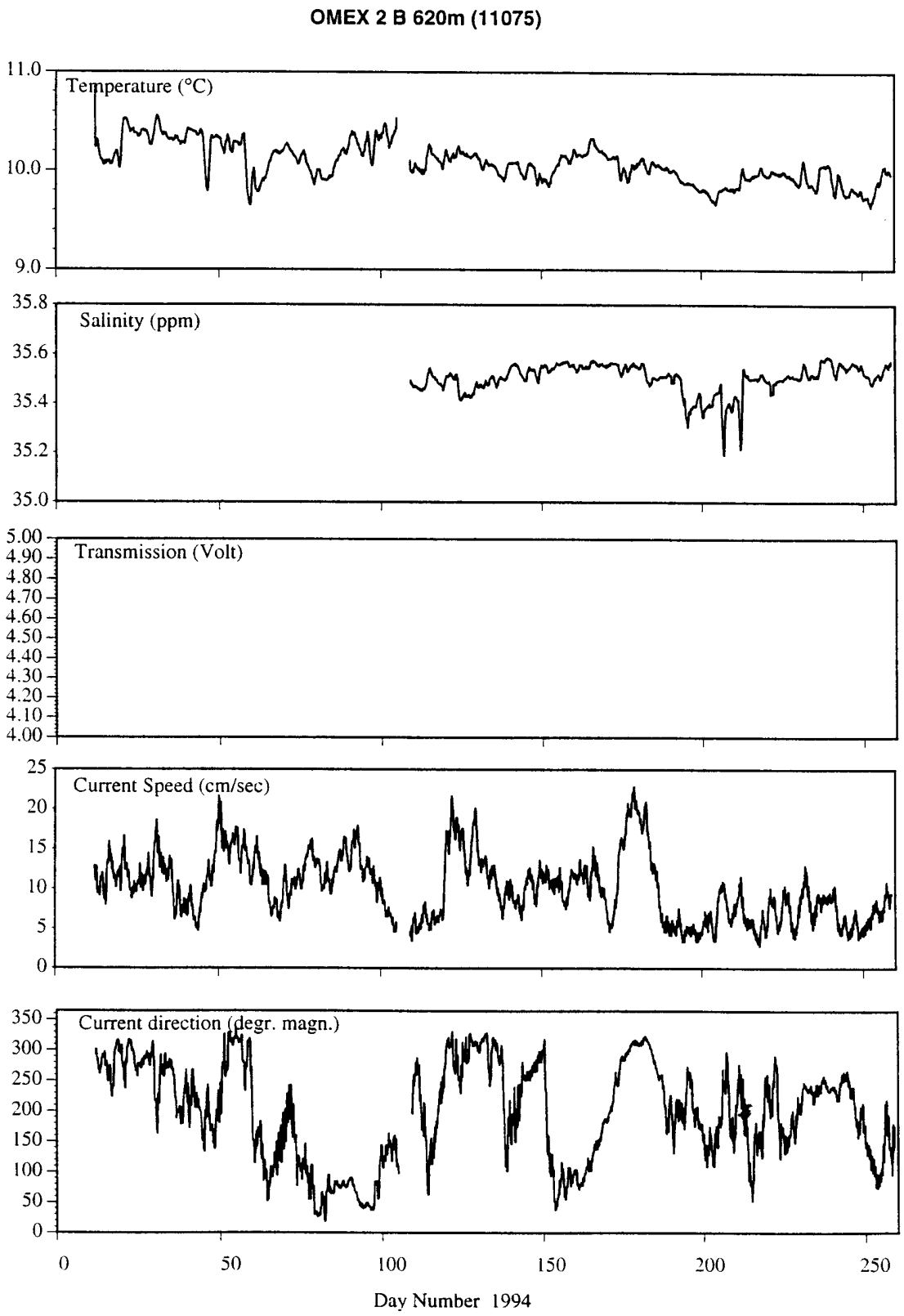

Fig. (4a) 24-hour running means of current meter data from OMEX 2 at 620 m from Jan - Sept 1994 (Day Nos. 11 - 260).

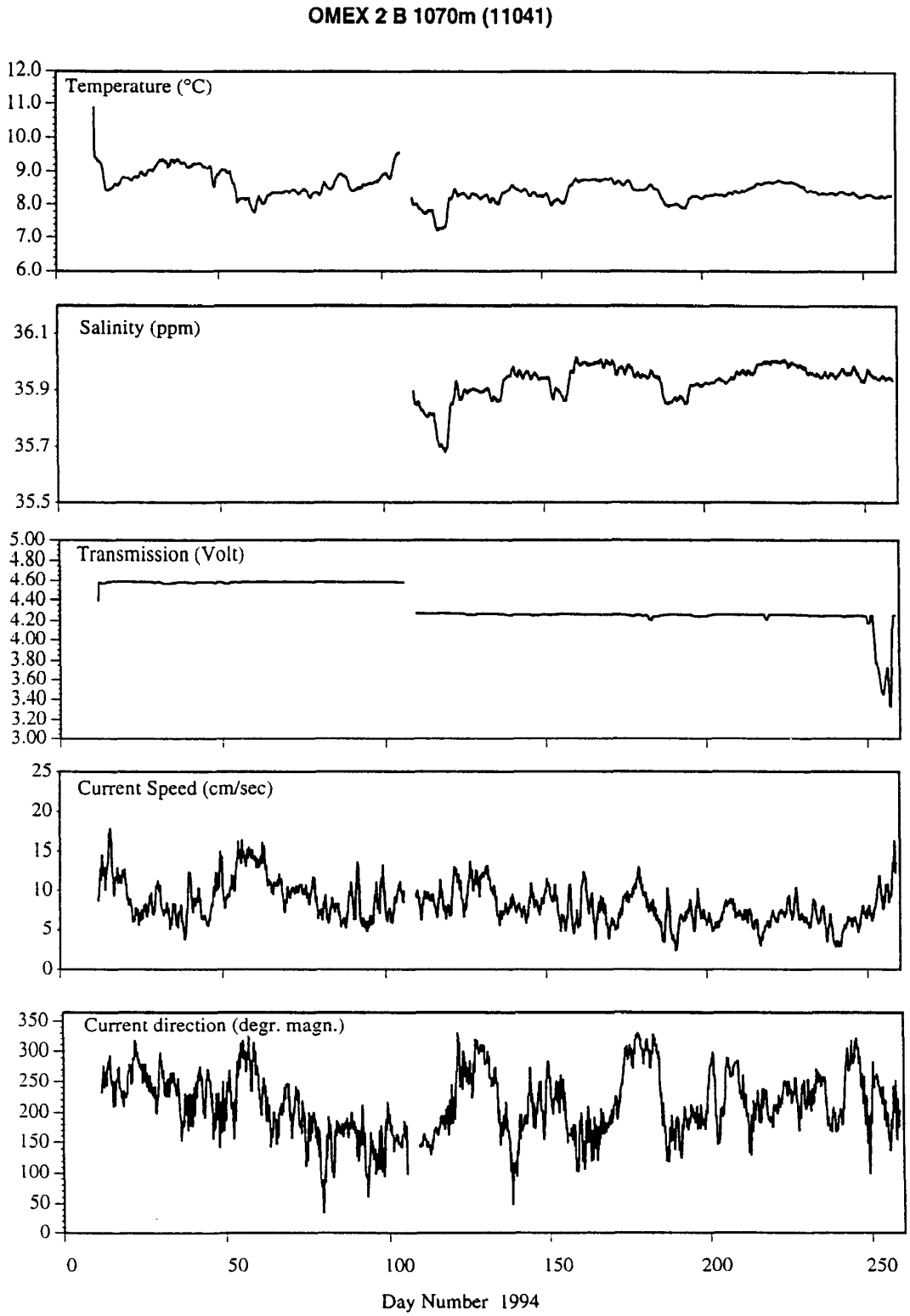

Fig. (4b) 24-hour running means of current meter data from OMEX 2 at 1070 m from Jan - Sept 1994 (Day Nos. 11 - 260). Jump in transmissometer data at day 108 is due to readjustment; transmissometer data are uncalibrated.

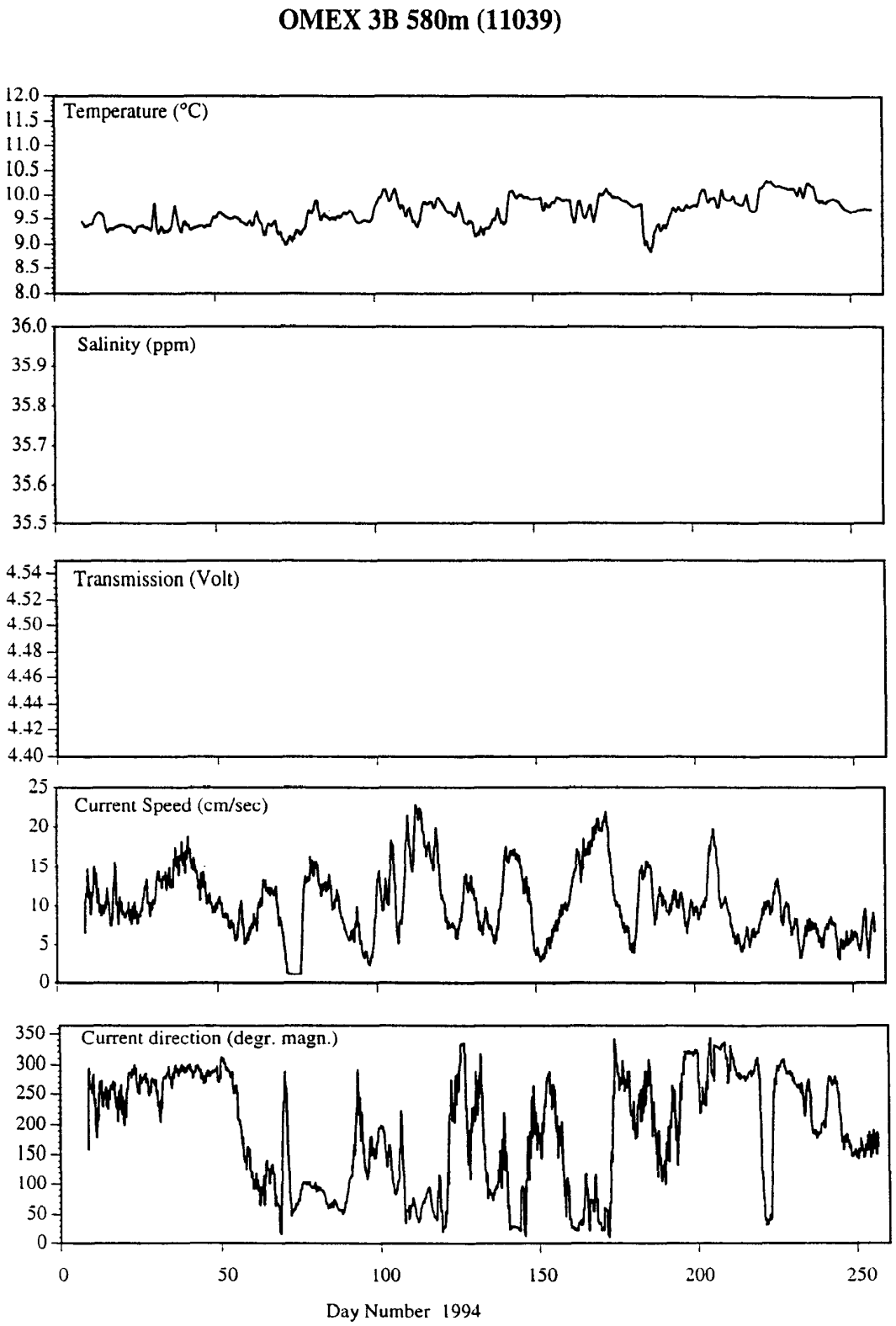

Fig. (4c) 24-hour running means of current meter data from OMEX 3 at 580 m from Jan - Sept 1994 (Day Nos. 11 - 260).

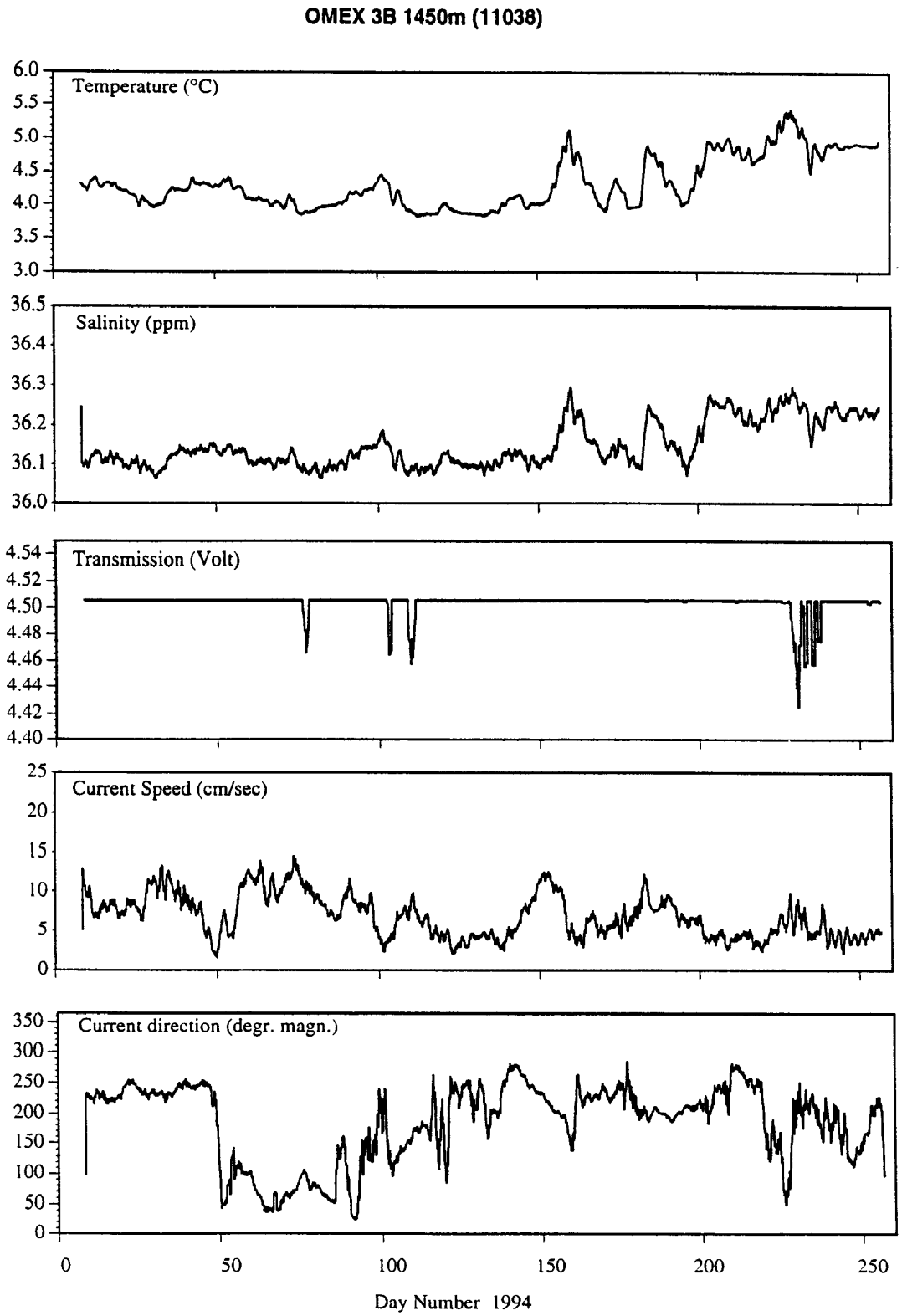

Fig. (4d) 24-hour running means of current meter data from OMEX 3 at 1450 m from Jan - Sept 1994 (Day Nos. 11 - 260). Transmissometer data (uncalibrated) are off scale at 4.505 Volt.

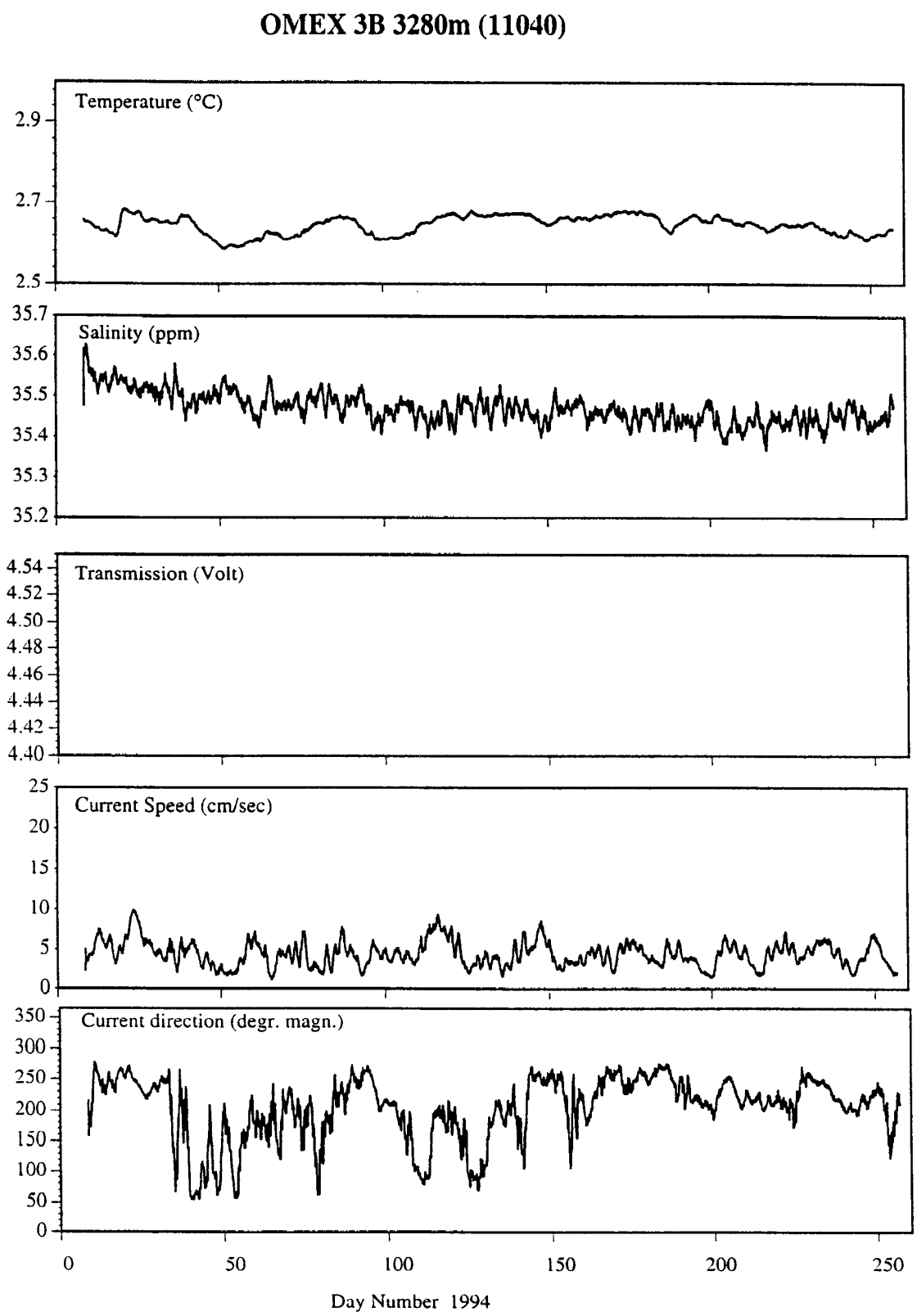

Fig. (4e) 24-hour running means of current meter data from OMEX 3 at 3280 m from Jan - Sept 1994 (Day Nos. 11 - 260).

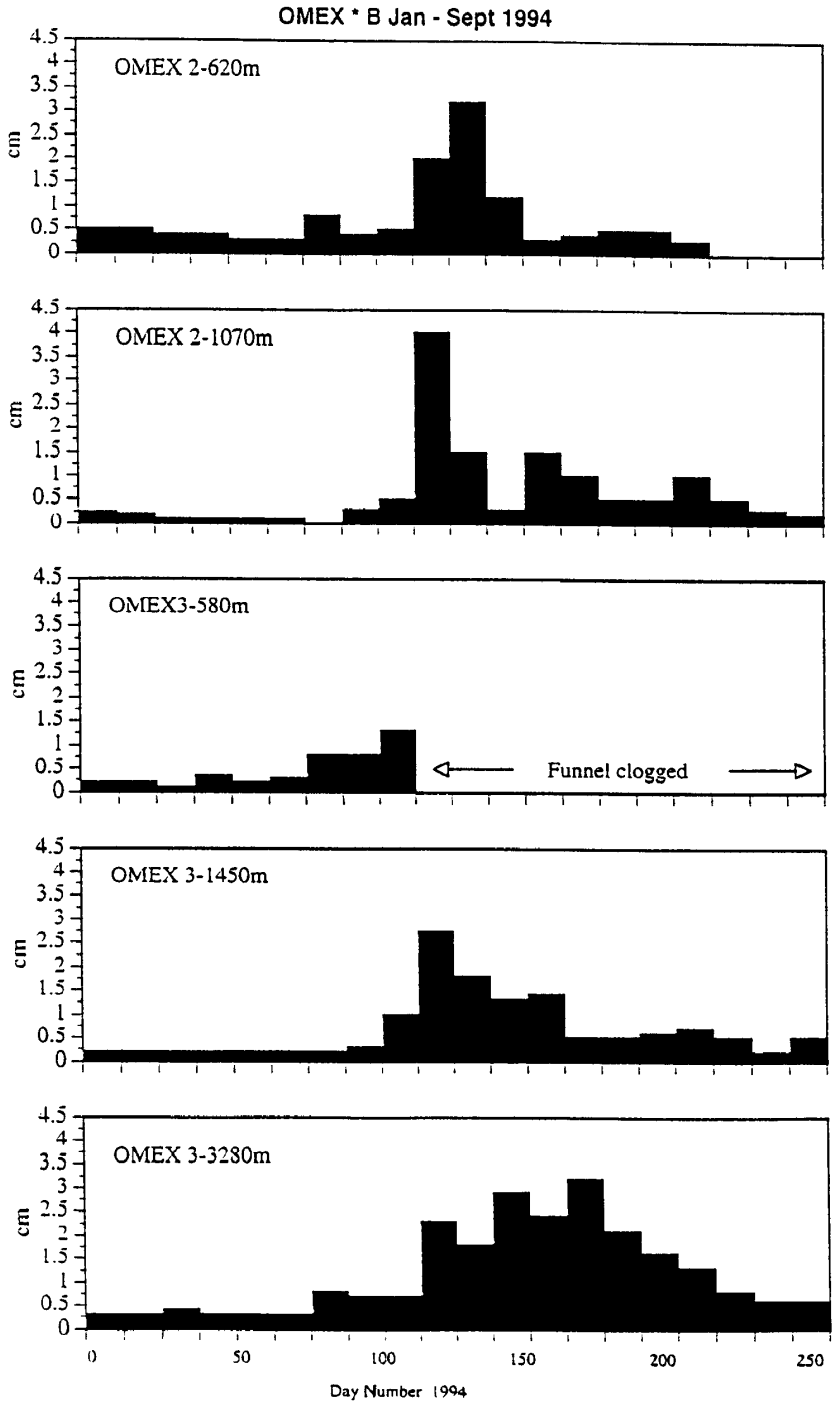

Fig. (5) A rough estimate of seasonality in sedimentation of the mooring OMEX 3 between January and September 1994 (x-axis, day numbers 11 - 260) as shown from the height of particle accumulation (y-axis, cm) in the sediment trap cups. Although these data are in no way quantitative, it is clear that a pulse of sedimentation following the spring bloom occurs in late April. Also conspicuous is the increase in bulk and duration of sedimentation in the deeper traps.

The weather conditions during the cruise were relatively good, so 4 sediment sampling at depths of 4805 m (the IOS-station in the Porcupine Sea Bight), 4471 m (close to the basis of Goban Spur), 2269 m and 1535 m (slope of Goban Spur) were possible. Generally, the found activity rates accorded to the range, which could be expected from our former measurements on VA 137. The rates were lower than on more shallow situated sampling sites (a detailed comparison of data is not possible in the moment, because the value are not exactly corrected on volume basis). Unusual high activity of protease and esterase (higher than at 1535 m) were found at 4471 m, which indicates that the basis of the continental margin acts as an accumulation zone for organic matter. Counting of bacterial abundance and must be performed later in the home laboratory.

- **Carbon Mineralization by the Benthic Community**
  (IHF, T. Soltwedel, Geomar, O. Pfannkuche)

Recent results from the temperate northeast Atlantic exhibited a strong seasonality in phytoplankton production and subsequently a varying supply of phyto-detritus to the benthos (Pfannkuche, 1993). Thus, benthic activity and biomass is subject to spatial and seasonal variations in response to the sedimentation of particulate organic matter. RV METEOR' cruise 30, leg 1 was part of a series of expeditions to survey the reaction of the benthic community to episodic (seasonal) food pulses and to assess the role of the benthic organisms for the carbon flux through the sediment.

Benthic sampling was carried out along a depth transect across the Goban Spur continental margin from the outer Celtic Sea to the adjacent deep-sea basin, the Porcupine Abyssal Plain (Fig. 1). A total of eight stations with water depths ranging from 200 m to 4800 m were sampled with a modified SMBA style multiple corer (MC).

To estimate the input of phytodetritus to the benthic community, we analysed chlorophyll/pheophytin concentrations within the sediments. Changes in activity and biomass of the benthic infauna was assessed by measuring a series of biochemical assays:

activity parameters:
- esterases with fluorescein-di-acetat, FDA
- adenosintriphosphate, ATP

biomass parameters:
- total adenylates, ATP+ADP+AMP
- desoxyribonucleinacid, DNA
- phospholipids
- particulate proteins

Additionally, samples were taken for grain size analyses and to determine the sediment water content (porosity). Our investigations restrict to the upper 10 cm of the sediments.

First results (Fig. 6) demonstrated the close relationship between food supply and benthic activity. Concentrations of sediment-bound chloroplastic pigments (indicating primary organic matter) and enzymatic activity (fluorescein-di-acetat turnover, FDA) showed a fairly similar pattern along the Goban Spur transect, with increasing values on the upper slope (1150 m, MC 31) and on the Pendragon Escarpment (3666 m, MC 27). So far, no explanation could be given for the unexpected high FDA values in 4500 m water depth (MC 26) while CPE values were lowest on that particular station. Results from other biochemical analyses might probably help to explain this discrepancy.

To assess the carbon flux through the sediment, measurements of *in situ* community respiration rates were planned using a new benthic lander system. Unfortunately the central command unit of the benthic chamber could not be activated caused by a leakage of the pressure cylinder. For time reasons a second mooring of the system was not possible.

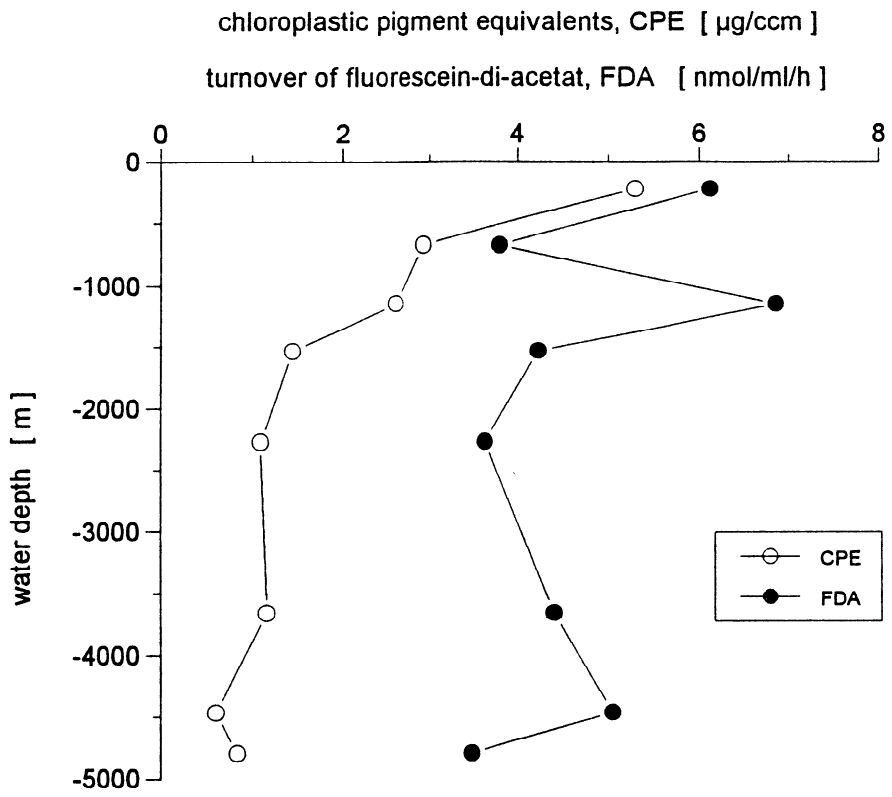

Fig. (6) Chloroplastic pigments and heterotrophic activity within the uppermost centimetre of the sediments

5.2 WOCE Programmes:

5.2.1 Physical and Chemical Oceanography on Leg M30/2

Operational Details
(BSH, K.P. Koltermann, K.C. Soetje, IORAS, V. Terechtchenkov)

Following the WOCE Hydrographic Programme requirements, the section WHP-A2 along nominally 48° has been worked as part of the One-Time Survey. In addition to the classical hydrographic parameters, nutrients, small and large volume tracer concentrations have been determined. Continuous ADCP (Acoustic Doppler Current Profiler) data provide the absolute vertical current shear of the top 500 m to calculate, from geostrophic transports, the absolute transport through this section. With a horizontal station spacing between 5 and 30 nm, a 24 x 10 l - rosette system was deployed to collect at up to 36 discreet depth levels water samples together with the quasi-continuous profiles of T, P, S and O_2 with a CTDO_2-probe. The track and station spacing essentially follows the Gauss section from 1993, covering, due to bad weather, 53 stations. Additional stations for performance tests of the CTD/rosette system, calibrations and for the instruments for the chemical analyses have been worked weekly. A distribution of the water samples along the section WHP-A2 is given in Fig. (7a).

CTD-Rosette Equipment and Procedures
(BSH, K.P. Koltermann, P. Wöckel)

The first few stations had to be used to find the most reliable and appropriate combination of CTD, rosette pylon and trip electronics and GO-bottle set. Problems were encountered with a rosette underwater unit that did not release properly and safely at pressures higher than 2600 dbar. To economize on ship time and allow for the time required to draw water samples properly from the shallow and deep rosette, a sequence of rosette deployments was tested where the first rosette/CTD was run deep, followed if required by the LVS casts. This was followed by a shallow rosette/CTD to provide close sample spacing in the top 1500 m. First, this second rosette was then deployed on the first, that is deep cast of the following station to avoid changing the rosette and CTD connections to the wire. This was abandoned rather early in the cruise in order to run all deep casts with the best CTD/rosette combination available, and deploy the shallow cast with the priority for water samples and ensuing trip CTD data only. This sequence has provided a much more secure calibration procedure and calibration data set for the full-depth CTD data, as in essence it will not be necessary to match data from two different CTD units for this section.

For the deep casts the CTD Neil Brown MkIII, labelled DHI1, was used on pylon no.7 with 24 x 10 l GO bottles uniquely marked. The shallow cast was run with the Neill Brown MkIII, labelled NB3 of IfM Kiel, with the Kiel pylon and 24 x 10 l GO-bottles. All bottles were equipped with stainless steel springs with grease-free O-rings to avoid contamination for CFC-sampling. The station routine was maintained throughout the cruise. Only few mistrips occurred and were accommodated for by standard oceanographic procedures.

In heavy weather and seas, particularly at the end of the cruise, on a few stations heavy wire wear was observed ca. 20 - 50 m above the rosette. This was seen as a result of the rosette package starting to kite. Extra weight was added to the package and the lowering speed decreased slightly to 1 m/s. No more problems occurred afterwards.

The acquisition software showed some mysterious problems at the beginning of the cruise where the acquisition at depth stopped and the system could not be restarted again. A simple software problem was solved after being identified.

More details of the sampling procedures are given in 5.2.3. The CTD- calibration coefficients for the M30/2 leg are essentially identical to those for M30/3. Both data sets have been processed similarly. Bottle data files for both leg are, again, processed according to the WHP guide-lines and with consistent meta-data file documentation.

The statistics of water bottle samples for the four calibration stations worked during M30/2 are given in Tab. 5.2.1.1.

BIO sample coding
(BSH, K.P. Koltermann)

On this cruise we used for both WOCE legs a sample labelling system introduced by the Bedford Institute of Oceanography, Canada. A uniquely numbered label is assigned to each water sampler at the rosette on each individual cast. The same number is assigned also to all subsamples of this particular sample bottle. Records of all groups analysing water samples maintain this unique number within their procedures until the hydrocast file is collated and merged with the trip data from the CTD of that cast. The uniquely identified sample can be traced back to the particular container/bottle of the cast it originates from. If mistrips have to be accommodated later, or sampling trip depths change due to recalibration of the pressure sensor, the sample is still tied to that volume of water/rosette bottle it was sampled from. Sampling depth was thus removed from being a sample identifier, and would later on be substituted as a parameter of the sample.

Almost all groups had not been familiar with this procedure prior to the cruise. They happily adopted it after only the first station. The CTD watch was particularly pleased with it as they were relieved of frequent curious questions as to what sampling depth the sample was supposed to come from.

Table 5.2.1.1 Precision of duplicate samples (i.e. from different rosette bottles fired at the same nominal depth) of calibration stations on WHP-A2.

	Stat. # 43601	**Stat. # 43603**	**Stat. # 45301**	**Stat. # 47601**
Duplicates:	N = 7	N = 24	N = 24	N = 24
Parameter	mean ± sdv	mean ± sdv	mean ± sdv	mean ± sdv
Pctd/db	3237.96 +1.52	3201.46 ± 0.27	4304.18 ± 2.1	3301.73 ± 0.87
(Pdsrt)	none	none	none	3304.25 ± 2.96
p/db				- 2.52
Tctd/mK	2.7192 ± .000	42.7410 ± .0019	2.5769 ± .0003	2.5766 ± 0.0005
(Tdsrt)	none	none	none	2.5807 ± 0.0044
ΔT				.0041
Sctd	34.9335 ± .0005	34.9284 ± .0004	34.9049 ± .0004	34.9200 ± 0.0003
Sali	34.9318 ± .0003	34.9332 ± .0008	34.9120 ± .0004	34.9185 ± 0.0004
ΔS	- .0017	.0048	.0071	-.0015
Oxygen (µmol/l)	251.99 ± .942	251.90 ± .694	249.87 ± .591	284.27 ± .472
Nitrate (µmol/l)	22.001 ± .083	none	22.507 ± .0079	16.992 ± 0.045
Phosphate (µmol/l)	1.561 ± .011	none	1.581 ± .0026	1.159 ± 0.014
Silicate (µmol/l)	36.324 ± .159	none	41.709 ± .314	19.541 ± 0.133

Thermosalinograph
(BSH, M. Stolley; IORAS, V. Terechtchenkov)

An Ocean Sensors OS200 thermosalinograph was mounted to the ship´s laboratory sea water pumping system. The data together with position and additional temperature data were logged at 1' intervals. Except for a few periods in heavy weather where air was caught in the system, the data are of good quality. Salinity samples were taken on each watch; the stability of the conductivity sensors and their statistics are promising.

ADCP
(BSH, M.Stolley)

The shipboard ADCP system with a RD unit was run throughout the cruise. Serious data quality problems occurred during heavy weather because of air being trapped under the ship. Data were recorded at 6 min intervals, a total of 6145 profiles down to 500 m depth was archived. From Oct 22 through 27 and between 21°W and 30°W computer problems impeded the data quality. During a gale on Oct 19, 1994 one transducer of the ADCP seems to have been damaged resulting in a reduced signal to noise ratio. The data from a new Ashtech 3D GPS system could not be successfully merged with the ADCP data stream. For the leg M30/3 new software was available only in St John's. For M30/2 the normal shipboard GPS data were logged with the ADCP data stream. All data are being processed at the level previously developed for M18.

- **Determination of the meridional transports of heat, salt and freshwater at 48°N in the North Atlantic along the WHP section A2**
  (BSH, K.P. Koltermann, A. Sy; IORAS, V. Terechtchenkov)

Preliminary results

The 48°N section was sampled for the fourth time since 1957. It was an exact repeat of the 1993 sampling with RV Gauss. By now we have a very clear picture of the main hydrographic features and spatial scales on this section, such as the deep boundary current regimes on both sides of the Mid-Atlantic Ridge (MAR), the spatial scales of the westward propagating Mediterranean Outflow and the eastward propagation of the Labrador Sea Water (Fig. 7 b-e).

The cooling of the LSW and deepening of the LSW core layer that was previously seen during 1993 (Koltermann and Sy, 1994) has continued during the autumn of 1994. But it now is seen more prominently also in the Eastern Basin of the North Atlantic. The LSW core temperatures had changed in 1993 since the 1982 occupation of this section by CCS Hudson by -0.45°C. The core layer had deepened in that same period by 641 dbar. From summer 1993 to autumn 1994 the temperature west of the MAR had cooled by another 0.057°C and deepened further by 27 dbar. From 1982 to 1993 the LSW core temperature east of the MAR at ca. 27°W had decreased by -0.154°C; in just over one year from 1993 to 1994 it cooled by another 0.096°C, deepening by ca. 152 dbar. Salinity changes in the Western Basin are small, order 0.001, compared to the temperature changes. The effect on the density is ca.0.045 kg/m^3 in the Western and 0.005 kg/m^3 in the Eastern Basin manifested in the increase in depth (Fig. 8 a-d). All this clearly shows how the LSW formed in the Labrador Sea in larger quantities since the late 1980s (Lazier, 1995) now invades the Eastern Basin (see also 5.2.3).

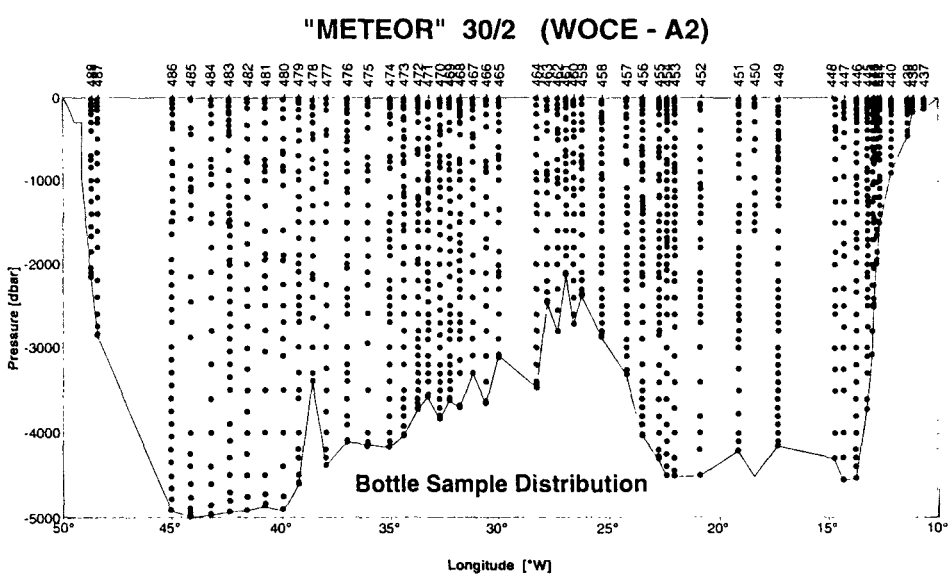

Fig. (7a) Distribution of water samples along section WHP-A2

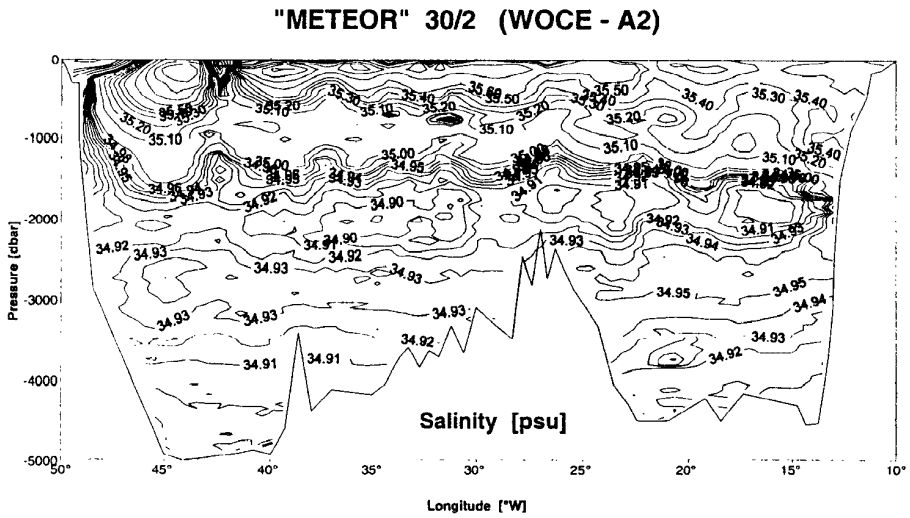

Fig. (7b) Salinity distribution from bottle samples along WHP-A2

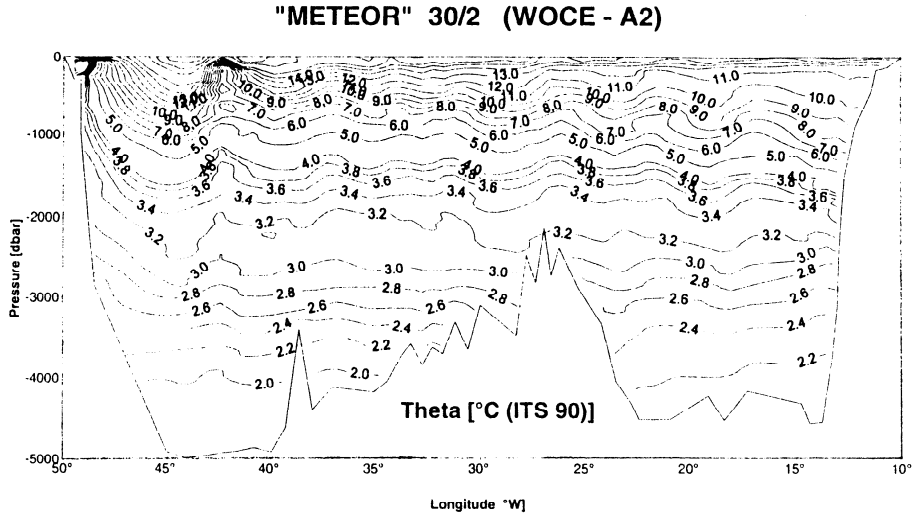

Fig. (7c) Potential temperature along WHP-A2

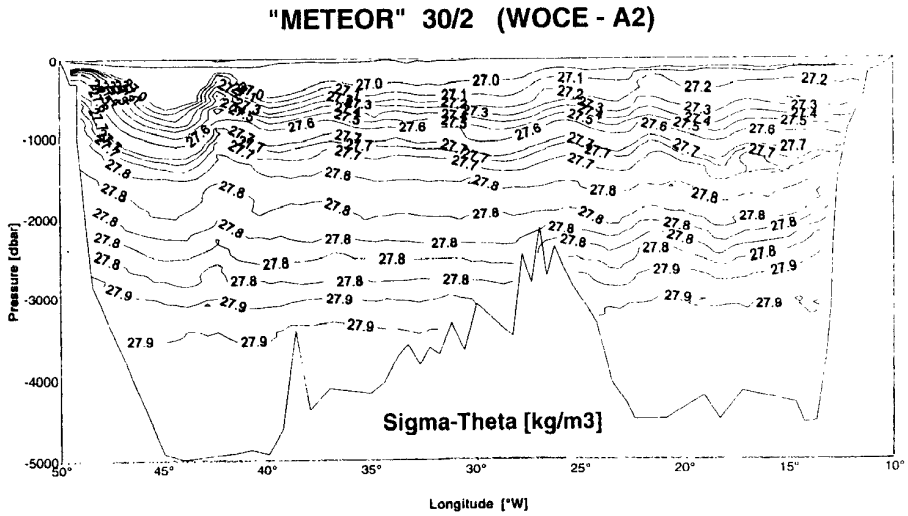

Fig. (7d) Density σ_θ distribution along WHP-A2

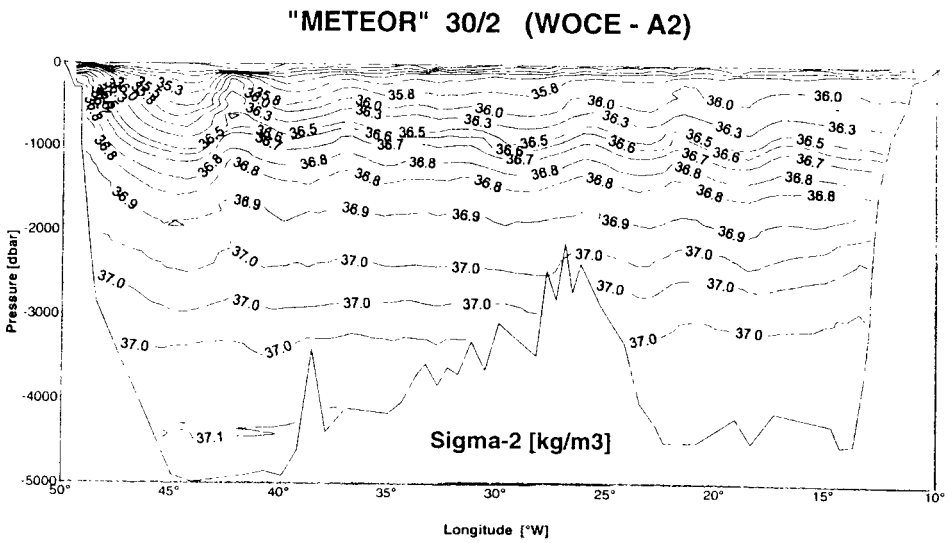

Fig. (7e) Density σ_2 (reference 2000 dbar) distribution along section WHP-A2

A feature not observed in that prominence on earlier cruises along A2/AR19 is the low surface salinity at #483, 42°26.5'W. This drop in salinity coincided with a drop in temperature by ca. 5°C. Only at 500 m depth both salinity and temperature level out to values comparable to neighbouring CTD stations. As this drop was already noticed in the thermosalinograph records approaching the station, closely spaced XBT-drops have resolved the temperature structure of an extensive eddy of northern origin on both sides of station 483. The effects of this eddy can be traced down to 2500 m in the density fields (Fig. 7d,e). CCS Hudson had surveyed the area only days earlier and had located the centre of this quasi-stationary feature, dubbed the "Mann Eddy", at 41°46'N and 44°10'W.

Long-term changes in the characteristics of the Labrador Sea Water LSW for the three comparable manifestations of this section along ca. 48°N are summarised in Fig. (8 a-d). All three cruises follow an identical track east of the Mid-Atlantic Ridge MAR, only in the Western Basin the tracks of Gauss 226 in 1993 and Meteor M30/2 in 1994 are identical. For CCS Hudson the track was chosen to follow 48°N exactly, crossing Flemish Cap and its local circulation regime.

An indication of the heat and salt available at 48°N and their changes since 1957, the year of the Discovery section during IGY, gives Fig. (8e,f). All available data have been interpolated on the same grid across the section. The Discovery and Hudson sections have been, for the Western Basin, projected onto the new track of the Gauss and Meteor sections. For each grid column potential temperatures and salinities have been averaged. The mean values are plotted against longitude west, and the bottom topography of the section has been included. For the continental shelf slope regions on both sides of the section the mean values are biased by the considerably shallower depths, not to be discussed here. From these figures it becomes obvious that outside the continental slope regimes the Eastern and Western basins show individual features. The Eastern Basin is much smoother, quieter at no distinct spatial scales below the basin scale. The MAR clearly separates both basins. Variations in the West show distinct spatial scales, order 300 km and much greater variability than in the East. The

Labrador Current on the shelf break and the Deep Western Boundary Currents on the continental slope are seen in the general decrease in temperature and salinity west of 44°W.

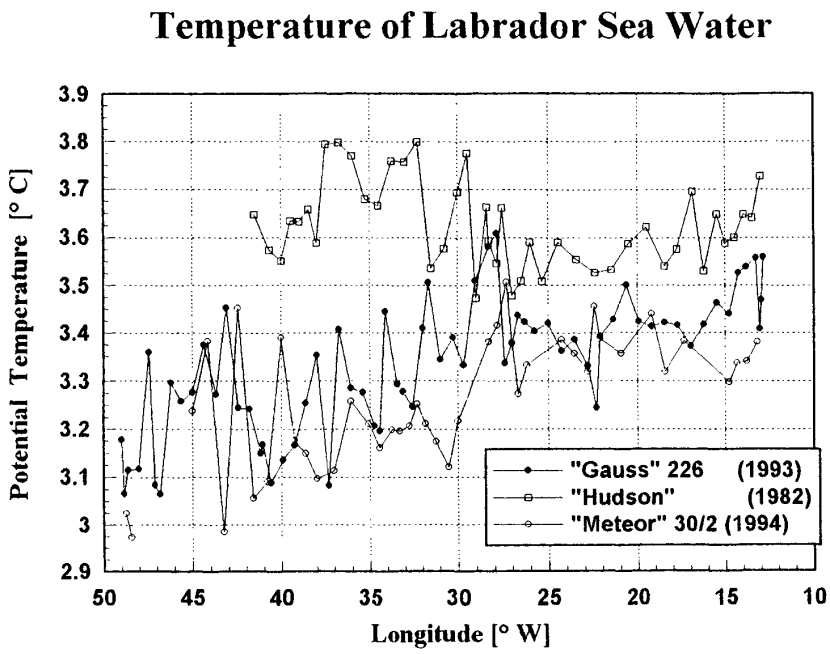

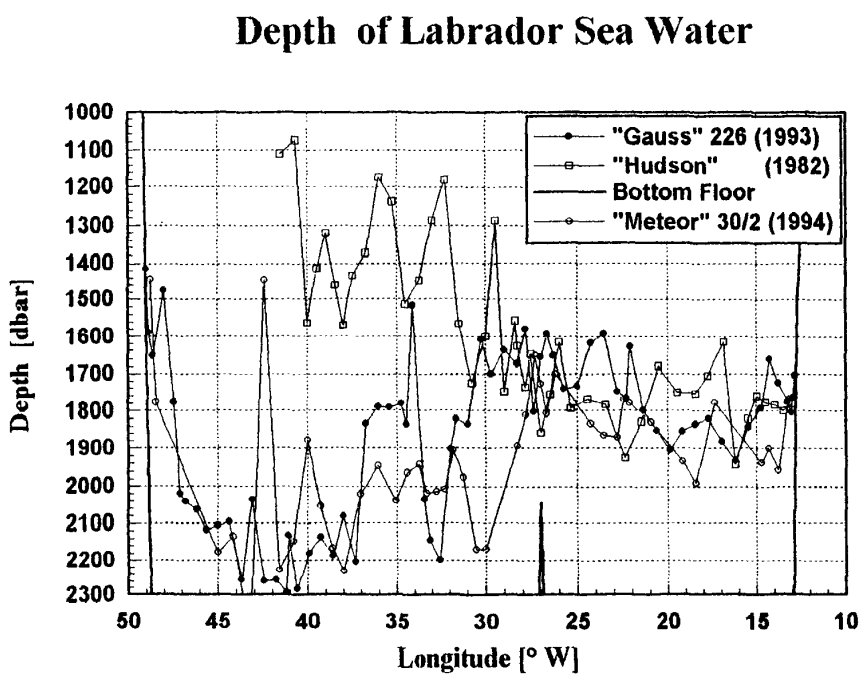

Fig. (8a,b) Potential temperature (8a) and depth (8b) of the Labrador Sea Water core along 48 °N for 1982, 1993 and 1994

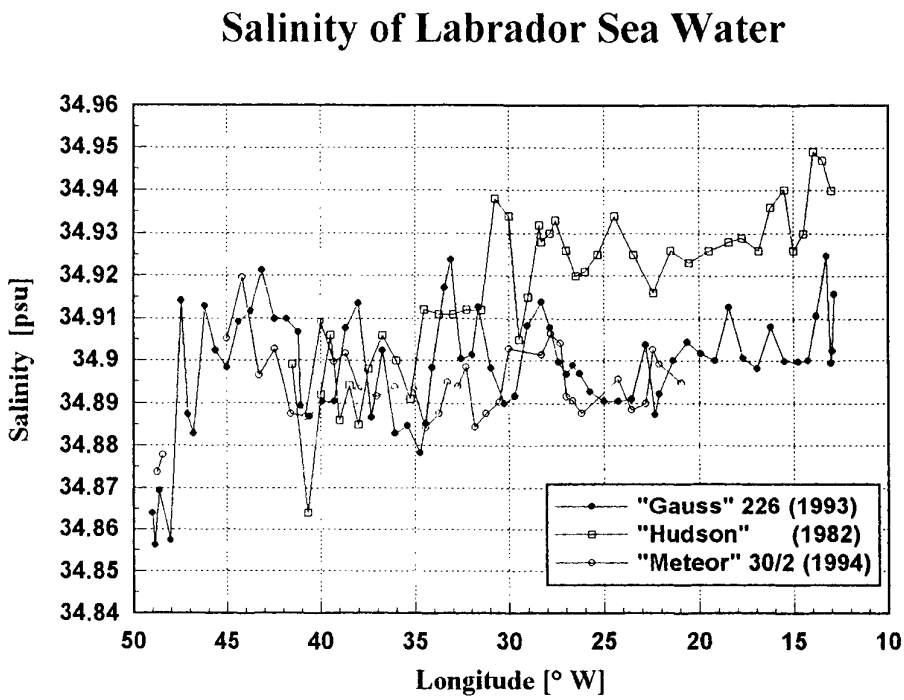

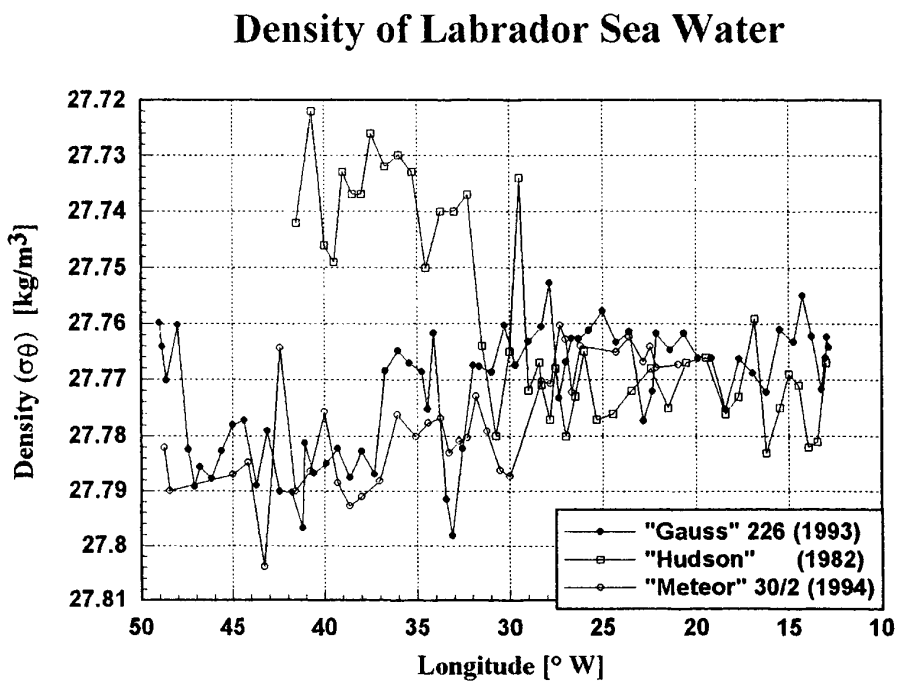

Fig. (8c,d) Salinity (8c) and density (8d) of the Labrador Sea Water core along 48°N for 1982, 1993 and 1994

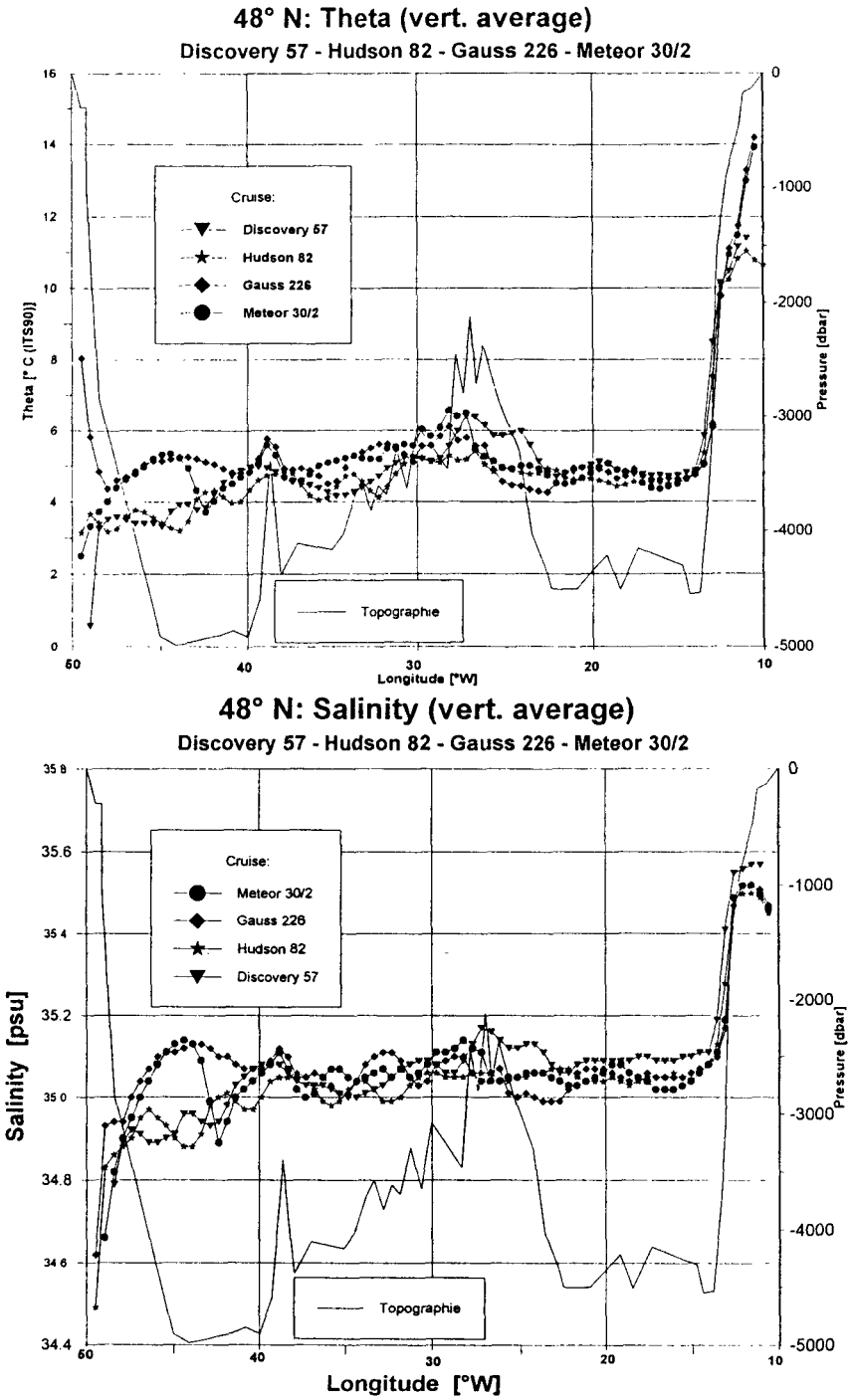

Fig. (8e,f) Depth-averaged potential temperatures (top) and salinities (bottom) along 48°N for 1957-1994

In the deep ocean we note the smooth curves in the Eastern Basin. For 1957 (Discovery) we find here the highest, for 1982 (Hudson) the lowest temperatures. The most recent survey in 1994 (Meteor) gives the lowest salinities, for 1957 with Discovery the highest. Disregarding potential accuracy questions with the Discovery salinities, we find that in 1982 and 1993 the mean salinities are almost the same, indicating that the cooling of the LSW we have observed already in the

Western Basin has now progressed into the Eastern Basin. Across the MAR the boundary currents on both sides leave their imprint by coherent changes towards higher or lower values at a given location. West of the MAR up to the Milne Seamounts at 39°W for 1993 and 1994 we find the highest mean temperatures and salinities, for 1957 and 1982 the coldest and freshest water. This tendency continues into the Western Basin proper, that is West of the Milne Seamounts. Here the warming between 1957/1982 and 1993/1994 amounts to about 1°C, and the salinity increase to ca. 0.2. Despite the considerable input of newly formed at great depth, the net vertically averaged property changes are towards higher temperatures and salinities.

- **Nutrients Measurements for Fine Resolution of Oceanic Water Masses on the Meteor Cruise M30/2 (section WHP-A2) in the North Atlantic**
  (IfMK, L. Mintrop, H. Johannsen, F. Malien)

Nutrient analyses as well as determinations of dissolved oxygen were carried out according to the WOCE WHP standards from the samples obtained from all hydrocasts. By sampling from every successfully closed bottle, a total number of 1692 and 1737 samples were analysed for nutrients (nitrate, phosphate, silicate) and dissolved oxygen, respectively, by the nutrient team from the Institute of Marine Sciences, Marine Chemistry Department, Kiel, Germany. The quality of the data was assured by carrying out the quality and reproducibility checks according to the WOCE standard operation procedures. These parameters were also measured from the samples (a total of 138) obtained with the large volume samplers of the C-14 group. The data from the measurements were made available to the participants at the end of the cruise to help in the fine resolution of oceanic water masses in the North Atlantic. Besides this goal, nutrient and oxygen distributions, especially in the upper water column, allow the interpretation of seasonal biological processes and therefore contribute to the CO_2-studies of this cruise.

The data are summarised in the Fig. (9 a-d).

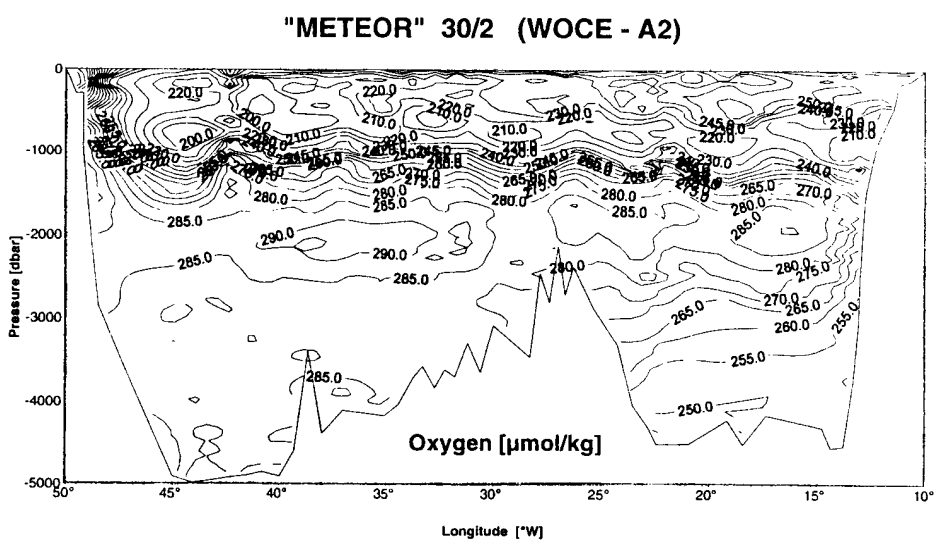

Fig. (9a) Distribution of dissolved oxygen along section WHP-A2

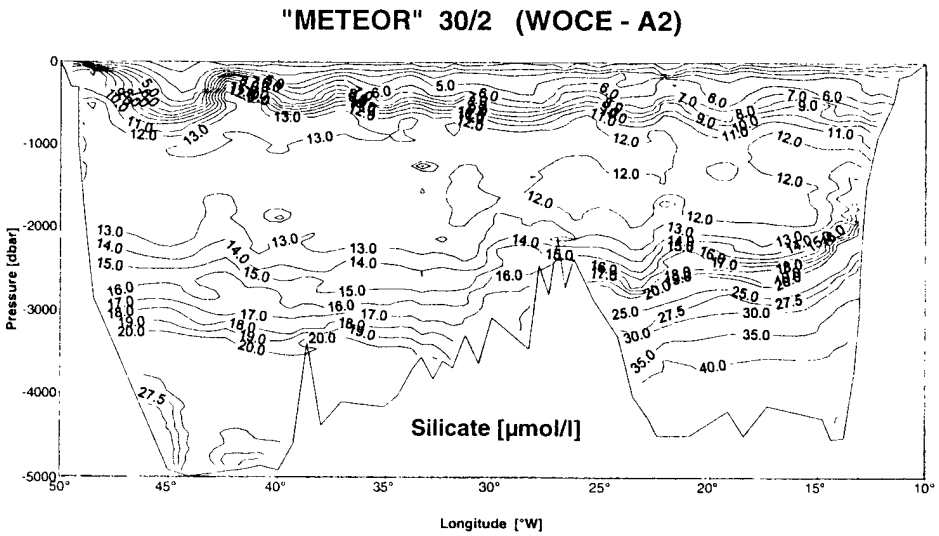

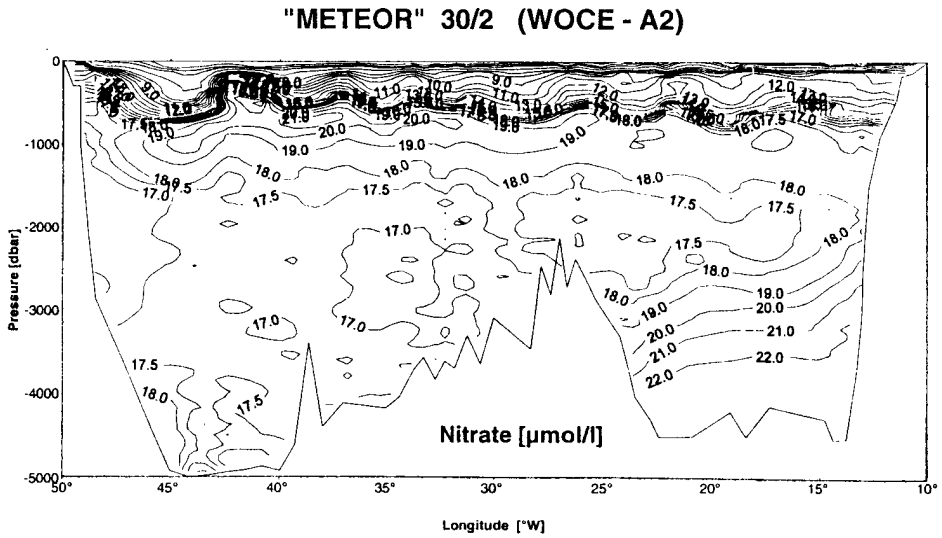

Fig. (9b-c) Distributions of silicate (8b), nitrate (8c) along section WHP-A2

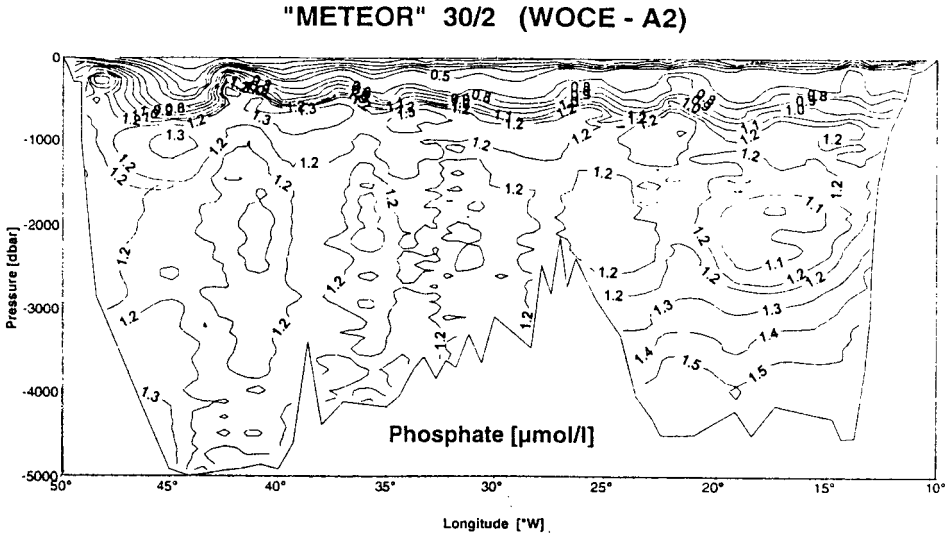

Fig. (9d) Distribution of phosphate along section WHP-A2

- **CFCs on the WHP section A2**
  (IUP-B, W. Roether, A. Putzka, K. Bulsiewicz, C. Rüth, H. Rose)

Operational Details

The CFC analyses are performed onboard. Except for shallower areas almost each station was sampled at up to 36 levels. The CFC samples were drawn from 10 liter Niskin bottles on large glass syringes. During sampling the contamination with ambient CFC had to be avoided and controlled. In all 1062 analyses for F11, F12, F113 and 978 analyses for CCl_4 have been performed, and the data were evaluated preliminary at sea.

The investigated tracers are the man-made chlorofluorocarbons (CFC) F11, F12, F113 and carbon tetrachloride CCl_4. Their time-dependent input at the ocean surface is known. The tracer concentration of the surface water is altered by mixing processes when the water descends to deeper levels of the ocean. Measuring the concentration of the tracers delivers information about time scales of ventilation processes of subsurface water. The atmospheric F11 and F12 contents increase monotonously with different rates since the forties. CCl_4 increases since 1920 while F113 started to increase in 1970. Hence the concentration ratios of the different tracers vary over wide time ranges and can be used to indicate the 'age' of water masses (age since leaving the surface). 'Younger' water is tagged with higher CFC concentration compared with 'older' water.

Sampling
Samples were taken according to the WOCE scheme.

CFCs: glass syringes, on 45 of 53 hydrographic stations 1048 samples were taken and measured on board.

Helium: 80 helium samples in copper tubes for on shore extraction, intercalibration purposes. Samples to be measured on shore.

Measurements:
All CFC measurements were done using a gas-chromatographic system especially improved because of problems with the analysis of F113 (chromatographic interference with CH_3I). The system is now equipped with a new designed micro-trap for collecting the different gases purged from a water sample, a special pre-column to improve especially the resolution between CH_3I and F113 and a electronic pressure regulator for a better baseline stability. Due to these changes we were able to measure F113 with sufficient chromatographic resolution and to produce for the first time a high quality set of measurements for the whole section.

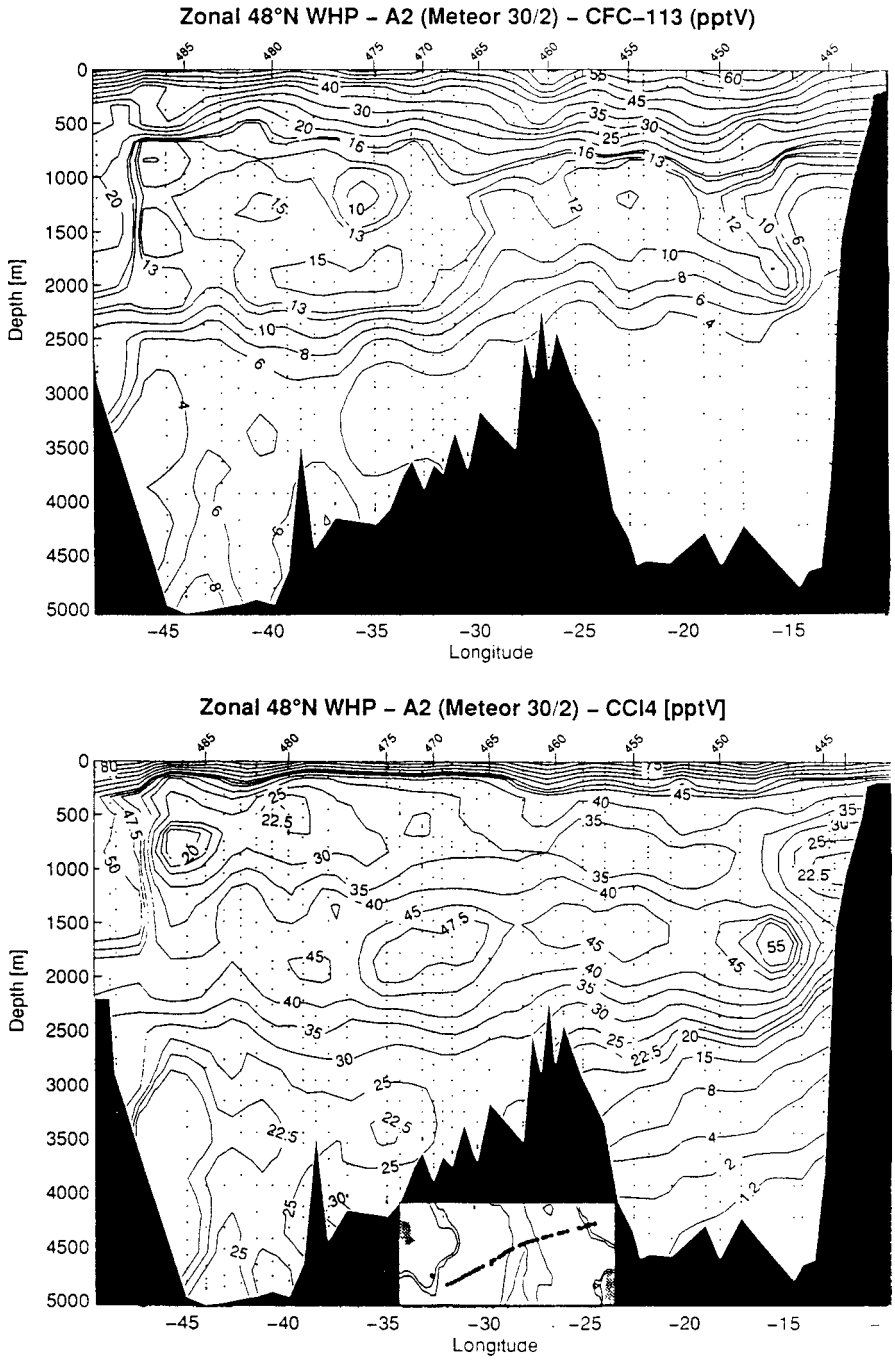

Fig. (10) F113 (upper part) and CCl_4 distribution on A2. Values given in ppt.

Preliminary results

In Fig. (10) sections for F113 and CCl_4 are shown. Within the eastern basin of the section the lowest F113 and CCl_4 values were found below about 3500 m indicating as expected the oldest water found on the section. For the deep western basin a layer of water with higher F113 concentration is found at the bottom due to the recently ventilated overflow water from the Denmark Strait. Lower concentrations were observed at a depth range between 3000 and

4000m on the western flank of the Mid Atlantic Ridge. This indicates most probable a re-circulating portion of a mid depth North Atlantic Deep Water (NADW). Most significant is a layer with higher F113 and CCl_4 concentrations indicating the Labrador Sea Water (LSW) at about 1900m depth which extends over the whole North Atlantic.

The Mediterranean Overflow Water (MOW) shows up slightly above 1000m depth at the eastern side of the West European basin. While the F113 and also F11 and F12 (not shown here) is here lower, the CCl_4 shows a much clearer minimum. It is known that CCl_4 degrades but only within water warmer than about 10-12˚C. The original overflowing Mediterranean Water is above that temperature and therefore the MOW found in the Atlantic has significant lower concentration in CCl_4 compared to Atlantic waters of comparable temperature or comparable concentration of the other CFCs.

- **Tritium/helium and ^{14}C-Sampling along WHP-sections A2 and A1**
  (IUP-HD, R. Bayer, B. Kromer, M. Born)

The experimental goal of the cruise was the collection and measurement of a representative data set of geochemical tracers along the WHP section A2. The data will be used to determine mixing rates and apparent ages of the water masses in the North Atlantic. A special focus is on the deep boundary currents along the continental margins and the Mid Atlantic Ridge. Sampling and interpretation will be done in close cooperation with all groups involved. The transient tracer data obtained will be compared with the 1972 GEOSECS data and the TTO/NAS data from 1980/81 in the Northern Atlantic. From the evaluation of the tracer fields further indications will be obtained how much and how fast the invasion of the tracer signals from the surface into the deep waters has proceeded.

The sampling programme was split into two components: small volume samples for analyses of the CFCs, helium isotopes, tritium and AMS-^{14}C to be collected with the rosette system, and a C-14 programme using large volume samplers.

During M30/2 468 tritium samples have been collected. About 1 liter of water is sampled in glass bottles for determination of the tritium concentration. In the home laboratory from a certain amount of water the helium is degassed quantitatively and the sample is stored in a vacuum container for several months. During that time tritium decays and the decay product, ^{3}He, is enriched. The latter will be detected with a special high sensitivity, high resolution mass spectrometer.

For helium measurement ca. 40 cc of sea water are sampled in a copper tube sealed with pinch-off clamps. Analyses will be performed on-shore with a dedicated helium isotope mass spectrometer after extraction of the helium dissolved in the water. A total of 474 samples were collected.

In addition samples have been taken to test a seagoing helium extraction system. In all 311 samples were taken both parallel and supplementary to the conventional sampling procedure. All samples have been processed onboard, and the measurements have been done in the home laboratory after the cruise. The duplicate samples obtained in copper containers as well as several seagoing replicate samples will be used to assess the performance of the new system.

Furthermore 60 AMS-^{14}C samples have been drawn from the rosette. This programme is supplementary to the large volume ^{14}C sampling and was restricted mainly to the upper water column.

For the large volume sampling ten Gerard-Ewing bottles with a volume of 270 liter each are used. The bottles are run in vertical series in two casts at the relevant stations. The shallow cast was followed by a CTD/rosette cast to give time to the onboard ^{14}C-extraction and the subsequent preparation of the large volume samplers for the deep^{14}C-cast. For the M30/2 section 8 large volume stations with a total of 204 ^{14}C samples have been worked.

Preliminary results

As a first example of the data from this cruise Fig. (11) shows selected profiles of tritium concentrations in the Western Basin. West of the MAR one can distinguish clearly separated depth ranges. For the LSW depth range we find tritium values of 1.2 -1.4 TU. Deeper, the distribution is more homogeneous, particularly in the central basin with a mean concentration of ca 0.75 TU. On the WHP-A1 section further north during leg M30/3 we find for these water masses significantly higher concentrations. We intend to use a multi-tracer approach to determine the mixing ratios and spreading rates for these water masses. We will also estimate the mean renewal times for the individual depth ranges.

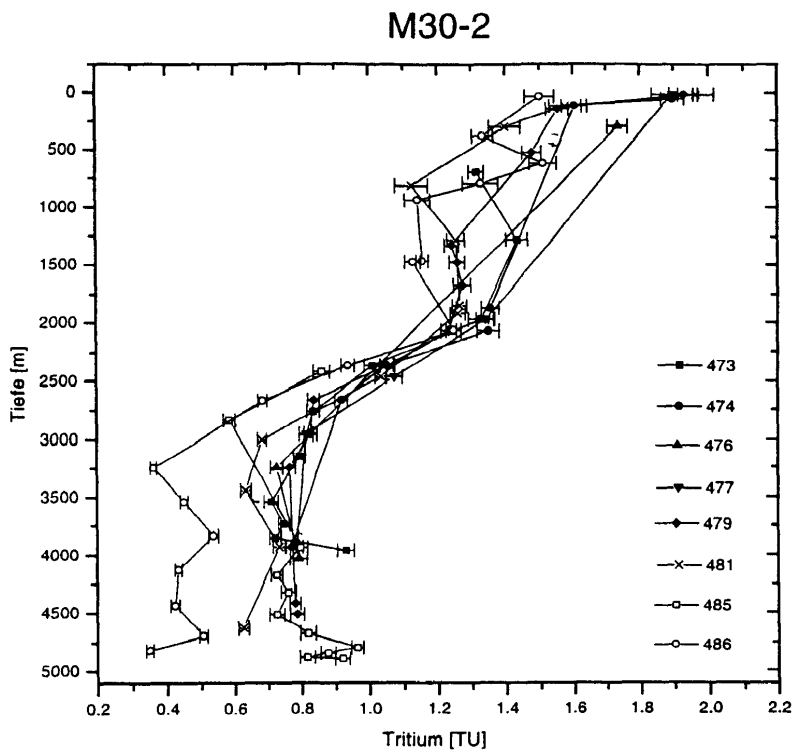

Fig. (11) Selected tritium profiles for the Western Basin on section A2

5.2.2 Mooring recovery on WHP- A2 and WHP-A1
(BSH, K.P. Koltermann and IfMHH, J. Meincke)

During the Gauss cruise no 226 in the summer of 1993 three moorings were deployed west of the Mid Atlantic Ridge on the WOCE section A2 to measure the fluctuations and spatial extent of a deep salinity maximum. These moorings could not be turned around in the summer of 1994 and thus a recovery was planned as part of this cruise. Two of the three moorings could be interrogated acoustically, one failed to answer. An attempt to dredge for the mooring K1 in a weather lull was not successful. Weather changes prevented other attempts to recover these moorings.

In summer 1995 the mooring K3 was completely and the mooring K1 partially recovered from RV Gauss by dredging. The mooring K2 could not recovered. From K3 some 640 days of data are now available.

The recovery attempts for the mooring D2 on leg M30/3 by dredging was not successful. Further attempts for dredging operations for other moorings had to be cancelled because of the prevailing weather and time constraints.

5.2.3 Physical, Chemical and Tracer Oceanography on Leg M30/3

- **Hydrographic Measurements on WHP-A1**
  (BSH, A. Sy)

Hydrographic casts were carried out with a NBIS MK-IIIB $CTDO_2$ unit (internal name: "DHI-1") mounted on a GO rosette frame with 24 x 10 litre Niskin bottles and owned by BSH. The mean constant maximum descent rate was 1 m/s. $CTDO_2$ data were collected at a rate of 64 ms/cycle using a PC based (HP Vectra 486) data acquisition software (CZHEAD rev. 18) designed by BSH. A video tape unit was used as a backup system on each cast. Hardware and software instrumentation ran without serious problems during the whole cruise leg. The rosette system used proved to be well adapted to the CTD unit, and thus only few tripping failures encountered.

Both pressure and temperature (ITS_{90}) were calibrated before (Sept./Oct. 1994) and after the cruise (February 1995) by the calibration facilities at IfM Kiel. The post cruise pressure calibration needed to be repeated in November 1995 due to uncertainties with results from the February calibration. Salinity was calibrated by comparison of CTD with sample salinities. 24 SIS digital temperature meters (RTM 4002) and 7 SIS digital pressure meters (RPM 6000), calibrated by the manufacturer in October 1994, were used in a rotating mode throughout this cruise leg to control the CTD sensors' stability. DSRT readings, along with salinity, oxygen and chemical data from the rosette water samples, were also used to detect erroneous depths of bottle firings. Unfortunately, 7 DSRTs were destroyed at the ship's side by heavy sea.

The bottle sampling sequence was as follows. Oxygen samples were collected soon after the CTD system was brought on board and after CFC and ^3He were drawn. The sample water temperature was measured immediately after the oxygen sample was drawn. The next samples drawn were TCO_2, ^{14}C, ^3H, nutrients (NO_2 + NO_3, SIO_3, PO_4), and salinity. All bottle

samples taken were linked to the rosette Niskin bottles by the "Bedford" sample identification system (see 5.2.1).

Salinity samples were drawn into dry 200 ml BSH salinity bottles with polyethylene stoppers and external thread screw caps. It was found by Kirkwood and Folkard (1986) that these bottles guarantee best long-term storage conditions, a problem encountered with the old soft glass seawater sample bottles (Sy and Hinrichsen, 1986). Bottles were rinsed three times before filling. Samples were collected as pairs of replicates (i.e. two samples from the same rosette bottle), one for shipboard salinity measurements and one for backup purposes, e.g. for the possibility of cross checks by later shore-based salinity analysis. The rosette sampling procedure was completed by readings of electronic DSRTs for a first quick check of the scheduled bottle pressure level and for in-situ control of the CTD pressure and temperature calibration.

In all 18 $CTDO_2$-rosette stations were occupied along section A1/West and 45 $CTDO_2$-rosette stations along section A1/East (Fig. 12a, List 7.1.3), of which the first two casts at station # 489 were used to test winch, cable, two CTD-rosette systems as well as the sampling procedure and the laboratory equipment. Three casts were used for rosette sample quality tests at stat. # 496, 517 and 542 by means of multi-trips at the same depth level (Table 5.2.3.1). An overview of the locations of water samples is given in Fig. (16 a). Activities, occurrences and measured parameters are summarised in the station listing (List 7.1.3).

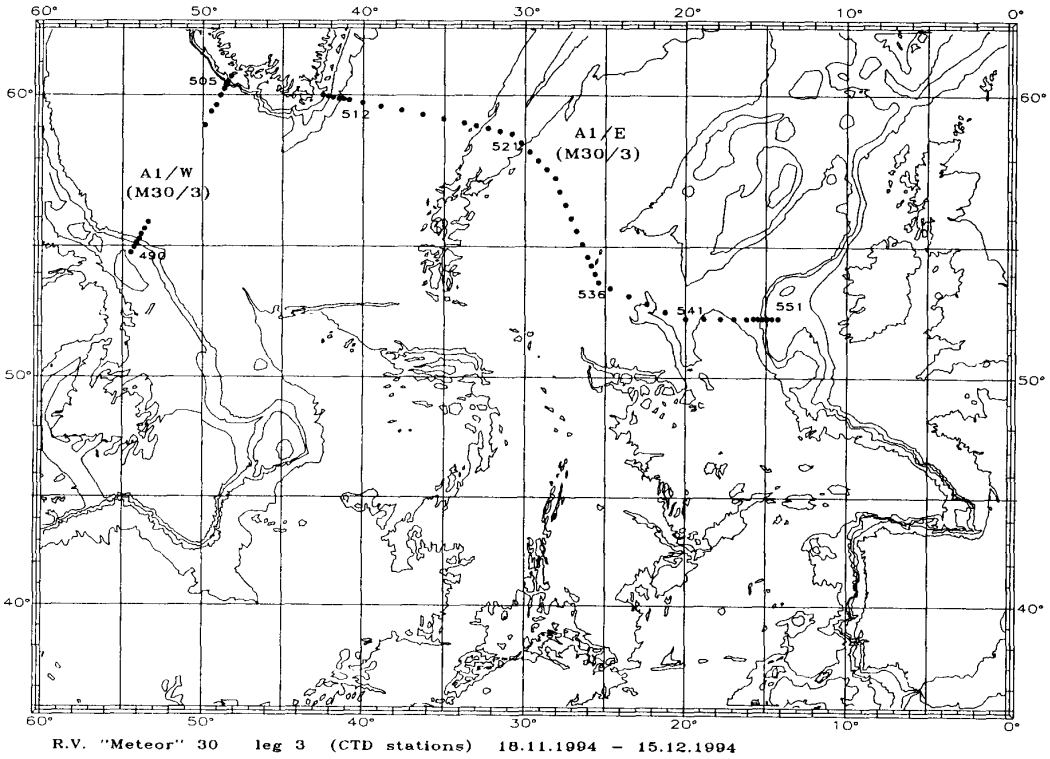

Fig. (12a) Positions of $CTDO_2$/rosette stations for R.V. "Meteor" cruise no. M30/3

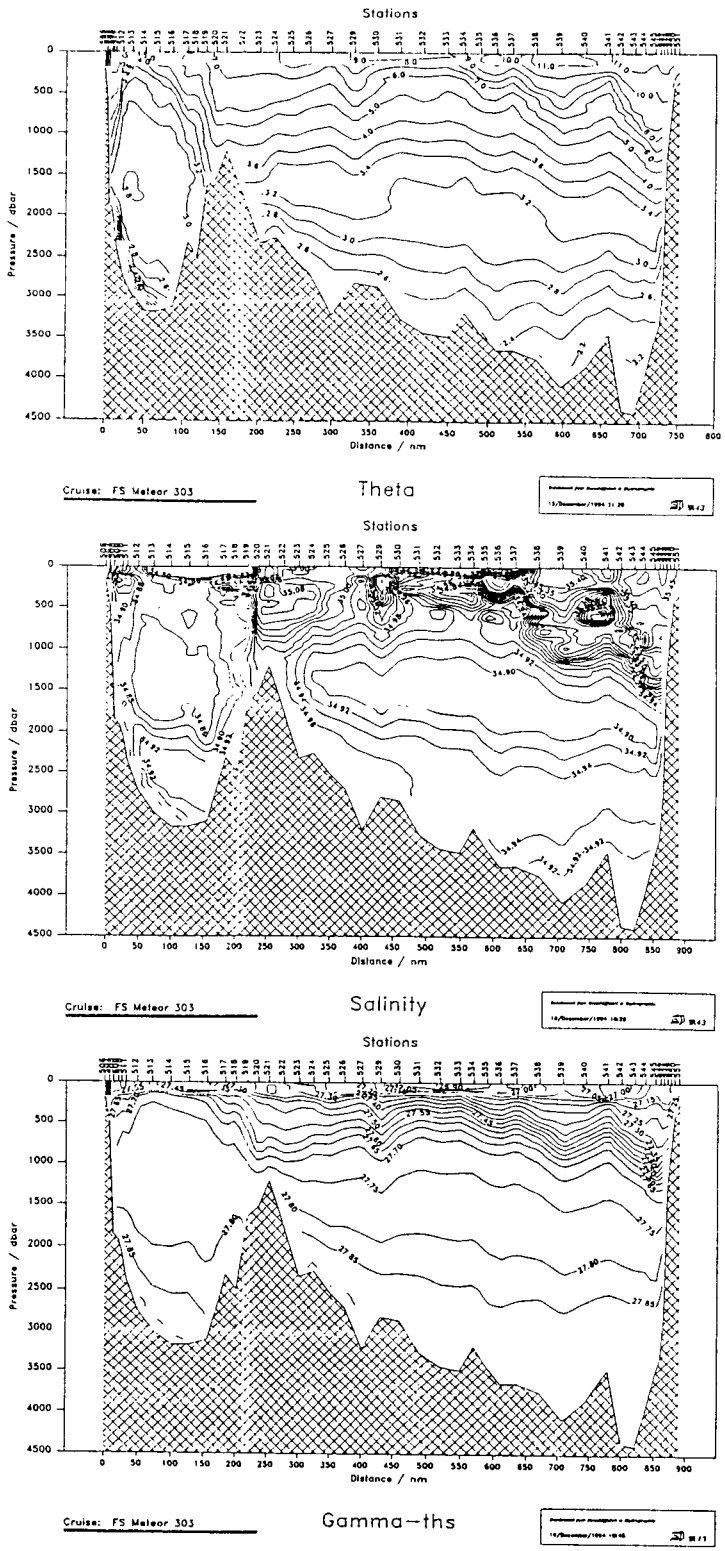

Fig. (12) CTD-sections A1/West, (b) potential temperature (°C), (c) salinity, (d) density (σ_t)

To meet WOCE quality requirements, the processing and quality control of CTD and bottle data followed the published guidelines of the WOCE Operations Manual (WHPO 91-1) as far as their realisation was technically possible on this cruise. Standard CTD data processing and bottle data quality control (including oxygen and nutrient samples) were carried out on board during the cruise using BSH designed software tools. The final CTD data processing was done in the laboratory at BSH and included the application of corrections to pressure, temperature and salinity and the oxygen calibration. Property sections from CTD data are presented in Fig. (12b-d). CTD data processing and quality evaluation will be discussed in greater detail in a separate data report. All hydrographic data are submitted for independent quality evaluation to the WOCE Hydrographic Programme Office.

The ADCP was serviced during the St. John's stopover. The antenna configuration of the new Ashtech GPS-system was re-initialised there. Measurements started on Nov. 15,1 1994 and had to be discontinued on Nov 28, 1994 in the Irminger Sea due to total collapse of the system due to transducer flooding in heavy weather. The third transducer had already failed on Nov 18, 1994. In all 2983 velocity profiles at 6 min intervals have been recorded are being processed with standard methods.

Table 5.2.3.1 Precision of duplicate samples (i.e. from different rosette bottles fired at the same nominal depth) of rosette test stations.

	Stat. # 496	**Stat. # 517*)**	**Stat. # 542**
Duplicates:	N = 19	N = 16	N =11
Parameter	mean ± sdv	mean ± sdv	mean ± sdv
Pctd/db	1473.7 ±5.7	1401.4 ± 1.2	3948.5 ± 4.0
(Pdsrt)	1471.9	1402.0 ± 3.5	none
Tctd/mK	2.8125 ± .0013	3.0466 ± .0100	2.4761 ± .0007
(Tdsrt)	2.8177 ± .0028	3.0542 ± .0077	none
ΔT	.0054 ± .0027	.0045 ± .00240	none
Sctd	34.8332 ± .0011	34.8621 ± .0012	34.9070 ± .0002
Sali	34.8320 ± .0004	34.8617 ± .0014	34.9050 ± .0003
ΔS	-.0013 ± .0004	-.0004 ± .0007	
Oxygen	6.9125 ± .0043	6.8764 ± .0124	5.5216 ± .0039
(ml/l)	(.06 % fs)	(.18 %)	(.07 %)
Nitrate	16.876 ± .061	17.217 ± .068	23.507 ± .0128
(µmol/l)	(.36 % fs)	(.39 %)	(.54 %)
Phosphate	1.0982 ± .0035	1.0982 ± .0082	1.5810 ± .0068
(µmol/l)	(.32 % fs)	(.75 %)	(.43 %)
Silicate	9.371 ± .043	9.746 ± .026	45.110 ± .056
(µmol/l)	(.46 % fs)	(.27 %)	(.12 %)

*) Water mass not as homogeneous as desired

It turned out that the pre- and post-cruise laboratory calibrations of pressure and temperature were stable (no significant differences) and thus these functions were used for the final correction of the field data (Fig. 13, Tab. 5.2.3.2).

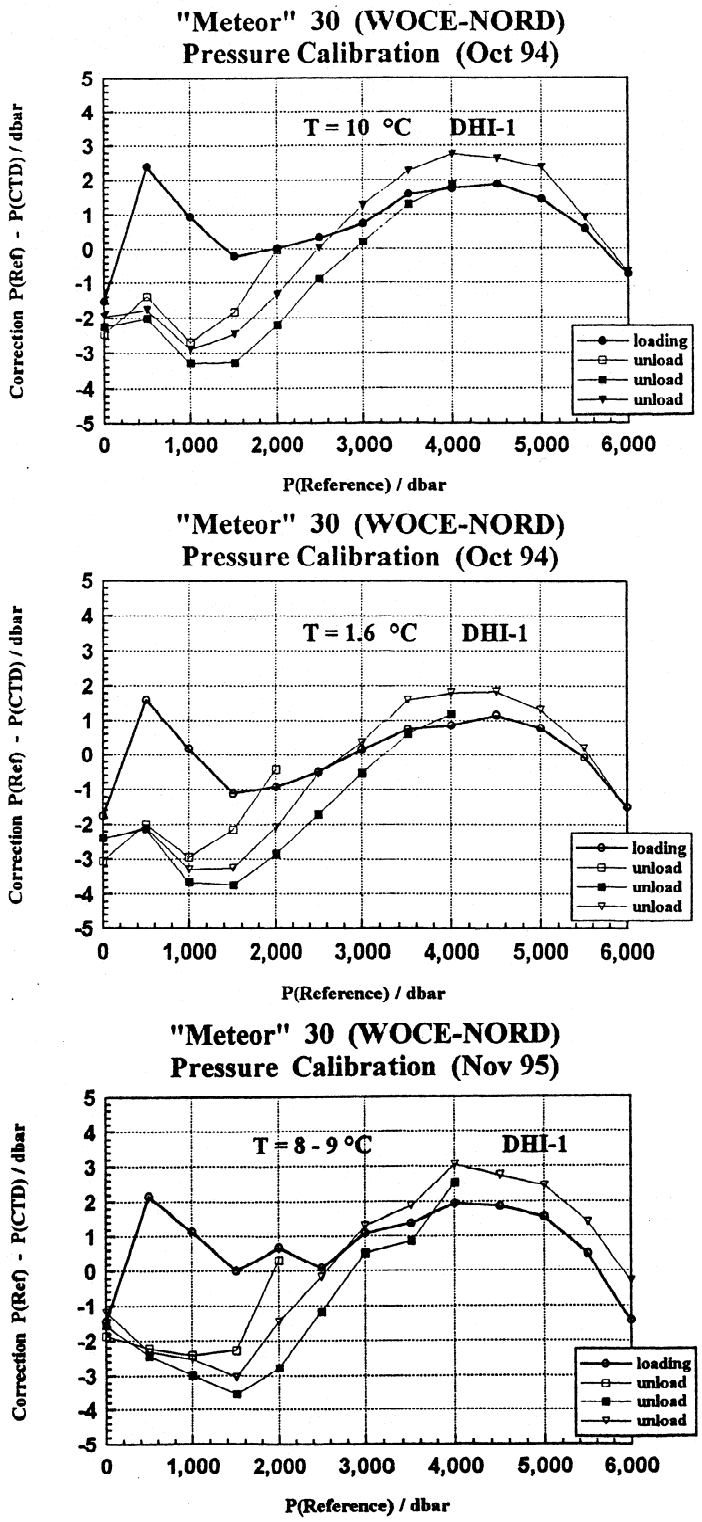

Fig. (13) Pre- and post -cruise calibration
(a) Pressure at T = 10°C (Oct 94)
(b) Pressure at T = 1.6°C (Oct 94)
(c) Pressure at T = 8-9°C (Nov 95)

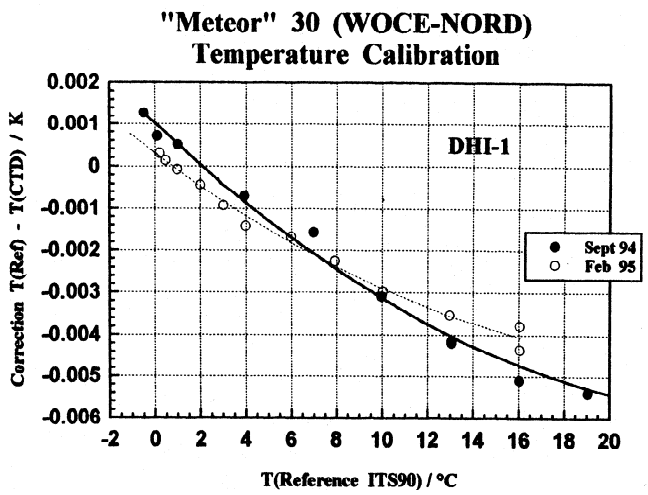

Fig. (13d) Pre- and post -cruise calibration, Temperature

The salinity correction was carried out by means of in-situ data. After pressure and temperature corrections were applied and salinity recalculated, the remaining salinity error consists of a small temporal drift only (Fig. 14). For salinity analysis of samples a standard Guildline Autosal salinometer model 8400 (s/n 56414) was used on board together with the processing software (SOFTSAL with ATS rev. 1.3 and ATSPP rev. 2.1) designed by SIS. One ampoule of IAPSO Standard Seawater (batch P 124) was used per 2 stations (48 samples). The instrument was operated in the ship's constant temperature laboratory at a bath temperature of 24°C with the laboratory temperature set to 23°C. Salinity was measured about 2 days after water collection. No backup seawater sample analysis was needed to be carried out.

Oxygen sample measurements were carried out by BSH technicians (see 5.2.3.4). Because CTD oxygen sensors cannot be calibrated satisfactorily in the laboratory, field calibration is the only alternative. This procedure was carried out in line with the guidelines given by Millard (1993) by merging the down-profile CTD data with corresponding up-profile water samples. Oxygen residuals of the final fit versus stations are shown in Fig. (15).

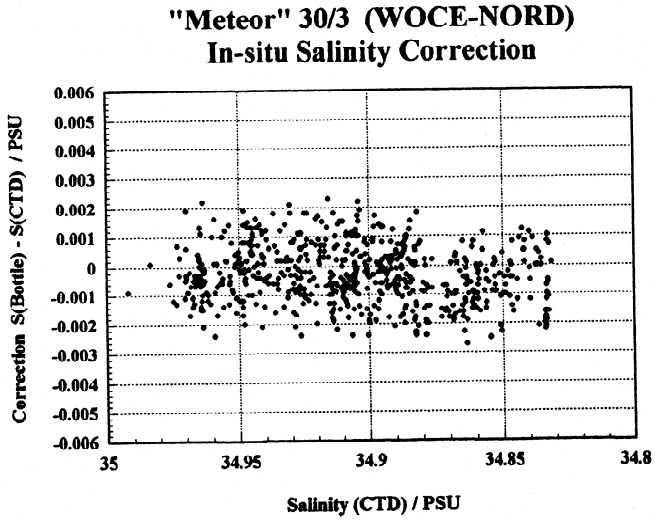

Fig. (14a) Salinity residuals, versus CTD salinity, M30/3

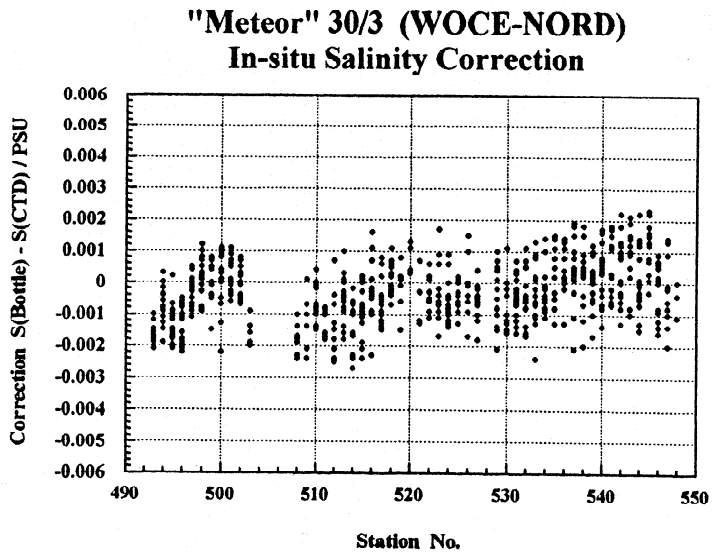

Fig. (14b) Salinity residuals, versus CTD stations, M30/3

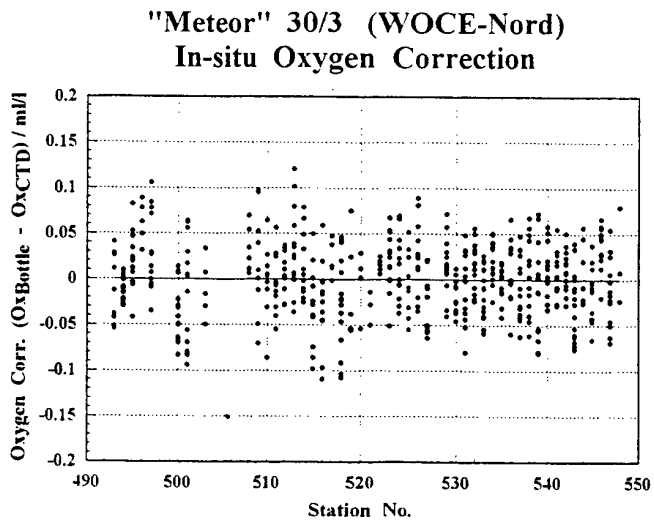

Fig. (15) Oxygen residuals of final fit versus CTD stations

Table 5.2.3.2: Laboratory calibration coefficients for CTD "DHI-1" temperature and pressure correction polynom P_{corr}, T_{corr} (e.g. $T_{new} = T_{old} + T_{corr}$)

	Temperature	Pressure (downcast)	Pressure (upcast)
a0	0.0010	-1.68	-2.31
a1	-0.000508	0.0140268	-0.001693
a2	9.3139 E-6	-2.14633 E-5	1.10129 E-6
a3		1.24996 E-8	-6.08444 E-11
a4		-3.39917 E-12	-1.21793 E-14
a5		4.39732 E-16	
a6		-2.19759 E-20	

Note: The a_0-coefficients for pressure are caused by the lab calibration procedure only and are not used for pressure correction. The actual pressure offset protocolled for each station is used as a_0.

Nutrients along WHP-A1
(BSH, A. Sy, MAFF. D. Kirkwood)

Along the entire two part of WHP-A1 concentrations of dissolved oxygen and nutrients have been analyzed from water samples. Details of the analyses and methods are given in 5.2.3.4 and 5.2.3.5, respectively. In Fig. (16a-e) we display the distribution of the sample positions and the data.

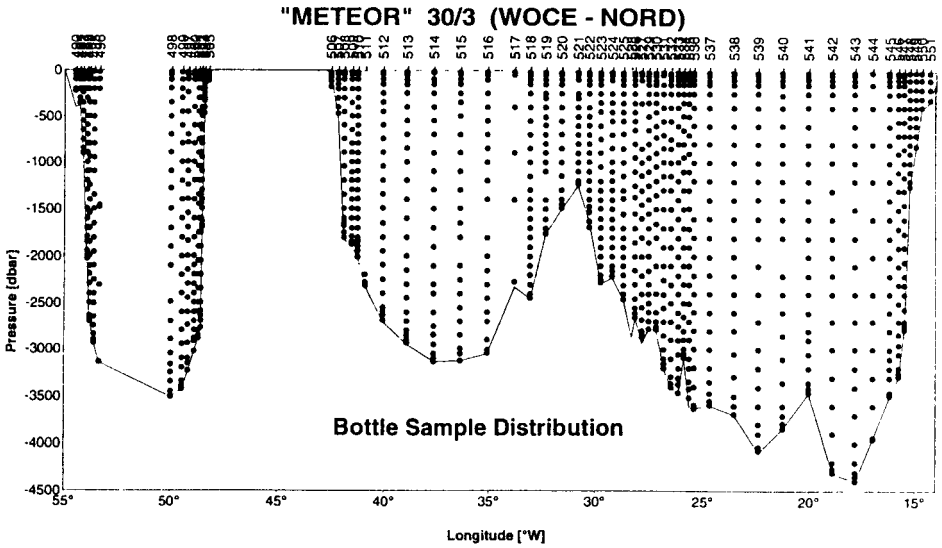

Fig. (16a) Distribution of water samples along WHP-A1

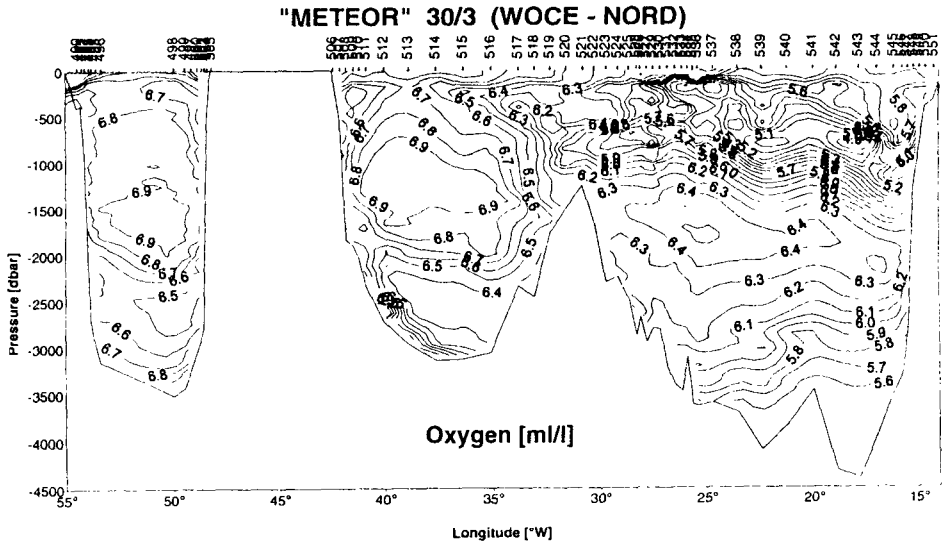

Fig (16b) Distribution of the concentrations of dissolved oxygen along WHP-A1

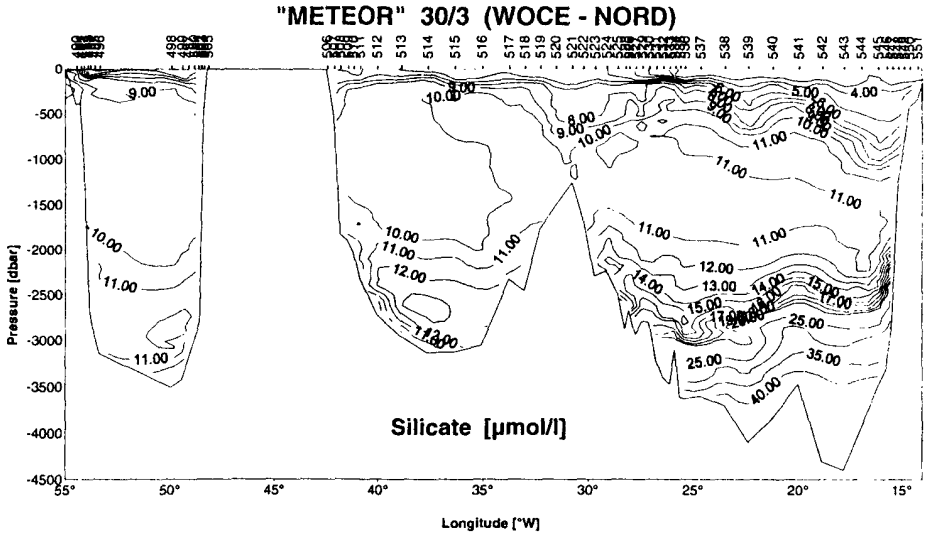

Fig (16c) Distribution of the concentrations of silicate (16c) along WHP-A1

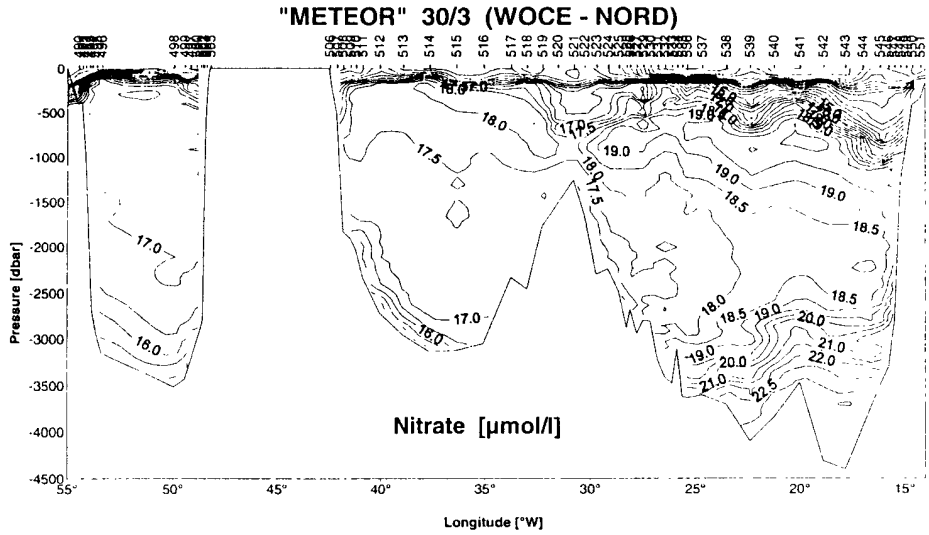

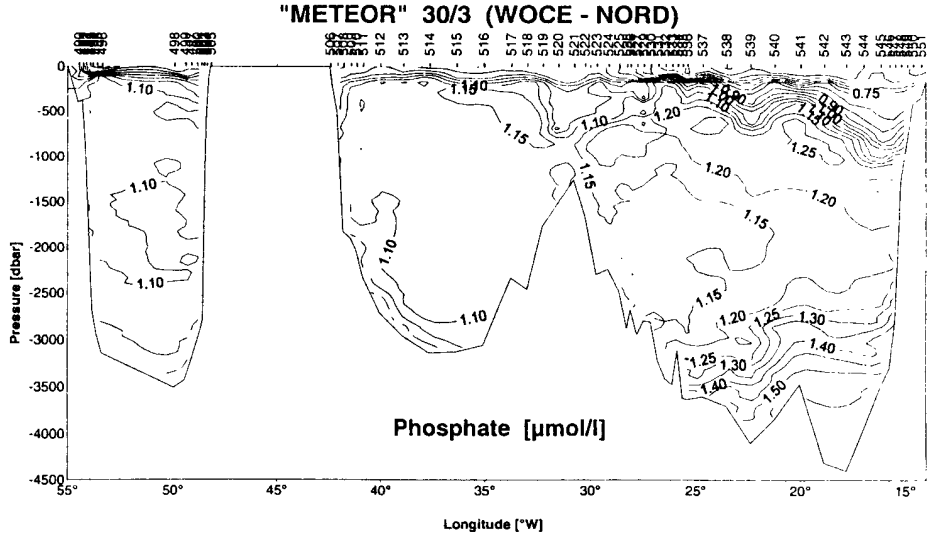

Fig. (16d-e) Distribution of nitrate (16d) and phosphate (16e) along WHP-A1

- **Spreading of Newly Formed Labrador Sea Water**
  (BSH, A. Sy)

As an outstanding event, comparable to the "Great Salinity Anomaly" of the mid 1970s (Dickson et al., 1988), a rapid cooling of the intermediate layer is taking place in the subpolar North Atlantic and in the transition zone between the subpolar and subtropical gyres during the last years (Koltermann and Sy, 1994). This cooling is attributable to a relatively fast spreading of new modes of LSW.

The comparison of the LSW core temperatures along section A1 for the years 1991, 1992 and 1994 (Fig. 17) reveals a clear cooling event in the Irminger Sea in the order of -0.23°C in 3 years. It looks as though every year a new mode of LSW arrives in the Irminger Sea ("LSW cascade"). Cooling in the Iceland Basin of -0.1°C also indicates the arrival of renewed LSW. The 3-year cooling rate from the Rockall Trough area was found to show the same value. But the arrival of the LSW cascade is probably 1 to 2 years later than that in the Iceland Basin.

For the other parameters we find an increase in density of the LSW of 0.018 kg/m^3 for the Irminger Sea and 0.012 kg/m^3 for the area east of the MAR (Fig. 18), and a deepening of LSW which is greatest in the Irminger Sea (250 dbar) and Rockall Trough area (200 dbar) (Fig. 19). However, there is no significant signal in salinity (Fig. 20).

The characteristic property change of the cascade of new LSW modes are cooling and deepening and only little or no freshening. Another striking but not surprising feature is the separation, by the Reykjanes Ridge, into two different hydrographic regimes, the Irminger Sea and the Iceland Basin. The erosion of the LSW core east of the central Iceland Basin (27°W) reflects the longer pathway with mixing and enhanced mixing over topography.

These results correspond well with observations of newly formed LSW in the central Labrador Sea reported by Lazier (1995). According to his findings, the recent period of LSW formation started in 1988. He showed that the characteristic signal of the new LSW period in its source region is the temperature decrease rather than a salinity decrease, and also a distinct density increase and deepening.

Because of the similarity of the LSW characteristics found in the Labrador and Irminger Seas, Lazier et al. (1995) estimated a circulation time of 8 to 20 months from the central Labrador Sea to the central Irminger Sea, or a speed of 1 to 3 cm/s. The pathway to the eastern North Atlantic is much longer and the arrival of the LSW signal will be years later. If the circulation scheme proposed by Talley and McCartney (1982) is adopted, then the water in the Iceland Basin should be of more recent origin than that south of the Rockall Trough. The erosion of the LSW core east of the central Iceland Basin is also indicative of a longer pathway (see Fig. 20).

It is assumed that the LSW observed in December 1994 south of the Rockall Trough is a product of the beginning of the cascade of new LSW modes because in 1991 and 1992 no significant change was detectable. That was not the case in the Iceland Basin where new LSW arrived earlier.

For the events observed east of the Reykjanes Ridge, it is concluded that the new LSW needed 5 to 6 years to propagate from the source region to the entrance of the Rockall Trough. That corresponds to a mean speed of about 1.5 cm/s which is about 3 times faster than suggested by Read and Gould (1992). From CFC measurements a travel time of 8 to 9 years is estimated (see 5.2.3.6).

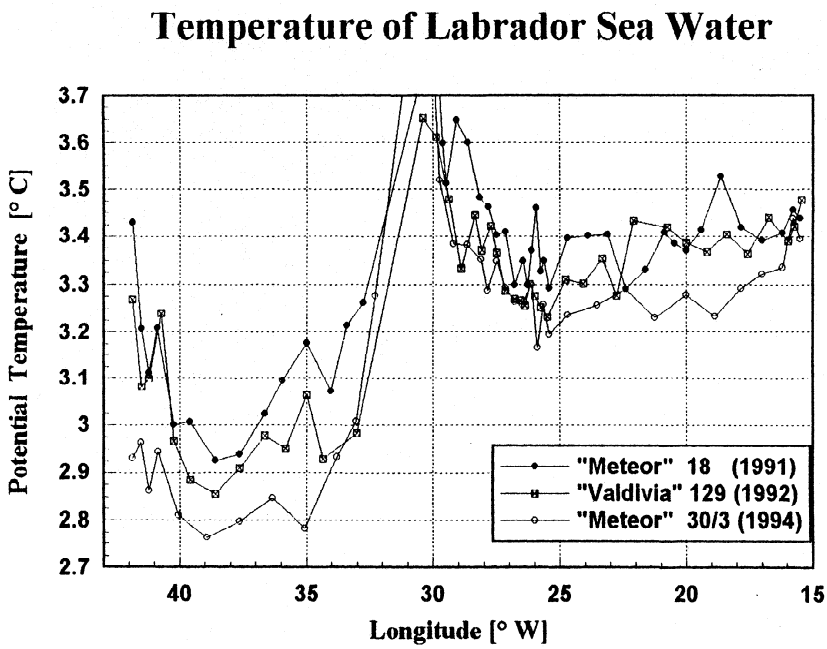

Fig. (17) Within 3 years the LSW in the Irminger Sea cooled down in the order of -0.23°C. The 3-year cooling rate from the Iceland Basin and the Rockall Trough area is in the order of -0.1°C

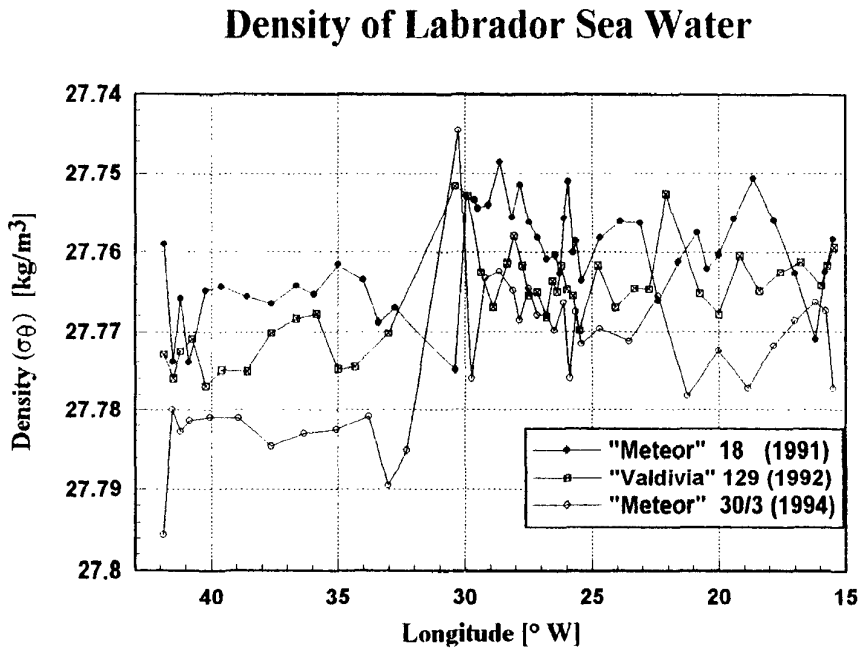

Fig. (18) Within 3 years the density of the LSW core increased by 0.018 kg/m^3 in the Irminger Sea and by 0.012 kg/m^3 in the area east of the MAR

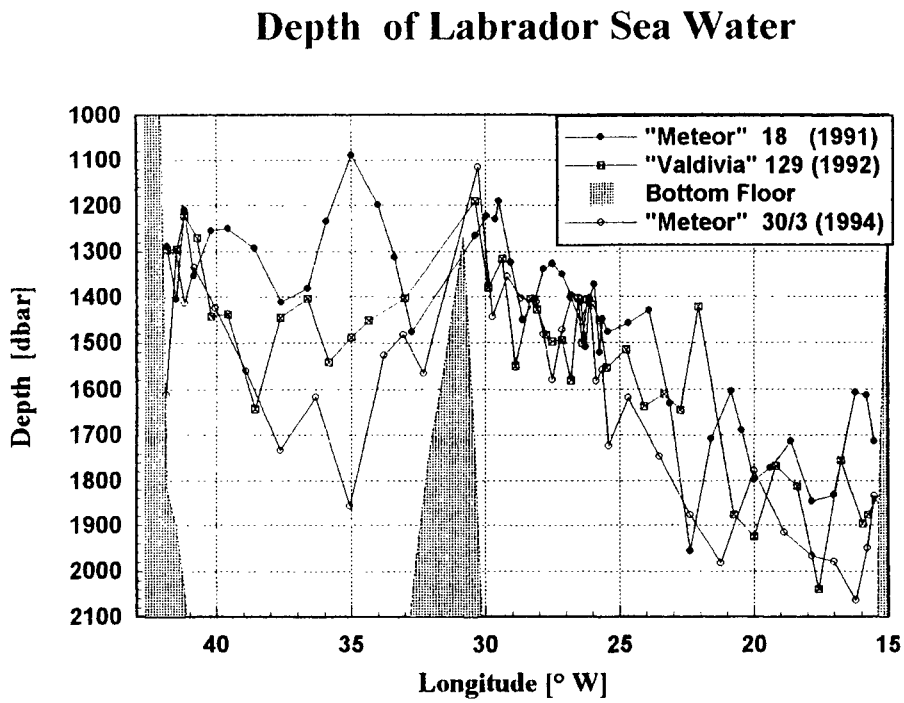

Fig. (19) A mean deepening of the LSW core of about 250 dbar was found for the Irminger Sea and of more than 200 dbar for the Rockall Trough area. For the Iceland Basin a deepening of only 53 dbar was found.

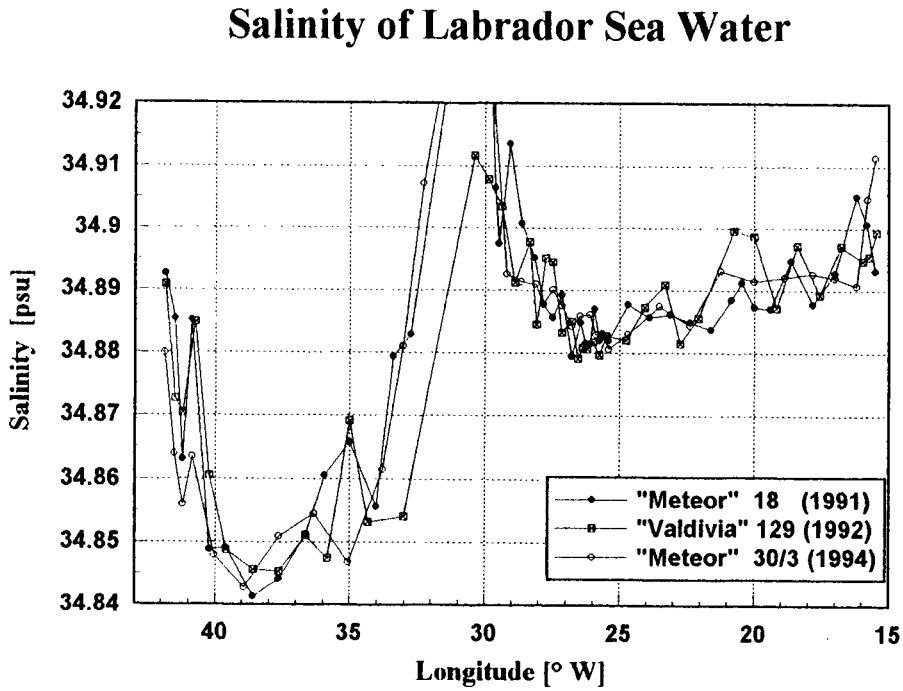

Fig. (20) No striking change of the LSW core salinity appeared within the 3 years of observation.

- **Thermosalinograph, XBT and XCTD Measurements**
  (BSH, A. Sy)

Unfortunately, underway measurements of surface temperature and salinity along section A1 failed, although an Ocean Sensors OS200 Thermosalinograph, which was mounted at the ship's laboratory sea water pipe system, worked without technical problems. However, due to the near surface sea water intake, rough sea over long periods and the absence of a bubble trap, the data quality was so badly affected by air bubbles, that the data were rejected.

XBT Sections
(BSH, A. Sy)

In order to improve the spatial resolution of the hydrographic sections XBT profiles were collected at least after each CTD station and halfway between two stations (Fig. 11). 157 Sippican T-5 probes (nominal depth range 1830 m) and 8 Sippican T-7 probes (760 m) were launched from the vessel's stern using a hand-held launcher. The data acquisition system used a Compaq SLT/286 laptop computer with extension unit, equipped with a Sippican MK-12 interface rev. J, firmware rev. 2.1 and NOAA SEAS-III software rev. 3.2. Where practicable, the measurements were carried out according to the guidelines given by Sy (1991).

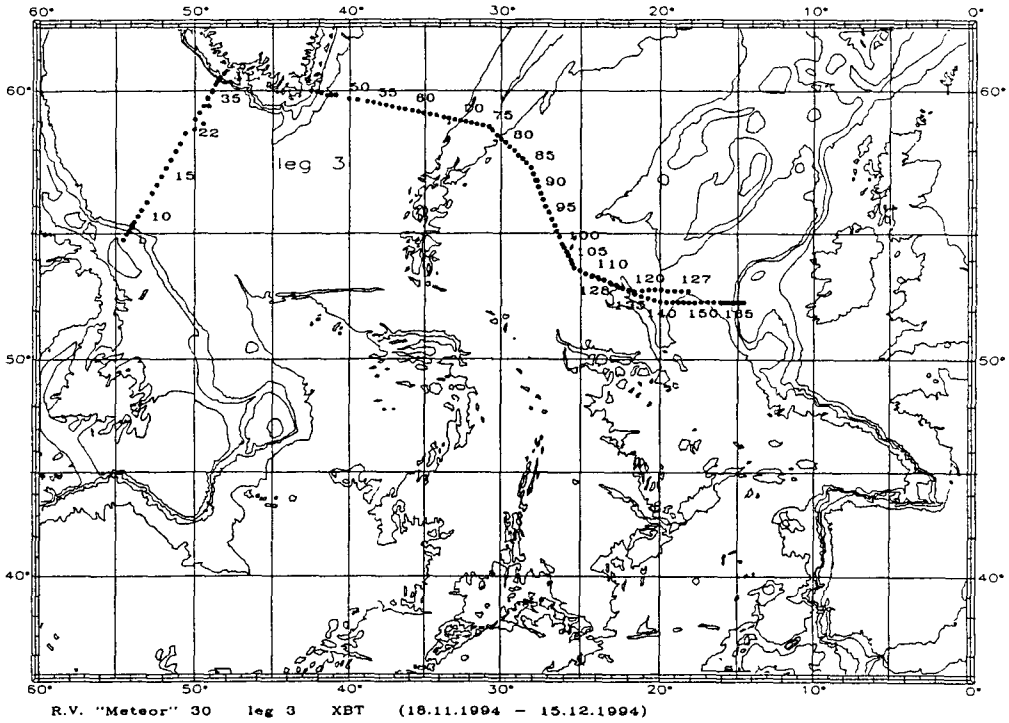

Fig. (21) Positions of XBT profiles for "Meteor" cruise M30/3

Vertical sections from XBT data are presented in Fig. (22). The inflection points calculated by the SEAS programme were transmitted as BATHY messages via BSH into the GTS network. The complete raw data were processed at BSH according the procedures described by Sy and Ulrich (1994).

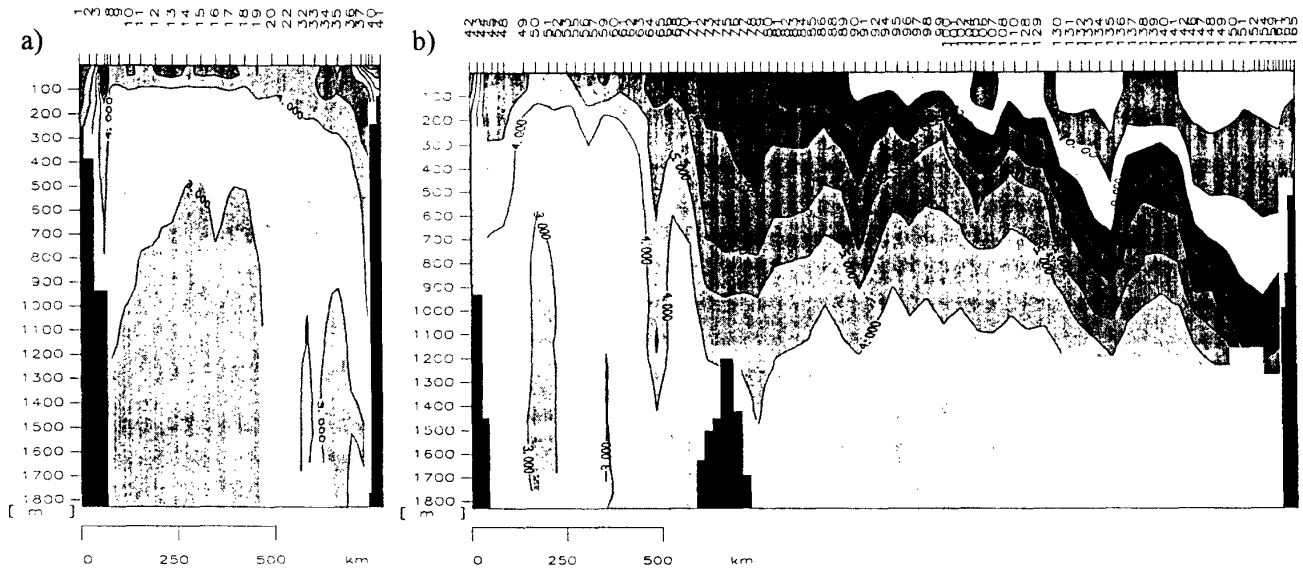

Fig. (22) XBT sections (a) A1/West, (b) A1/East

For test reasons XBT probes were launched at selected CTD stations in parallel to the CTD casts. The purpose of this test was to provide data from the North Atlantic for the international co-ordinated re-evaluation of T-5 and "Fast Deep" probe's depth fall rate with the aim of developing community-wide accepted recommendations for a new depth formula as already published for T-7, T-6 and T-4 probes (Hanawa et al., 1995).

XCTD Field Test
(BSH, A. Sy)

An XCTD field evaluation in the eastern North Atlantic from 9 to 14 December 1994 has completed a series of field trials started in 1992. The first at-sea tests revealed significant deficiencies in the system's performance (Sy, 1993). The urgent need to improve the reliability and accuracy of XCTD measurements led to the development of various modified devices by the system's manufacturer, Sippican, Inc. The combined modifications result in a new configuration of the MK-12 hardware, firmware and software, and also include changes of the XCTD probe. After several field and laboratory tests carried out by the manufacturer (Elgin, 1994), the results were sufficiently promising to convince the customer of significant improvements of the overall system performance. The purpose of the last field evaluation was to check the manufacturer's specification of the final product independently, i.e. from the customer's point of view. The system's accuracy for XCTD measurements is claimed by the manufacturer to be ±.03°C for temperature, ±.03 mS/cm for conductivity, and ±5 m or 2% for depth (Sippican, 1992; 1994).

A total of 12 XCTD probes were calibrated by Sippican, Inc. in September 1994 and made available for this test. The data acquisition system was the same as for the XBT measurements except a faster Compaq LTE/33C and Sippican's software rev. 2.2.1. The XCTD test sites are located west of the British Isles, because this ocean area provides favourable conditions due to its well developed hydrographic stratification in both temperature and salinity.

Severe weather conditions forced a premature end of our regular research programme before we had the opportunity to carry out the planned XCTD field trial. Therefore, it was decided to use a combination of T-5 XBT and test XCTD probes en route home as a poor makeshift substitute to complete our hydrographic section in a rough-and-ready way (XCTD test part A). After successful and problem-free launching of 6 XCTDs at a ship's speed of about 6 knots, we were surprised by a sudden unpredicted favourable change of the weather situation. We returned to the break-off point of the hydrographic section to resume our field work including the originally planned XCTD versus CTD inter-comparisons (XCTD test part B). This field test part was carried out with XCTD drops at 2 regular CTD stations (stat. # 542 and # 546) side by side with the down-profiling of the CTD.

All 12 probes launched gave traces from the sea surface to below 1000 m depth. No calibration failure and no increasing signal noise with depth was detectable. The range of temperature differences between XCTD and CTD traces does not exceed the ±0.03°C limit in the homogeneous mixed layer (Fig. 23) and remains within this limit also for the deeper ocean (Fig. 24).

The conductivity, however, is low with respect to the reference CTD in the upper layer (Fig. 25). This difference becomes smaller with increasing probe depth and eventually falls inside the ±0.03 mS/cm limit in the deeper ocean (Fig. 26). At some profiles a significant discrepancy in conductivity (slow start-up) appeared in the upper 30 to 60 m (Fig. 25). Ordinary air bubbles seem to be responsible for this effect. Trapped in the conductivity cell they cause too low a conductivity measurement until they collapse by increasing pressure. On the other side, micro air bubbles seem to be responsible for the generally reduced conductivity accuracy in the profiles' upper part.

As for XBT probes (Hanawa et al., 1995) the XCTD probes fall faster than specified. The depth fall rate variability is small and the depth error is estimated to be about -30 m at 900 m depth (or about 3.3%). The review of the XCTD depth fall rate will be the next action to be taken by the IGOSS Task Team on Quality Control of Automated Systems (TT/QCAS).

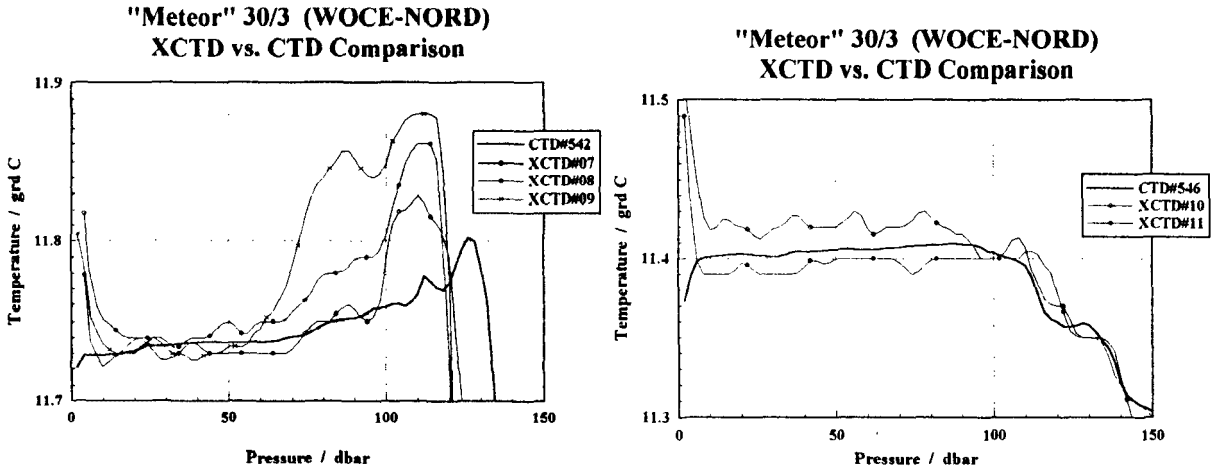

Fig. (23) CTD and XCTD temperature profiles of the upper 150 dbar (a) at stat. # 542, (b) at stat. # 546

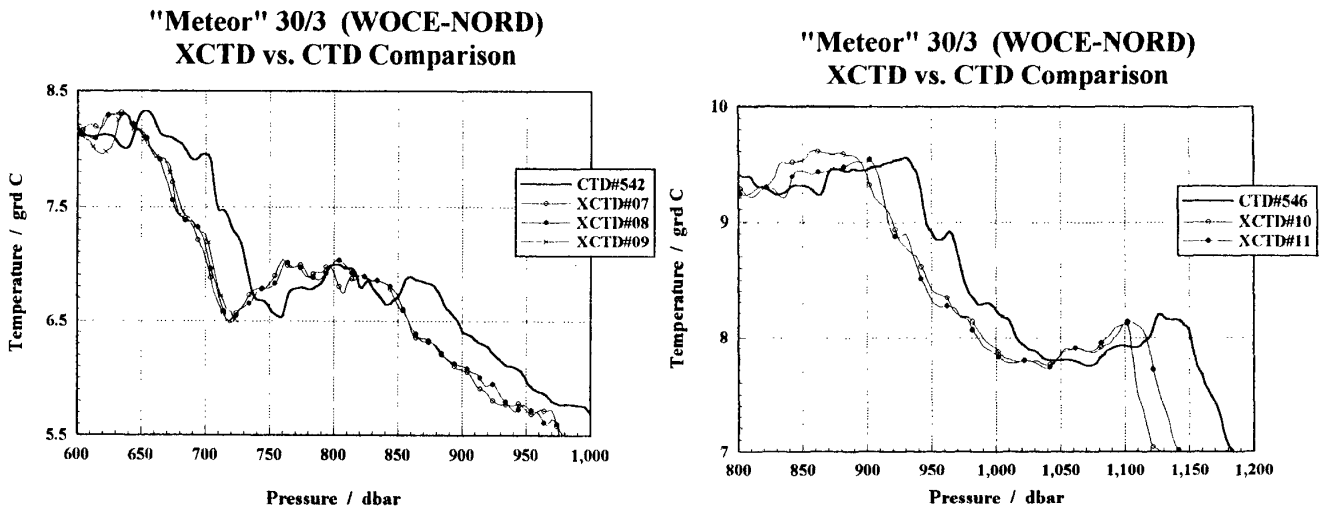

Fig. (24) CTD and XCTD temperature profiles of deeper layers
(a) at stat. # 542, (b) at stat. # 546

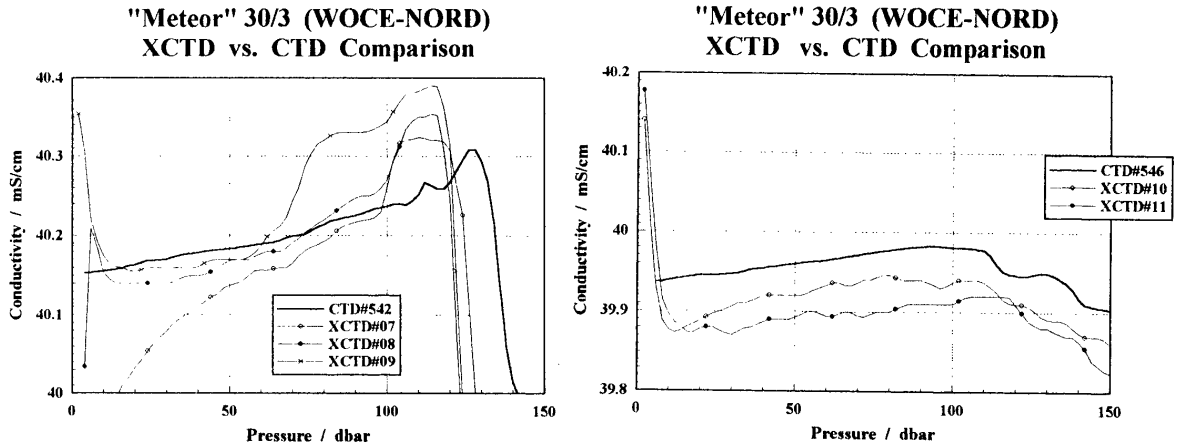

Fig. (25) CTD and XCTD conductivity profiles of the upper 150 dbar
(a) at stat. # 542, (b) at stat. # 546

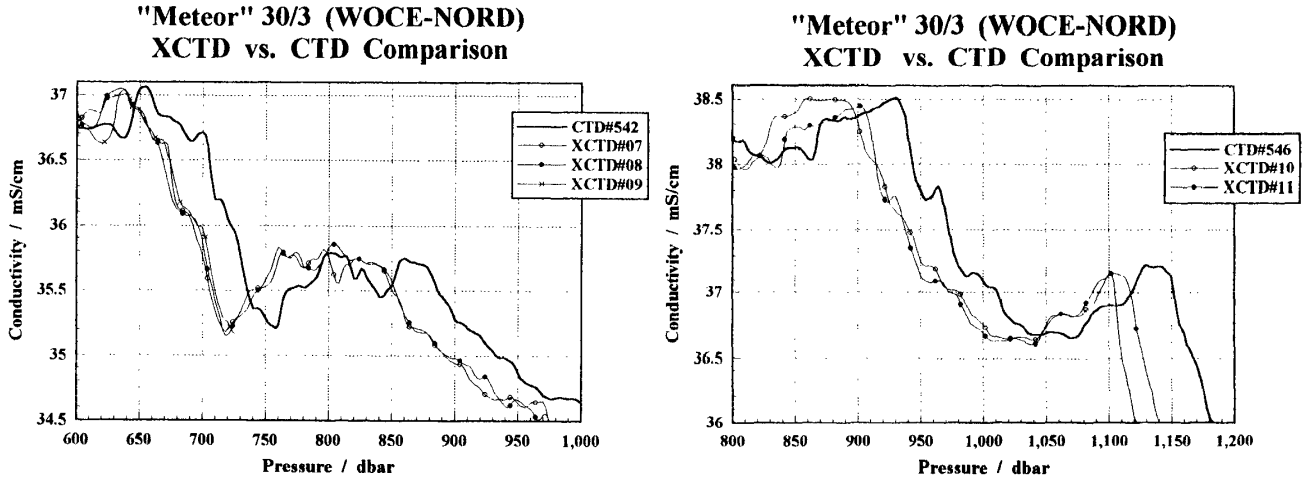

Fig. (26) CTD and XCTD conductivity profiles of the deeper layers
(a) at stat. # 542, (b) at stat. # 546

The results of the field evaluation conclusively reveal that modification efforts of the manufacturer during the last years have resulted in a significant MK-12/XCTD system performance improvement. Obviously most performance difficulties encountered at previous sea trials have been successfully solved and the system is close to the point of meeting the claimed specification. Unsolved deficiencies are the slow conductivity start problem, the reduced conductivity accuracy at low pressure, and the inaccurate depth formula.

- **Sample Oxygen Measurements on WHP-A1**
  (BSH, I. Horn, R. Kramer, F. Oestereich)

Oxygen samples were taken from the rosette bottles right after freon and helium samples. A silicone tube of 20 cm length was slipped over the outlet valve of the Niskin bottle and used as drawing tube. Oxygen flasks were rinsed twice before filling, then filled with at least a 3 bottle volume overflow to avoid the inclusion of air bubbles. Immediately after each oxygen sample was drawn, the reagents $MnCl_2$ and NaI/NaOH were added with the tips of the pipettes below the neck of the oxygen flask. After adding the reagents the flask was stoppered and shaken for about two minutes. Meanwhile the seawater temperature in the rosette bottle was measured with a NTC sensor.

Further analysis was carried out in the laboratory. After removing the stopper 1 ml H_2SO_4 reagent was added and the titration was performed with the oxygen flask. Therefore any loss of iodine was avoided.

Dissolved oxygen analysis was carried out according to the Winkler method modified by Carpenter with a Metrohm Titroprozessor 686 and a double platinum electrode. Polarisation titration was used. The electrodes were driven by a constant current of 1 μA. The resulting voltage was measured as a function of the titrant. Because of the dependence on the sample material (blank, standard, seawater sample) an endpoint determination before any measurement was necessary. During the cruise the voltage of the endpoint was verified and in case of a drift (>20 mV/4-5 samples) an additional correction was applied. The point of equivalence determined from the titration plot is 90- 95% of the endpoint voltage which is the voltage minimum. The calculations were carried out with Microsoft Excel 4.0.

An overview on instrumentation and reagents used, standardisation and calculation procedures carried out and precision estimated follows.

<u>Technical equipment:</u>
Metrohm Titroprozessor 686,
Dosimat 665+ stirrer E649,
Polarizer E585,
Thermometer Testotherm 1100, NTC sensor, accuracy 0.1°C,
calibrated oxygen flasks,
calibrated pipettes for standard solution,
calibrated volumetric flask for standard solution,
calibrated Eppendorf-pipettes for reagents.

Reagents:

Potassium Iodate Stand.: 1 hour at 105°C in a dryer, aliquots of about 0.3567 g; each portion was dissolved in 1 liter pure water; water temperature was measured for correction. The weight of KIO_3 was corrected for air buoyancy.

Sodium Thiosulphate: Merck Titrisol ampoule, 0.01 mol/l; 2 ampoules within 1 liter, 0.02 molar.

Alkaline Sodium Iodide: 600 g NaI/l, 4 molar; 320 g NaOH/l, 8 molar.

Manganous Chloride: 600 g ($MnCl_2$ x $4H_2O$)/l, 3 molar.

Sulphuric Acid: 280 ml concentrated H_2SO_4/l, 5 molar.

All reagents were dissolved into demineralized water.

Blank Determination:

Blanks were determined in demineralized water weekly according the following procedure:

$$1 \text{ ml } KIO_3 + 100 \text{ ml } H_2O + 1 \text{ ml } H_2SO_4 + 1 \text{ ml NaI/NaOH} + 1 \text{ ml } MnCl_2$$

After titration another 1 ml KIO_3 was added followed by a second titration. The difference of the thiosulphate volumes was regarded as reagent blank. Five blanks were determined and the difference between them should be within 0.004 ml. The blank value (mean) is an important part of the calculation of oxygen concentrations.

Standardization:

Standards were determined in demineralized water daily according the following procedure:

$$10 \text{ ml } KIO_3 + 100 \text{ ml } H_2O + 1 \text{ ml } H_2SO_4 + 1 \text{ ml NaI/NaOH} + 1 \text{ ml } MnCl_2$$

The titration of the standard was repeated three times. The scatter of the thiosulphate titer should be less than 0.05% (0.002 ml). For further calculations the mean was used. While standard determination the ambient temperature was measured and included in the calculation.

Calculation of Oxygen Concentrations:

$$O_2 = \frac{\dfrac{\left(V_x - V_{blk,dw}\right) * V_{I03} * N_{I03} * 5598}{\left(V_{std} - V_{blk,dw}\right)} - 1000 * DO_{reg}}{\left(V_{bot} - V_{reg}\right)}$$

V_x = thiosulfate titer of sample

$V_{blk,dw}$ = thiosulfate titer of pure water blank (cm^3)

V_{std} = thiosulfate titer of standard (cm^3)

V_{bot} = volume of sample bottle (cm^3) at sampling temperature

V_{reg} = volume (2 cm^3) of sample displaced by reagents

V_{IO3} = volume of iodate standard (cm^3) at temperature of standardization

N_{IO3} = normality of iodate standard (= 6 molarity) at temperature of standardization

DO_{reg} = absolute amount of oxygen added with reagents, 0.0017 ml (Murray et al, 1968)

O_2 = oxygen concentration in sample (ml/l)

Calculation of KIO_3 Standard:

$$N_{I03}(t_p) = \frac{W_{KI03} * F_{buoy,KI03} * 6}{V(t_p) * 214.001}$$

$$V(t_p) = V(20) * \left[1 + \alpha v (t_p - 20)\right]$$

$N_{IO3}(tp)$ = normality of iodate standard (= 6 molarity) at t_p°C
W_{KIO3} = weight of KIO_3 in air
$F_{buoy,KIO3}$ = buoyancy correction for solid KIO_3 (=1.000159)
214.001 = 1987 molecular weight KIO_3
t_p = preparation temperature of KIO_3 solution
$V(t_p)$ = volume of volumetric flask at temperature, t_p°C
V(20) = volume of volumetric flask at 20 °C reference temperature
αv = cubial coefficient of thermal expansion $1.0*10^{-5}$ for borosilicate glass

Normality of KIO_3 standard at reference temperature 20°C:

$$N_{I03}(20) = N_{I03}(t_p) * \left[p_w(20) / p_w(t_p)\right]$$

$N_{IO3}(20)$ = normality KIO_3 at reference temperature 20°C
$N_{IO3}(t_p)$ = normality KIO_3 at preparation temperature
$p_w(20)$ = density of pure water at reference time 20°C
$p_w(tp)$ = density of pure water at preparation temperature

Density of pure water:

p_w = $0.999842594 + 6.793952*10^{-5}*t - 9.095290*10^{-6}*t^2 + 1.001685*10^{-7}*t^3 - 1.120083*10^{-9}*t^4 + 6.536332*10^{-12}*t^5$
t = water temperature in °C

Normality of KIO_3 standard at standardization temperature:

$$N_{I03} = N_{I03}(20) * \left[p_w(t_{std}) / p_w(20)\right]$$

$N_{IO3}(20)$ = normality of iodate standard at 20°C
$p_w(t_{std})$ = density of pure water at standardization temperature
$p_w(20)$ = density of pure water at reference temperature 20°C

Precision:

With the three calibration stations (# 496, 517, 544) the overall error of oxygen measurement between 0.06% fs and 0.18% fc was determined. Between twelve to twenty rosette bottles were released at the same depth to provide independent samples of the same water mass. The results are presented in Fig. (27).

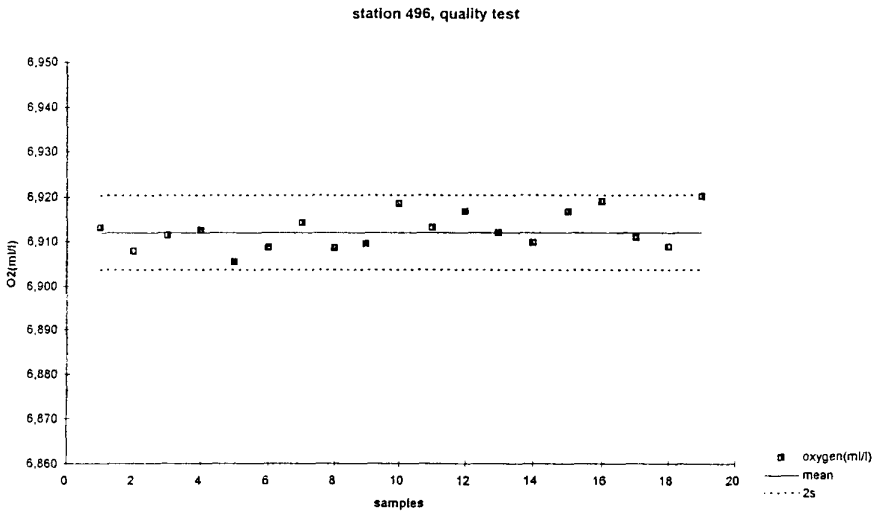

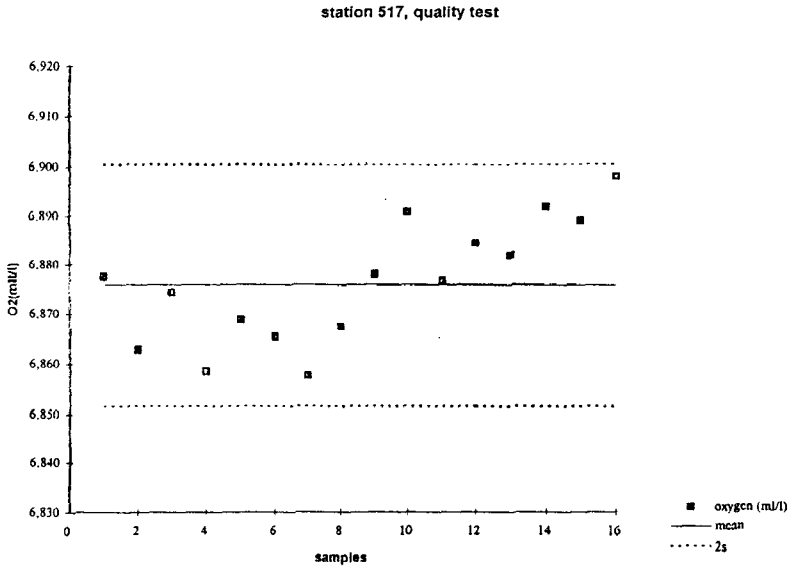

Fig. (27a,b) Results of oxygen measurements at calibration stations, (a) #496,(b) #517

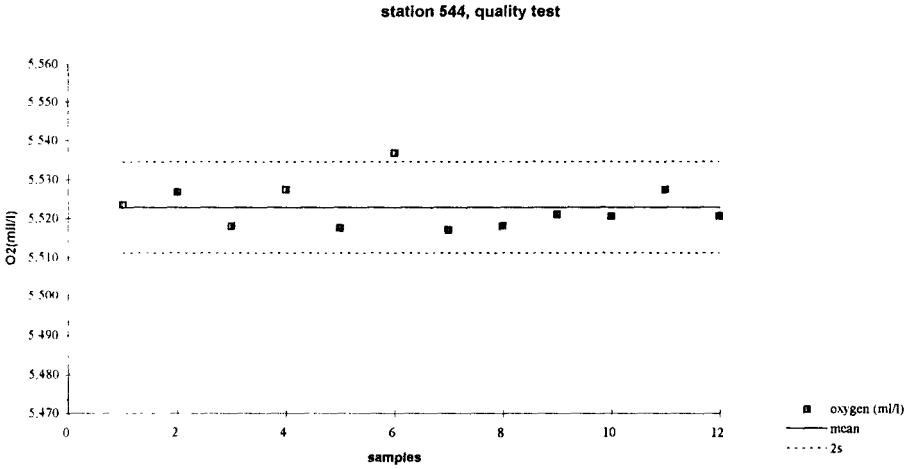

Fig. (27c) Results of oxygen measurements at calibration stations, (c) #544

- **Nutrient Measurements on WHP-A1**
  (MAFF, D. S. Kirkwood)

The Skalar SA-4000 auto-analyser and data-system gave trouble-free service throughout the cruise. 1257 seawater samples from 63 CTD stations were analysed for nitrate, phosphate and silicate. 142 additional analyses were undertaken in the course of quality control procedures.

Equipment and methods:

Nitrate, phosphate and silicate were determined simultaneously using the SA-4000 segmented continuous-flow auto-analysis system manufactured by Skalar Analytical BV, Breda, Netherlands. The data acquisition and processing software was version 6.1. The chemical methods used are contained in Skalar's (1994) booklet on seawater analysis and are summarised briefly here.

Nitrate: Following on-line reduction of nitrate to nitrite by passage through a packed column of copperised cadmium granules, a diazo-couple compound is formed at pH < 2.4 as described by Bendschneider and Robinson (1952). Strictly speaking, it is the sum (nitrate + nitrite) that is measured, as nitrite, but on the assumption that in oceanic work the nitrite contribution is negligible, the term nitrate is used throughout.

Phosphate: Murphy and Riley's (1962) procedure is followed in respect of sulphuric acid and molybdate concentrations, but their antimony-containing salt is omitted and the reducing agent is hydrazine at 65°C, as in the Oregon State University method (Atlas et al., 1971).

Silicate: As the sensitivity of the method is lab-temperature dependent, the entire manifold is made from polypropylene tubing and is wound externally around the heat exchanger simultaneously used in the phosphate method. This is very similar to the construction proposed by Grasshoff et al. (1983), and the chemistry is identical.

These methods are fully discussed and described by Kirkwood (1995), and using them, the MAFF (Lowestoft) laboratory has produced high-quality results in the two most recent ICES nutrients inter-comparison exercises (Kirkwood et al., 1991; Aminot et al., 1995).

Procedures:

Samples were drawn from the rosette bottles directly into 1-litre polyethylene bottles having a separate neck-insert seal secured by a screw cap. Bottles and seals were rinsed twice with sample and the same two crates (2 x 24) of bottles were re-used continuously throughout the cruise with no cleaning between samples other than the rinsing procedure.

The sub-sample for analysis was decanted into an 8 ml sampling cup, rinsing copiously. Cups were used new, as supplied, without any pre-cleaning other than the rinsing with sample and a dummy-run at the first CTD station. The same 40 cups were re-used throughout the cruise and at no time were they allowed to dry out. As a protection against contamination, this regime has

proved to be as good as any, better than some, and is simple. Filled cups were placed on the carousel in small batches (six or seven) to minimise the period they might be exposed to airborne contamination, and to prevent significant bias due to evaporation.

Working calibration solutions were freshly prepared daily. A full calibration accompanied each CTD station's samples and consisted of five concentration levels with linear intervals in the ranges 0 - 24, 0 - 2, and 0 - 24 μmol/l for nitrate, phosphate and silicate respectively, utilising second-order curve-fitting although the response to concentration is essentially linear in these ranges, 0 - 0.66, 0 - 0.12 and 0 - 0.50 absorbance, respectively. For deeper waters in the later part of the cruise (station 535 onward), these ranges were extended as required, to accommodate silicate concentrations approaching 40 μmol/l.

A single analysis of each sample was considered sufficient unless a result appeared to be in any way oceanographically inconsistent, in which case the analysis was repeated. Such events were rare and were generally attributable to slight but significant phosphate contamination. Analyses were, in most cases, completed within three hours of the rosette's arrival on board. Results were obtained initially on a μmol/l basis and subsequently recalculated to μmol/kg taking account of salinity and laboratory ambient temperature, 18 - 20°C.

Quality Control:

On November 16th at the first CTD station (# 491/1), twenty-three sampling bottles were closed at the same nominal depth as part of rosette and CTD testing procedures and residual water from these bottles was collected in a 25-litre carboy for nutrients quality control purposes. This bulk (QC) sample was kept cool (in the rosette handling laboratory) but not refrigerated. A 150 ml sub-sample was taken daily and analysed, in duplicate, in the course of the analysis of rosette samples from each CTD cast.

Note: Each analytical run begins with a full calibration, which is then followed by the rosette samples (in decreasing order of depth) interposed between two replicates of the QC sample. These two replicates are also designated drift samples; they are analyzed over an hour apart, and are a check on any (chemical) sensitivity drift that may occur during the run. Sensitivity drift, detected as a difference in net peak heights (i.e. after subtraction of the baseline), is assumed by the data-system to be linear, and the signal from each rosette sample is individually corrected, pro rata, according to its position in the run, before its concentration is calculated using the calibration data. Apparent concentrations are calculated (uncorrected) for the two 'drift' peaks so that the extent of any drift can be visualised.

No significant drift was observed in phosphate or silicate during any analytical run, but for nitrate a consistent trend was evident, the second QC replicate almost invariably producing a slightly lower result than the first, the difference between their means being 0.24 μmol/l (1.4%). This observation is entirely consistent with the chemistry and hydraulics of the nitrate determination, negative drift resulting from a degradation of the reduction column's wash-out characteristics due to increasing dead-volume as metal is consumed. It follows that the result produced by the first QC replicate is the more accurate because its analysis occurs immediately after calibration and is therefore

virtually unaffected by drift. The summary of the QC data takes account of this by treating only but for phosphate and silicate, data from both QC replicates are treated as equivalent and are pooled. Full QC data are depicted in Fig. 18. Standard deviations are as follows:

	nitrate	phosphate	silicate
relative s.d. (%):	1.38	1.27	0.85

Fig. (28) show a gradual increase in nitrate and phosphate concentrations in the QC sample with time, but no such trend in silicate. This suggests some remineralisation during the 31-day measuring period. The purpose of the sample was to check day-to-day comparability, thereby avoiding serious systematic errors. High stability for this sample over the duration of the cruise was not assumed. It therefore follows that the above standard deviations for nitrate and phosphate are over-estimates, and the true day-to-day precision for nitrate and phosphate is similar to that shown for silicate. Errors from a variety of other sources contribute to these standard deviations:

1. Sub-sampling: (contamination of intermediate container and auto-sampler cups)
2. Calibration: (contamination, stability of calibration materials, gravimetric/volumetric errors)
3. Auto-analyzer: (repeatability of the chemistry, measurement of the chemistry)

Of these, auto-analyzer performance is most amenable to evaluation. A typical sample from station # 535 was analyzed in replicate (x 24) by repeat sampling from a 75 ml container suitably positioned on the auto-sampler after removal of the carousel. Standard deviations are as follows:

	phosphate	nitrate	silicate
relative s.d. (%):	0.36	0.29	0.11

Phosphate performance is the least satisfactory, but its precision approaches the noise level of the system. It is clear that the Skalar SA-4000 analyzer and data-system contribute only a small proportion of the total imprecision associated with the measurement of typical samples.

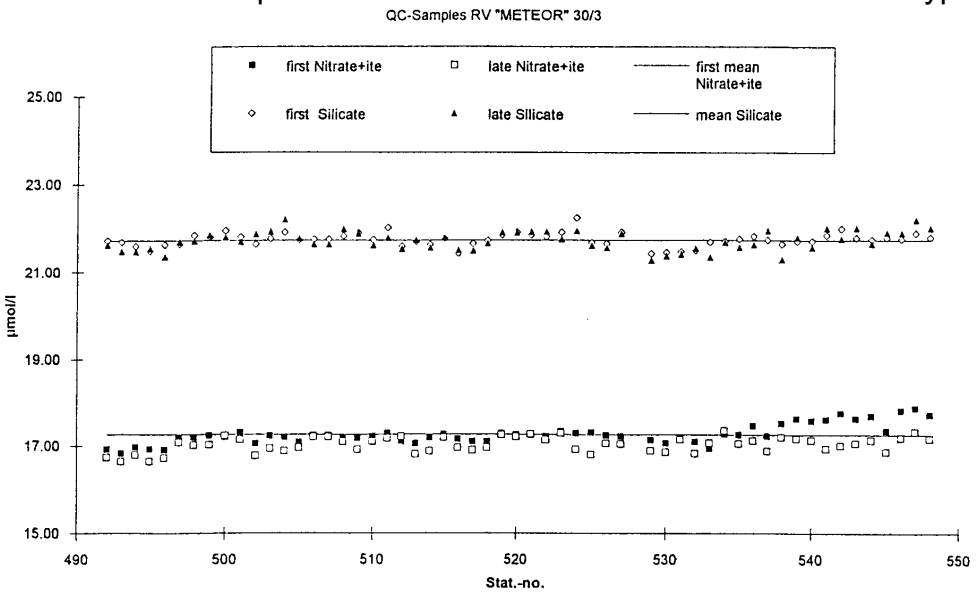

Fig. (28a) Quality control samples, (a) nitrate + nitrite and silicate

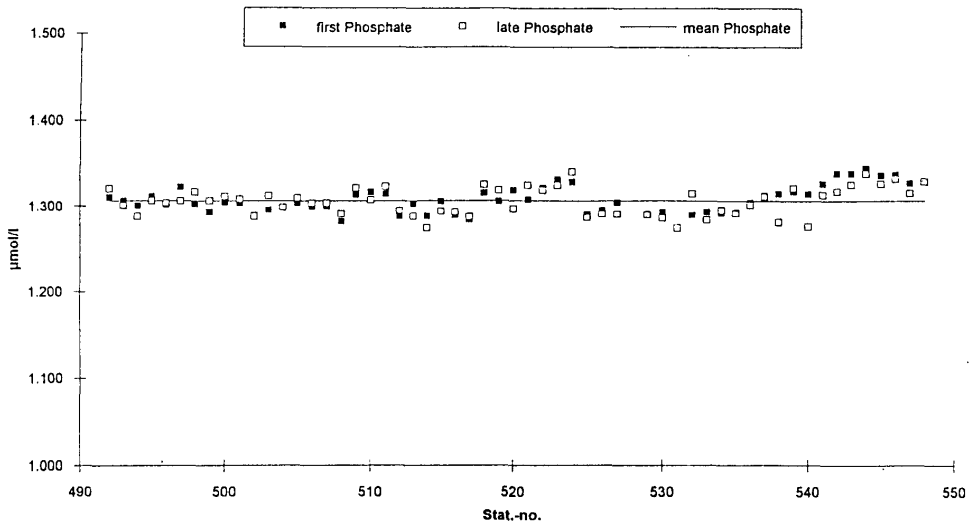

Fig. (28b) Quality control samples, phosphate

- **Tracer Studies on WHP-A1**
  (IUP-HD, R.Bayer and IfMK M.Rhein)

The experimental goal of the tracer programme is the collection and measurement of a representative data set for geochemical tracers along the WHP section A1. The data will be used to determine mixing rates and apparent ages of the water masses in the North Atlantic. Special focuses are on the North Atlantic overturning, the deep boundary currents as observed along the continental margins and the Mid Atlantic Ridge and the formation and spreading of Labrador Sea Water.

The interpretation of the data will be done in close cooperation with all groups involved. The tracer information will be compared with the 1972 GEOSECS data, the TTO/NAS data from 1980/81 in the Northern Atlantic, the data obtained during the first occupation of WHP-A1/E in 1991 and other data available from the region. The evaluation of the tracer fields yields further indication how much and how fast the invasion of the tracer signals from the surface into the deep waters has proceeded. The observations will specifically give starting concentrations for the North Atlantic Deep Water. Tracer concentrations within the overflows will also yield information on the turnover of the water masses feeding the overflows. Moreover, all tracers studied have transient distributions and may be used to study the temporal evolution further on.

Onboard measurements were carried out of the CFCs F11 and F12. Samples for ^{3}He, tritium and ^{14}C (large volume programme) were taken for measurement at the tracer laboratory at Heidelberg. Additional ^{14}C samples for Accelerator Mass Spectrometry (AMS) were obtained and the subsequent analyses will be performed at the Eidgenössische Technische Hochschule Zürich (ETH). Furthermore a new seagoing extraction line for ^{3}He was tested. All measurements were designed to meet the WOCE quality standards.

Tracer Oceanography: Tritium/Helium and Radiocarbon
(IUP-HD, R. Bayer, M. Born, E. Gier, F. Müller)

Operational Details

The sampling programme was divided into two components: small volume samples for analyses of the helium isotopes, tritium and AMS-^{14}C were collected with the rosette system, and on the other hand a large volume ^{14}C-sampling programme was run. Helium and tritium samples were obtained on 58 stations. Seven large volume casts were performed and a total of 70 LV-^{14}C samples was collected.

About 580 helium and tritium samples were collected. About 1 litre of water was sampled in glass bottles for determination of the tritium concentration. In the home laboratory the helium is degassed quantitatively from a certain amount of water and the sample is stored in a vacuum container for several months. During that time tritium decays and the decay product, ^{3}He, is enriched. The latter will be detected with a special high sensitivity, high resolution mass spectrometer. For helium measurement ca. 40 cc of sea water was sampled in a copper tube sealed with pinch-off clamps. Analyses will be performed on-shore with a dedicated helium isotope mass spectrometer after extraction of the helium dissolved in the water.

In addition samples were obtained to test a new seagoing helium extraction system. About 330 samples were taken from the rosette both parallel and supplementary to the conventional sampling procedure. All samples were processed onboard, and the measurements will be done in the home laboratory soon after the end of the cruise. The duplicates to the samples obtained in copper containers as well as several seagoing replicate samples will be used to check the performance of the new system.

Furthermore 32 AMS-^{14}C samples were obtained from the rosette. This programme is supplementary to the large volume ^{14}C sampling and was restricted to the upper water column. The total inorganic carbon dissolved in the samples will be extracted in the home laboratory. Measurement of the carbon isotope ratio will be done at the AMS facility of the ETH in Zürich/Switzerland.

For the large volume programme Gerard-Ewing bottles with a volume of 270 litre each were used. Ten depth levels were sampled on each cast, and a total of 7 stations (Labrador Sea 5, Irminger Sea 1, Icelandic Basin 1) was occupied. The total inorganic carbon dissolved in the samples was extracted onboard using two separate extraction lines, and the CO_2 derived was trapped in sodium hydroxide solution. Further processing of the samples (low-level proportional gas counting) will be done in the home laboratory, and the C14 content will be determined with a precision of 2 permille or better.

Preliminary results

The section WHP-A1W (Fig. 29) shows at the southern (A,C) and northern (B,D) boundaries of the Labrador Sea close to the surface influences of river run-off with its high tritium values. The deep boundary current system at more than 2500 m of DSOW is marked with higher

tritium concentrations from its source region, the Irminger Sea, compared to the water masses of the central Labrador Sea. It also shows a lower $^3H/^3He$ age. The LSW shows a smooth tracer distribution: the mean tritium concentration is ca. 1.65 TU and the characteristic $^3H/^3He$ age ca 7.5 a. The tracer gradients of the deeper GFZW (or NADW) indicate the low ventilation of this water mass.

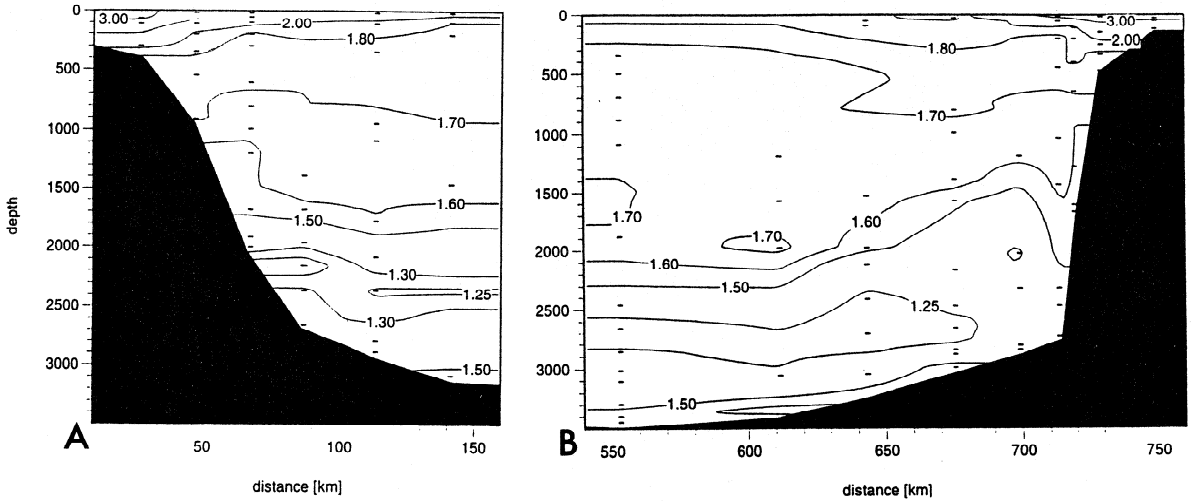

Fig. (29a,b) Distribution of tritium (A, B) along a section across the Labrador Sea (M30/3, WHP-A1W).

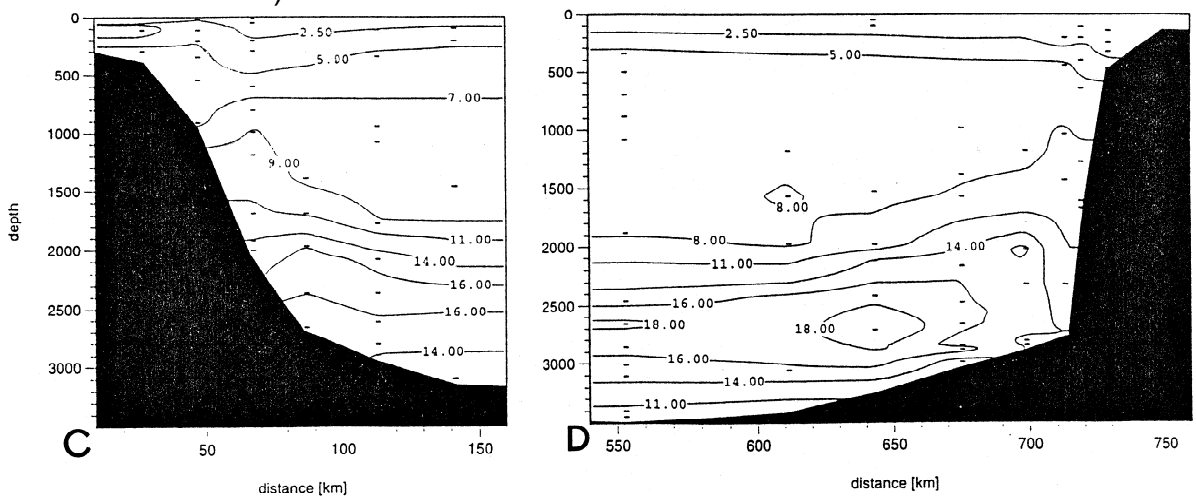

Fig. (29c,d) Distribution of $^3H/^3He$ age (C, D) along a section across the Labrador Sea (M30/3, WHP-A1W).

Tracer Oceanography: CFCs
(IfMK, M.Rhein, P.Heil, A.Schaub)

Operational details

During leg M30/3, the CFC components F11 and F12 have been sampled on 54 stations and about 700 water samples have been analyzed. About 10 to 30 ml of seawater are transferred from 10 liter Niskin bottles to a Purge and Trap device using 100 ml glass syringes. The O-rings

and valves as well as the stainless steel springs of the 10 liter Niskin bottles have been precleaned. The gases are separated on a ss packed column, and detected by electron capture detection, following the procedures described in Bullister and Weiss, 1988. Blanks of the measurement system and the syringes are determined by degassing CFC free water, produced by purging ECD clean Nitrogen permanently through 10 liter seawater. The blanks were lower than 0.005 pmol/kg for both, F11 and F12. Calibration is done using a gas standard with near air concentrations kindly provided by R. Weiss, SIO. The values are therefore reported according to the SIO scale. Calibration curves with 7 points are carried out before and after the water analysis of a station. It is assumed that the efficiency changes linearly in time between the two calibration curves. CFC concentrations are calculated by using the two neighboured calibration points, assuming, that the calibration curve is linear between these points. Reproducibility was checked by replicate measurements, at least 4 pairs at each station. The mean reproducibility for single stations varied for both components from ± 0.5% to ± 2.0% with a mean of ±1.1%.

Preliminary results

Although the Labrador Sea section could not be completed due to bad weather, some of our stations (497-499) represent the central Labrador Sea (Fig. 30). The CFC-11 concentrations of LSW (Labrador Sea Water) were as high as 4.5 pmol/kg, reflecting the recent vigorous convection activities. Similar high values are observed near the bottom in the Denmark Strait Overflow Water (DSOW). This high tracer burden originates north of the Denmark Strait, where the overflow water was subject to convection. After overflowing the sill, the neighboured water masses in the Irminger Sea (mostly LSW) are entrained. Between those tracer maxima, a CFC minimum zone connected to the intermediate salinity maximum is found. They characterize the Gibbs Fracture Zone Water (GFZW), which is a mixture of CFC poor Iceland-Scotland Overflow Water and entrained North East Atlantic Water. The NEAW adds the salt and the small CFC signal characteristic for this water mass in the sub-polar North Atlantic.

The CFC concentrations in the LSW of the Irminger Sea (Fig. 31) are only slightly lower than in the Labrador Sea. These surprisingly high values found in the Irminger Sea, indicates that most likely newly formed LSW invades the Irminger Sea within 8 months, which is faster than previously thought.

The horizontal CFC distribution shows the CFC minimum of the GFZW in the Irminger Sea spreading along the basin except the western edge. On the bottom of the western flank, the high tracer signal of the DSOW can be observed in two or even three near bottom patches, indicating that probably more than one flow core of the DSOW exists. These features were also observed in the tracer distributions measured in 1991 (Meteor cruise M18).

The CFC concentrations in the LSW of the Iceland basin are drastically lower than in the Irminger Sea (Fig. 32); they reach at the maximum 2.8 pmol/kg CFC-11 above the Eriador seamount, whereas the Labrador Sea and the Irminger Sea exhibit water with 4.4 pmol/kg CFC-11. Moreover the LSW in the Iceland basin is warmer and saltier. These features point to a LSW component in the Iceland sea which is older than the one in the Irminger Sea. On both cruises, M18 and M30, the most pronounced LSW was found above the Eriador Seamount, which could be a topographic guidance to the inflow of LSW into the Iceland basin.

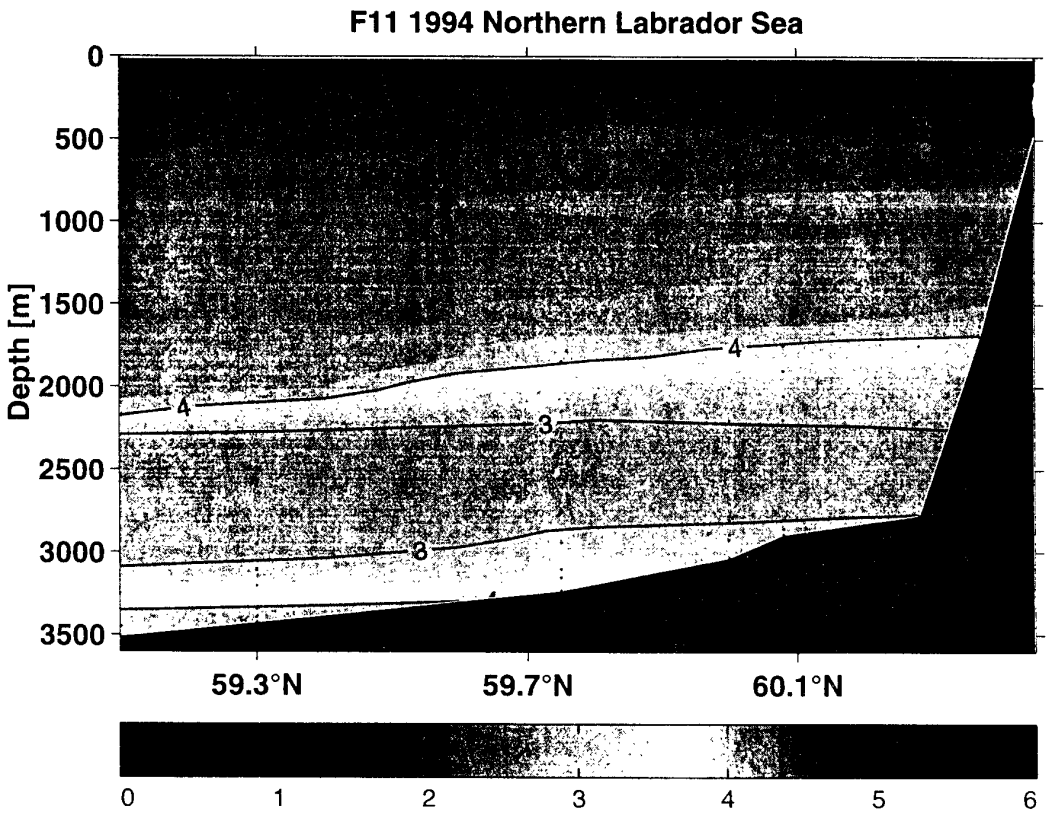

Fig. (30) CFC11 section (pmol/kg) of the northern part of the WHP-A1W Labrador Sea section

On the eastern flank of the MAR, the tracer core of the GFZW water is found with high salinities near 34.97 and a CFC-11 signal of 2.5 pmol/kg. The salinity and the tracer maxima decrease off the ridge. Below the GFZW, water with decreasing CFC concentrations and, similar to the results from 1991, decreasing F11/F12 ratios near the bottom are observed.

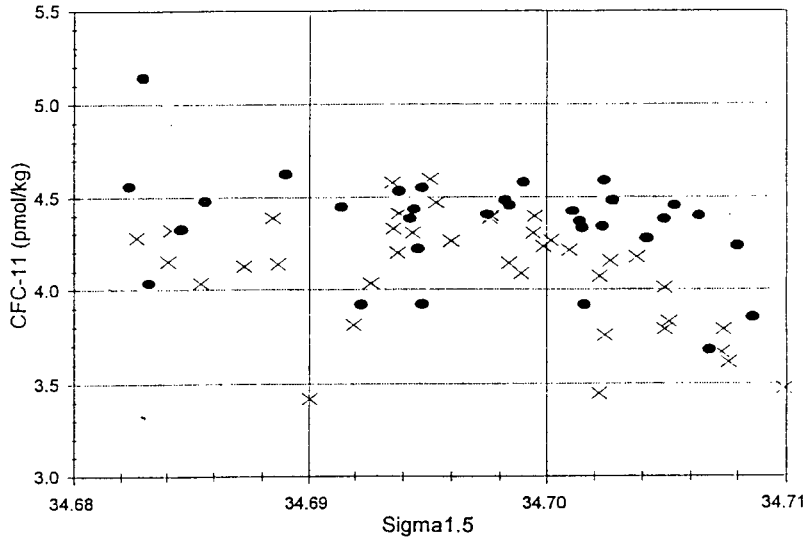

Fig. (31) CFC11 concentrations vs $s_{1,5}$ for the stations in the Labrador Sea (l) and the central Irminger Sea (x). This density range characterizes the Labrador Sea Water (LSW)

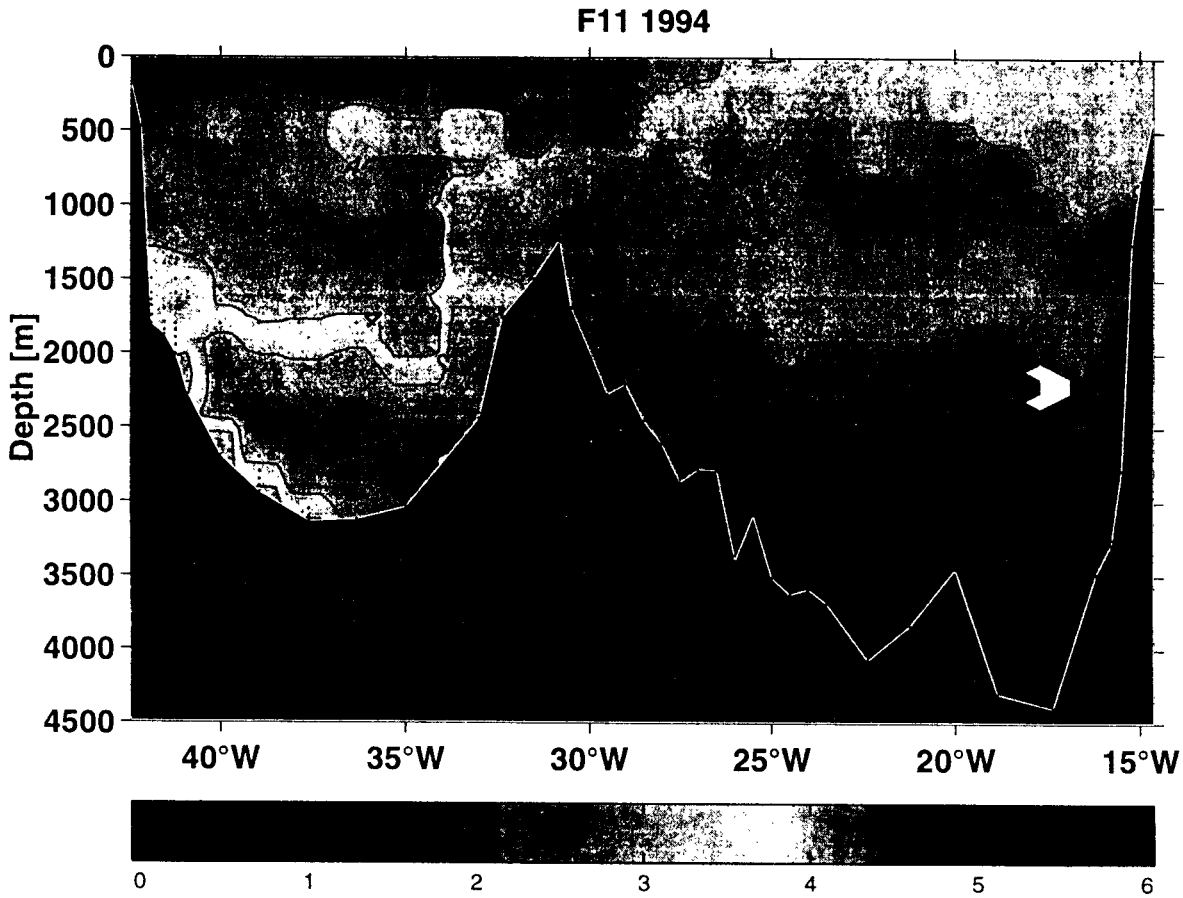

Fig. (32) CFC11 section (pmol/kg) along section WHP-A1E

The lowest concentrations are observed in the Lower Deep Water (LDW) which enters the Eastern Atlantic through the Romanche (near the equator) and Vema Fracture zones (at 11°N). LDW is a mixture of water from the Circumpolar Current (salinity poor, cold and freon poor) and overlying remnants of the overflow water masses mostly from the Denmark Strait. The CFC-11 concentrations found in LDW entering the Eastern Atlantic through the Vema Fracture Zone was 0.05 pmol/kg in March 1994. The CFC-11 concentrations in LDW in the subpolar North Atlantic was found to range between 0.05 to 0.07 pmol/kg, indicating further mixing of LDW with neighboured water masses carrying CFCs.

Surprisingly high CFC values (2.6 pmol/kg) and low salinities were observed near 16°W, in the density range characterizing LSW. The Salinity/CFC-11 correlations of this water compared to the correlations in the Labrador and Irminger Sea in 1994 shows that despite the low salinities the water was not formed in 1994 or 1993 but after 1990. The water could not be older, because of its high CFC content. The original CFC level the water received during its formation in the Labrador Sea has to be higher than the values observed at 16°W. Thus the time scale of the spreading of LSW in the subpolar North Atlantic is significant faster than previously thought.

5.3 JGOFS Programmes:

5.3.1 The Control Function of the Carbonate-System in the Oceanic CO_2 Uptake, WHP-A2

(IfMK/J. Duinker, SIO/C. Atwood, IfMK/A. Körtzinger, S. Schweinsberg, A.v. Hippel, C. Senet)

The parameters to determine the oceanic carbonate system are partial pressure of CO_2 (pCO_2) in seawater, total carbonate concentration (TCO_2) , alkalinity and pH. The goal is to investigate the CO_2 exchange between ocean and atmosphere in a regional and seasonal resolution to contribute to a global budget assessment. Alkalinity and TCO_2 were determined by potentiometric (alkalinity) and coulometric titration (TCO_2) from hydrocast samples taken at 28 out of the 53 stations of the cruise (694 samples in total). During the whole cruise two automatic systems were operated to continuously measure the pCO_2 and the pH, respectively.

While these two systems measured the properties of surface seawater obtained by the ship's pumping device, with the latter system also several samples from the hydrocast bottles were measured for evaluation of system performance. At some occasions, samples for alkalinity and TCO_2 determination were drawn from the seawater line to perform a consistency check between all four parameters (21 samples).

To detect the anthropogenic signal in dissolved carbon, a recalculation of pre-formed values can be carried out using information about the 'history' of the water obtained from oxygen, nutrient, alkalinity and TCO_2 values. The nutrient and oxygen data obtained during this cruise will be used for this purpose.

Another way to follow the invasion of anthropogenic CO_2 into the ocean is by monitoring the C-12/C-13 ratio, since CO_2 emitted by fossil fuel combustion is depleted in C-13. From the hydrocasts, samples were taken for C-13 analysis at 18 stations (359 samples). These are being measured at the Institute for Pure and Applied Physics at Kiel University, Germany. From the same samples the O-16/O-18 ratio can be measured. This will be done for selected samples.

The pCO_2 of seawater is controlled by physical (cooling, wind stress) and/or biological (photosynthesis/respiration) processes. As a means to trace the relevance of biological processes, seawater samples from the upper 200 m of the water column were filtered for the determination of chlorophyll a were taken and filtered at about 30 stations (123 samples).

Preliminary Results

The surface waters along the entire transect contain almost its full component of anthropogenic CO_2 (ca. 62 $\mu molkg^{-1}$). Anthropogenic CO_2 has penetrated through the entire water column west of the Mid-Atlantic Ridge: even in the deepest waters (ca. 5000 m) a mean value of 10.4 $\mu molkg^{-1}$ excess CO_2 was estimated (Körtzinger et al., 1996).

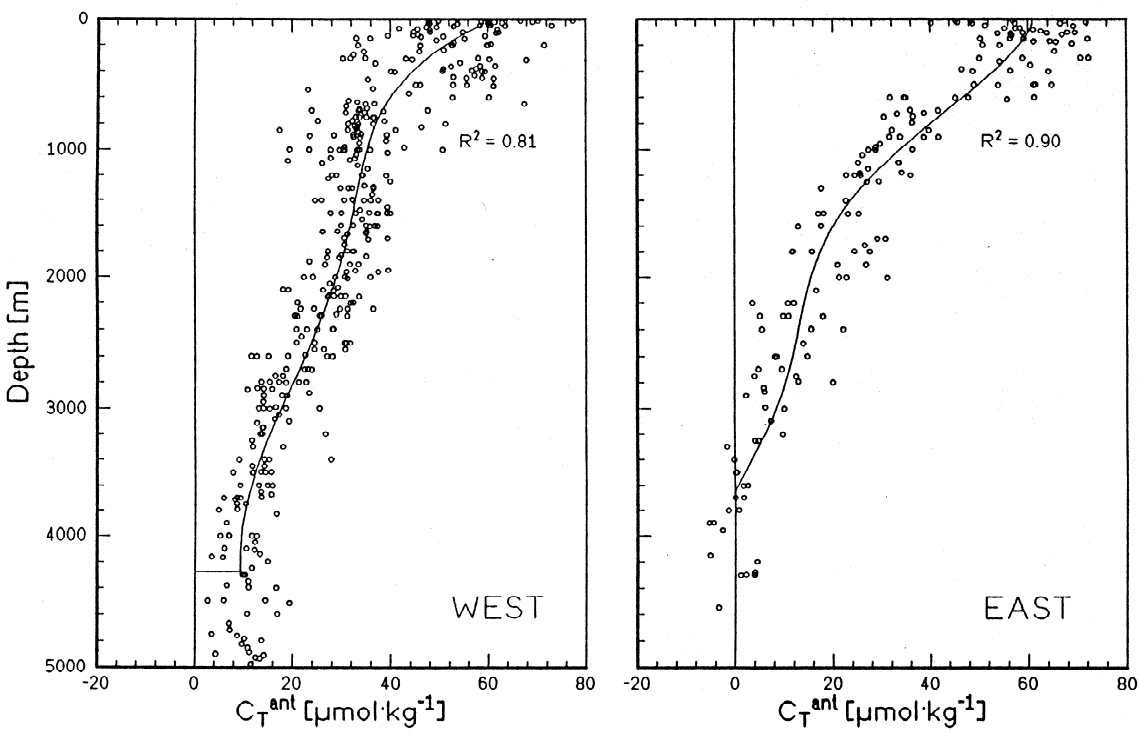

Fig. (33) Cumulated depth profiles of C_T^{ant} for the western (left) and eastern (right panel) basins of the North Atlantic Ocean along WHP-A2 in 1994. Also shown are the third polynomial least squares fit functions.

5.3.2 The Ocean as a CO_2 Sink: complimentary Studies of the Baltic Sea and the North Atlantic, WHP-A1

(IOW, B. Schneider, H. Thomas, R. Prado-Fiedler)

During the cruise leg M30/3 measurements of two parameters of the oceanic carbonate system were performed along the WOCE lines WHP-A1W and WHP-A1E: the CO_2 partial pressure in surface water (pCO_2) was measured continuously and total carbonate (TCO_2) profiles were recorded at all stations in 8-12 depths.

The aim of the measurements is the calculation of fluxes of inorganic, dissolved carbon. With the data from the pCO_2 measurements the exchange between the atmosphere and the surface of the ocean can be estimated. In addition with data of water masses and their movement it is possible to get an idea of horizontal and vertical transport of carbon in the subarctic North Atlantic. In addition to these three parameters we make an attempt to develop a model of all fluxes of dissolved inorganic carbon in the ocean and between the ocean and the atmosphere.

<u>Analytical methods:</u>

TCO_2 was determined by a coulometric method (SOMMA). The analytical precision was better than ± 1 µmol/kg. The results were checked by measurements of standard waters and by determination of the standard deviation. Also comparisons of the TCO_2 contents of very

deep water with results of the earlier cruise M18 showed a very good agreement. pCO_2 was determined by equilibration of an air stream with a continuous flow of sea water and subsequent detection of CO_2 by an infra red spectrometer. Due to the missing of standard water it is difficult to determine the error of the measurement.

Preliminary results

The calculation of the pCO_2 requires data from the ship's meteorological station, but they have not been available yet. So instead of exact results only a first view of the pCO_2 data can be given:

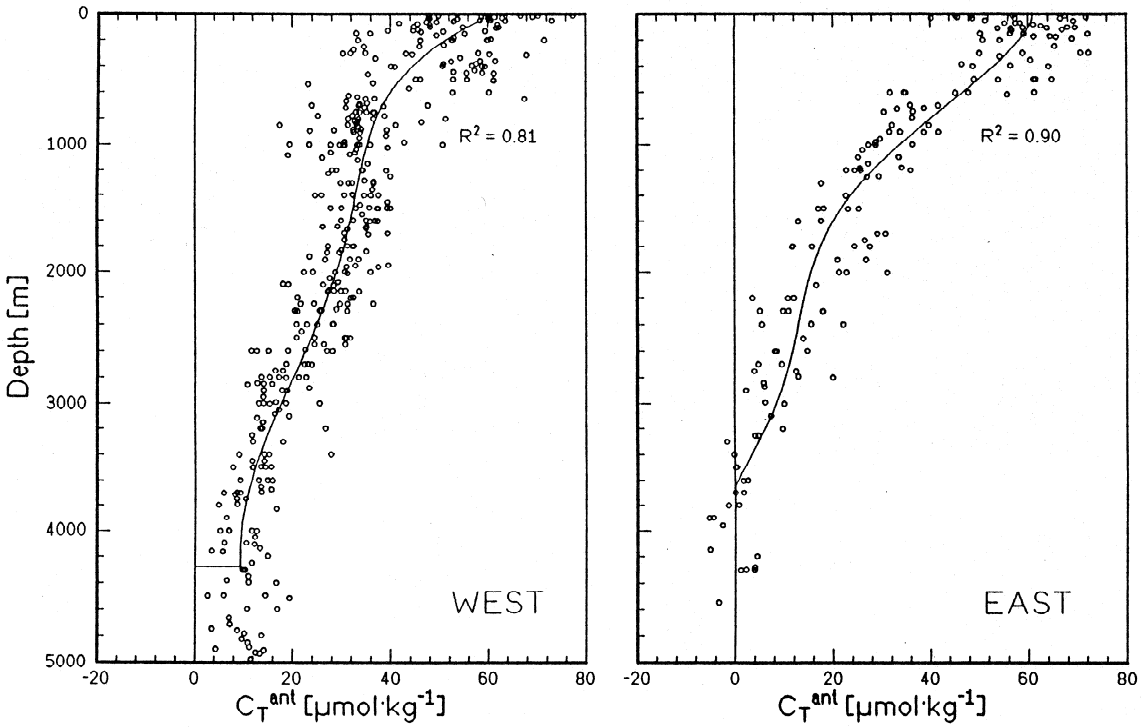

Fig (34) Profiles of total carbonate concentrations for selected stations (#515, #529, #541) of M30/3, section WHP-A1

The range of the pCO_2 of the surface water was approx. 360 ppm ± 20 ppm except in coastal areas. Thus it was very close to the pCO_2 of the air (≈360 ppm). This means that the pCO_2 of the surface water was in the range of the saturation partial pressure and that only low CO_2 fluxes occur between the surface of the ocean and atmosphere.

Fig. (34) shows three profiles as examples for the TCO_2 data, which were determined on the WOCE line WHP-A1E, stat. 515 situated in the Irminger Sea, stat. 529 in the Iceland Basin and the (JGOFS) stat. 541 in the Rockall Plain. The profile of stat. 515 shows the typical behaviour of TCO_2, in the Irminger Sea and also in the Labrador Sea, which is similar to the nutrients. In all profiles the lowest TOC_2 values can be observed in the mixed surface layer (MSL). The profile of stat. 529 shows a typical behaviour of the eastern part of the Northern Atlantic Ocean. In depths between 300 m (stat. 515) and 800 m (stat. 529 and 541) the Subpolar Mode Water (SPMW) is identified in different distances to its origin: at the stations 529 and 541 is the older

water mass with higher TCO_2 values (2160 µmol/kg) than in station 515 (2153 µmol/kg). The water between 1500 m and 2000 m you can identify as the young Labrador Sea Water (LSW) with its low TCO_2 contents (2145-2150 µmol/kg). The increase in TCO_2 (2160-2170 µmol/kg)in the depth between 2500 m and 3000 m is caused by the older Iceland Scotland Overflow Water (ISOW). At the deepest station 541 occurs the Antarctic Bottom Water (AABW) with the highest TCO_2 values 2190 µmol/kg), which are caused by the highest degree of remineralisation of organic matter. Only in the area around stat. 529 there was in the depth between 300 m and 500 m a water mass as well with low TCO_2 contents (2150 µmol/kg) as with low nutrient contents. This is a small stream of Subpolar Surface Water (SPSW).

5.4 Individual Programmes:

5.4.1 ^{129}I from Nuclear Fuel Processing as an Oceanographic Tracer
(CSCSM-CNRS, G. M. Raisbeck)

We have collected 78 samples of 1 l each from WOCE sections A2 and A1. Samples should be resolving the depth profile as good as possible. Stations sampled are typical of the oceanographic regime encountered; four stations per North Atlantic Basin, one in each BC region, two in the centre of the basin are now ready for analysis. The samples have been prepared for measurement. This will proceed in the next year.

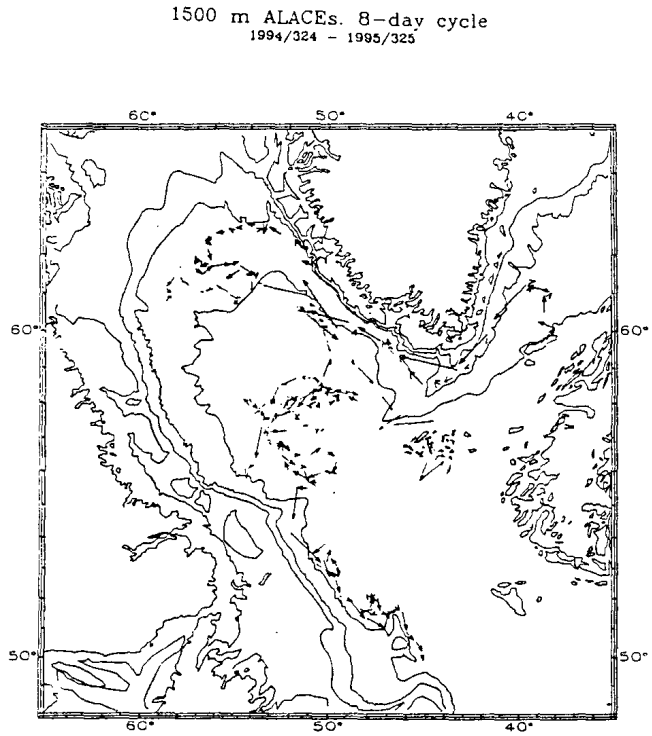

Fig (35) One year of ALACE data in the Labrador Sea at 1500 m depth. One arrow represents one week's displacement of a float. Individual floats are grey-coded. The bathymetry is overlaid to indicate regions where its effect seems to result in rectified or sluggish flow.

5.4.2 ALACE Float Deployments
(SIO, R. Davis; WHOI, B.Owens)

During Leg M30/3 in all six ALACE floats were deployed. Two had additional CTD-sensors, four only temperature sensors. After deployment all floats stayed as planned for 24 hours on the surface and then sank to the pre-assigned pressure level of 1500 dbar. One S-PALACE (CTD) died after one week, a temperature P-ALACE died in May 1995. Four floats are still working. The tracks of the floats for the first year of deployment are shown in Fig (35).

6 SHIP'S METEOROLOGICAL STATION

6.1 Leg M30/1
(DWD/SWA, G. Kahl)

When "Meteor" left Las Palmas de Gran Canaria on September 6th, 1994, the Azores High was at position just south and west of the archipelago thus blocking a cold front extending from an Icelandic gale center. The Northeast Trade Winds were blowing, force being 6 Bft.

This synoptic situation did not last long, however. The gale center moved from southwest of Iceland to the northern part of Azores and then to the southwest, reaching the Bahamas and swinging into the Caribbean. South of this transatlantic front the subtropical high had sent a wedge into Portugal. Consequently, light northerly winds only were experienced by the "Meteor". Winds backed west the next day as the research vessel progressed north, force being 5 Bft on September 10th, too.

By then, however, a gale center had developed in the Gulf of St. Lawrence, and a secondary low had made its way across the ocean to the Celtic Sea where it intensified. North 6 Bft resulted for "Meteor". During September 12th, the next low arriving from the west developed into a gale center even before reaching our research vessel's longitude to that northwesterly gales force 7 to 8 Bft tried to impede our journey on September 13th and 14th, subsiding by then. While the low responsible for that kind of weather developed further into a storm center creating havoc in the North Sea, a high was building over Iceland, its wedge reaching "Meteor"'s working area. Having arrived at our site, the wedge strengthened into a high by itself. As a result, winds were light to that scientific work was not impeded. Even the swell did subside. Favourable conditions accompanied the "Meteor" into the Channel while conditions in the North Sea took their time to calm down on September 18th. Meanwhile, another low had arrived to the southwest of Iceland and its secondary low west of Ireland. During the last days of the voyage this secondary low moved southeast to east, thereby intensifying. "Meteor" strived to keep just ahead of it, experiencing moderate winds from southerly to southeasterly directions.

6.2 Leg M30/2
(DWD/SWA, E.Röd)

The behaviour of the atmosphere was controlled by the vicinity of a quasi-permanent westerly jet with a continuous series of ridges and troughs and proved to be very close to the climatic average of this belt of prevailing westerlies. The weather was somewhat better than expected

before, because in spite of the advanced season no really extreme pressure was recorded. The lowest value at the ship was 984 hPa, the mean 1010 hPa, the deepest low over the northern Atlantic just around 970 hPa. Prevailing wind direction was 245°.

Six well developed cyclonic events were responsible for a remarkably high mean wind speed of 25 knots. These eddies originated over the western subtropical Atlantic or south of the Great Lakes over the central USA and moved east or northeast. This movement however was so slow, that a long lasting intense cold sector flow could persist for several days. The series of cyclonic curls ended with a low that had formed over Kentucky and then swept in a large curve to Belle Isle Strait and the Grand Banks. In connection with this low quite an unusual exciting development took place: already since the 25 October at low latitudes about 27°N the birth of a tropical disturbance could be seen by the spreading of a bright cirrus field that formed a distinct frontal system later on. Finally, when this depression had assumed the typical structure of a tropical hurricane, it was named "Florence" and remained stationary on its position at first. On 6 November 1994 it was caught by the circulation system of the low over the St. Lawrence Gulf and accelerated towards north- east. On the 8th it reached 41°N just at a distance of 180 nm ESE of Meteor. Here the northern spiral arm of "Florence" met the warm front of the Newfoundland low. At the occlusion point in addition a secondary low pressure core had formed. This oblong shaped complex low now swung towards northeast giving free way to a northwesterly flow from Labrador down to subtropical latitudes.

The temperature changed widely between 11°C and 21°C depending on warm sector- or cold sector conditions. Even higher was the variation of the dew-point: 1°C in fresh arctic air and 19°C within moist subtropical warm air. It was astounding, that also in warm air over colder water no significant fog patches could form. Only twice during the hole cruise visibility was reduced for less than one hour by frontal fog. Due to the cold air advection also the ill-famed Newfoundland Banks were free of fog. The small statistic given below shows a quasi-Gaussian distribution of wind-force with a maximum of frequencies at 6 Bft.

The absolute maximum of wind speed was 64 knots. Calm air was not observed at all. The sea was rather rough at times but didn't exceed 7 m of height. Ship's manoeuvres and scientific station work were temporarily hampered by hard weather but not seriously jeopardized.

Distribution of wind directions and wind force in Beaufort in percent of a total number of 568 hourly observations during M30/2

First obs: 15.10.94, 01 h
Last obs : 08.11.94, 23 h
Number of hourly observations: 568

N	NE	E	SE	S	SW	W	NW	VRB
6	1	1	12	9	13	39	20	0%

0	1	2	3	4	5	6	7	8	9	10	11	12 Bft
<1	1	2	6	13	18	21	18	14	6	<1	<1	0

Rem.: Between the hourly observations different values may have occurred.

6.3 Leg M30/3

(DWD/SWA, E. Röd)

The meteorological conditions during the operational phase of the cruise M30/3 between Hamilton Bank and Porcupine Bank from the 16th of November to the 15th of December 1994.

This leg of the voyage back to Europe was located approximately 900 nm north of the preceding one from Europe to Newfoundland and therefore much closer or even directly underneath the axis of the polar jet stream. Very frequently in the daily radio-soundings maximum winds ranging from 80 to 160 kts could be seen a few thousand feet under the tropopause, which in polar cold air came down as far as 7 to 8 km with temperatures higher than -50°C. Whereas hurricane "Florence" could approach the route of "Meteor" during the preceding leg and join a strong polar front low lateron, the second hurricane "Gordon" - extraordinarily late in the season - remained in subtropical latitudes far away in the south and faded away near Florida. In brief, conditions might be summarized as a typical jetstream weather with rapidly alternating lows and ridges. Cyclonic regime however was prevailing, which may also be seen in the average atmospheric pressure of 990 hPa. Corresponding to these circumstances wind was rather strong with a mean value of 28 kts, that is by 17% more than on the southern leg. Cyclogenetic processes were mostly intense, but not extreme. The most spectacular pressure fall reached 17 hPa in 3 hours deepening a frontal wave into a vigorous storm centre of 950 hPa in the Irminger Sea and Denmark Strait. This vortex produced the heaviest storm of the cruise on the 26th and 27th of November with nearly constant W 10 gushing up frequently into full 12 Beaufort.

This storm was followed by a less windy week which opened a large "weather window" for station work. Between the 5th and the 11th of December a new stormy period made research impossible: rapid pressure fall of nearly 5 hPa/h announced the approach of a vortex nearly equally intense (963 hPa) as the preceding one. The sharp pressure rise in its cold sector originated a long lasting northwesterly to westerly flow. On the 6th of December hurricane-like gusts exceeding 100 knots marked the absolute wind maximum of the whole cruise. Towards the end of November at 59°N/34°W as a counterpart to subtropical hurricanes a typical Polar Low could be observed near the ship. Under weak gradient conditions, which geostrophically could have brought only 2 or 3 Bft, wind remained nearly constantly about 7 Bft. Examining closely the satellite image the sub-scale polar eddy with its characteristic structure could be detected.

On 9 December, 1994 dramatic numerical forecasts suggested to leave the ship's position as soon as possible heading towards the English Channel. Fortunately already on the following day this prognosis was replaced by a quite optimistic one which proved to be correct when "Meteor" had returned to the working area. Under high pressure conditions the transect could be completed without any meteorological problems. This case was quite a good lesson about the reliability of medium range forecasts. It was striking during this cruise that several depressions were born on the leeward side of the Rocky Mountains west of the Great Lakes, but even more originated over the area between the Caribbean Sea and the Bermuda. This is to be ascribed to the fact, that frequent Anticyclones over the North American continent drove arctic cold air far down into the south against subtropical warm air, whereas cyclogenetic processes in more or less uniform cold air masses over Canada remained rather weak.

Visibility was nearly always good, mostly unlimited. The duration of the extremely rare fog events due to frontal processes was less than half an hour. The average atmospheric pressure amounted to 995 hPa with a lowest value of 956,5 hPa and a maximum of 1031,5 hPa. The mean wind was 234°/28 knots.

Statistics for the period 16.11.-14.12.94

Distribution of wind directions and wind force in Beaufort in percent of a total number of 695 hourly observations.

Wind Directions

N	NE	E	SE	S	SW	W	NW	VRB
11.5	2.4	5.0	5.6	10.8	16.5	28.6	19.3	0.0%

Wind Force

0	1	2	3	4	5	6	7	8	9	10	11	12 Bft
1.0	1.2	1.9	3.9	0.4	17.4	16.1	12.9	18.6	9.2	4.9	1.6	1.0%

Distribution of wave heights in meter in percent of a total number of 160 visual observations during daylight.

0	1	2	3	4	5	6	7	8	9	10	11	12
0.6	4.4	10.6	31.9	25.6	16.9	6.3	2.5	0.6	0.6	0	0	0%

In the hourly wind measurements and the three-hourly wave observations higher values might have occurred. Thus the absolute wind maximum of 100 kts and the highest waves exceeding 10 m do not show up in that list.

7 LISTS

7.1 List of Stations

7.1.1 Lists of sampling stations M30/1

Water samplers:	Go-Flows, Rosette sampler, Marine snow catcher
Sediment samplers:	Multiple corer, Box grab
Water column profiling:	CTD

Station No.	Date (1994)	Gear	Coordinates °N	Coordinates °W	Sampling depth (m)
422	09.09.	Multiple corer	38°28,5’	15°53,0’	4989
		(failed)			
423	09.09.	CTD/Rosette	39°18,3’	15°55,7’	0-3500
424	10.09.	Multiple corer	41°49,8’	16°03,7’	5330
425	12.09.	Go-Flows	48°56,9’	16°26,7’	0-1200

Station No.	Date (1994)	Gear	Coordinates °N	°W	Sampling depth (m)
		Multiple corer	48°58,4’	16°28,4’	4805
		(failed)			
		Multiple corer	48°58,3’	16°28,3’	4805
		Go-Flows	48°59,7’	16°26,7’	0-200
		Go-Flows	48°59,8’	16°26,7’	0-200
		Multiple corer	48°59,7’	16°26,5’	4807
426	13.09.	Multiple corer	48°59,1’	13°45,1’	4500
		Box grab	48°59,4’	13°45,3’	4469
		(failed)			
427	14.09.	Go-Flows	49°03,2’	13°24,6’	0-1500
		Bottom lander	49°04,0’	13°23,4’	3635
		(partly failed)			
		CTD	49°05,5’	13°24,7’	0-500
		Multiple corer	49°05,5’	13°24,8’	3665
428	15.09.	CTD	49°08,9’	13°05,2’	0-500
		Rosette	49°08,9’	13°05,2’	0-1500
		Multiple corer	49°09,0’	13°05,6’	2268
428		Box grab	49°09,0’	13°05,5’	2277
		(failed)			
		Box grab	49°09,0’	13°05,6’	2260
		Go-Flows	49°09,8’	13°08,7’	0-2200
429	15.09.	Marine snow	49°04,7’	13°24,2’	50
		catcher			
		Marine snow	49°04,7’	13°24,4’	50
		catcher			
		CTD	49°04,6’	13°25,0’	0-500
		Go-Flows	49°04,4’	13°25,1’	0-50
		Multiple corer	49°03,7’	13°23,3’	3629
430	16.09.	CTD	49°11,0’	12°50,8’	0-500
		Rosette	49°11,0’	12°50,8’	0-1400
		Multiple corer	49°11,1’	12°51,0’	1535
		Box grab	49°11,1’	12°50,9’	1529
431	16.09.	Go-Flows	49°14,0’	12°30,2’	0-1100
		Multiple corer	49°14,0’	12°30,0’	1165
432		Go-Flows	49°13,2’	12°48,9’	0-1300
433		Box grab	49°14,2’	12°29,6’	1158
		CTD	49°14,5’	12°29,4’	0-500m
	17.09.	Rosette	49°14,0’	12°28,9’	0-1000
434	17.09.	Multiple corer	49°24,1’	11°32,1’	674
		Box grab	49°24,0’	11°32,2’	674
		CTD	49°25,2’	11°32,2’	673
		Go-Flows	49°24,9’	11°32,2’	0-650
		Rosette	49°25,0’	11°33,8’	0-650

Station No.	Date (1994)	Gear	Coordinates		Sampling depth (m)
			°N	°W	
435		Multiple corer	49°27,9’	11°12,2’	227
		Multiple corer	49°28,0’	11°12,5’	230
		Multiple corer	49°28,0’	11°12,4’	231
		CTD	49°28,0’	11°09,4’	0-200
		Go-Flows	49°28,4’	11°08,7’	0-200
		Rosette	49°28,4’	11°08,5’	0-200
		Multiple corer	49°28,6’	11°08,0’	231

7.1.2 Station List Leg M30/2 Section WHP-A2

EXPO-CODE	WOCE WHP-ID	Stat. No.	Cast No.	Cast Type	Date	Time UTC	Code	Position Latitude	Longitude	Code	Bottom Depth	Meter Wheel	Max Pres	Bottom Dist.	No.of Btls	Parameters	Comments
06MT30/2	A2	436	01	ROS	101594	1232	BE	48 09.9 N	11 44.9 W	GPS	3422						
06MT30/2	A2	436	01	ROS	101594	1338	BO	48 09.9 N	11 44.9 W	GPS	3422		3236		12	1-4,6,7,8,27,28	
06MT30/2	A2	436	01	ROS	101594	1511	EN	48 09.9 N	11 45.2 W	GPS	3422						
06MT30/2	A2	436	02	LVS	101594	1605	BO	48 09.9 N	11 45.0 W	GPS	3430		300		5	1,12,13	
06MT30/2	A2	436	03	ROS	101594	1648	BE	48 10.0 N	11 45.3 W	GPS	3418						
06MT30/2	A2	436	03	ROS	101594	1810	BO	48 10.1 N	11 45.7 W	GPS	3418		3201		24	1-2	
06MT30/2	A2	436	03	ROS	101594	1952	EN	48 10.1 N	11 46.3 W	GPS	3418						
06MT30/2	A2	437	01	ROS	101694	0444	BE	49 14.1 N	10 40.0 W	GPS	0154						
06MT30/2	A2	437	01	ROS	101694	0449	BO	49 14.0 N	10 39.7 W	GPS	0154		132	20	7	1-4,6	
06MT30/2	A2	437	01	ROS	101694	0507	EN	49 13.9 N	10 39.6 W	GPS	0154						
06MT30/2	A2	438	01	ROS	101694	0658	BE	49 11.6 N	11 11.1 W	GPS	0192						
06MT30/2	A2	438	01	ROS	101694	0702	BO	49 11.6 N	11 11.1 W	GPS	0192		173		10	1-4,6,7,8,27,28	
06MT30/2	A2	438	01	ROS	101694	0718	EN	49 11.6 N	11 10.9 W	GPS	0192						
06MT30/2	A2	439	02	ROS	101694	0928	BE	49 10.7 N	11 25.6 W	GPS	0478						
06MT30/2	A2	439	02	ROS	101694	0943	BO	49 10.7 N	11 25.6 W	GPS	0478		461		11	1-4,6	
06MT30/2	A2	439	02	ROS	101694	1003	EN	49 10.7 N	11 25.6 W	GPS	0478						
06MT30/2	A2	440	01	ROS	101694	1257	BE	49 06.4 N	12 11.7 W	GPS	1001						
06MT30/2	A2	440	01	ROS	101694	1318	BO	49 06.4 N	12 11.7 W	GPS	1001		985	20	17	1-4,6,7,8,27,28	
06MT30/2	A2	440	01	ROS	101694	1356	EN	49 06.4 N	12 11.6 W	GPS	1001						
06MT30/2	A2	441	01	ROS	101694	1600	BE	49 03.1 N	12 42.3 W	GPS	1502						
06MT30/2	A2	441	01	ROS	101694	1630	BO	49 03.3 N	12 42.3 W	GPS	1502		1501	20	21	1-4,6,7,8,27,28	
06MT30/2	A2	441	01	ROS	101694	1720	EN	49 03.5 N	12 42.1 W	GPS	1502						
06MT30/2	A2	442	01	ROS	101694	1853	BE	49 01.2 N	12 51.4 W	GPS	1986						
06MT30/2	A2	442	01	ROS	101694	1934	BO	49 01.2 N	12 51.4 W	GPS	1986		1994	20	24	1-4,6,7,8,27,28	
06MT30/2	A2	442	01	ROS	101694	2034	EN	49 01.2 N	12 51.3 W	GPS	1986						
06MT30/2	A2	443	01	ROS	101694	2159	BE	49 00.0 N	12 58.8 W	GPS	2500						
06MT30/2	A2	443	01	ROS	101694	2245	BO	49 00.2 N	12 58.5 W	GPS	2500	2500	2510		24	1-4,6,7,8,27,28	
06MT30/2	A2	443	01	ROS	101694	2359	EN	49 00.4 N	12 57.9 W	GPS	2500						
06MT30/2	A2	444	02	ROS	101794	0425	BE	48 59.9 N	13 02.6 W	GPS	3068						
06MT30/2	A2	444	02	ROS	101794	0523	BO	49 59.8 N	13 02.6 W	GPS	3068		3127	20	23	1-4,6	
06MT30/2	A2	444	02	ROS	101794	0642	EN	48 59.8 N	13 02.7 W	GPS	3068						
06MT30/2	A2	445	01	LVS	101794	0925	BO	48 55.0 N	13 16.5 W	GPS	3725		1700		10	1,12,13	
06MT30/2	A2	445	02	ROS	101794	1106	BE	48 55.5 N	13 17.1 W	GPS	3718						
06MT30/2	A2	445	02	ROS	101794	1220	BO	48 55.6 N	13 16.5 W	GPS	3718		3735	20	23	1-4,6,7,8,27,28	
06MT30/2	A2	445	02	ROS	101794	1349	EN	48 55.4 N	13 16.7 W	GPS	3718						
06MT30/2	A2	445	03	LVS	101794	1616	BO	48 55.2 N	13 16.8 W	GPS	3726		3670		10	1,12,13	
06MT30/2	A2	445	04	ROS	101794	1908	BE	48 55.2 N	13 16.8 W	GPS	3726						

EXPO-CODE	WOCE WHP-ID	Stat. No.	Cast No.	Cast Type	Date	Time UTC	Code	Position Latitude	Longitude	Code	Bottom Depth	Meter Wheel	Max Pres	Bottom Dist.	No.of Btls	Parameters	Comments
06MT30/2	A2	445	04	ROS	101794	1938	BO	48 55.2 N	13 16.9 W	GPS	3726		1180		19	1-4,6,7,8,27,28	
06MT30/2	A2	445	04	ROS	101794	2029	EN	48 55.1 N	13 16.7 W	GPS	3726						
06MT30/2	A2	446	01	ROS	101794	2242	BE	48 51.4 N	13 46.0 W	GPS	4495						
06MT30/2	A2	446	01	ROS	101794	2302	BO	48 51.3 N	13 46.2 W	GPS	4495		1049		16	1-4,6	
06MT30/2	A2	446	01	ROS	101794	2341	EN	48 51.2 N	13 46.5 W	GPS	4495						
06MT30/2	A2	446	03	ROS	101894	0352	BE	48 51.6 N	13 46.2 W	GPS	4490						
06MT30/2	A2	446	03	ROS	101894	0513	BO	48 51.5 N	13 46.1 W	GPS	4490		4562	20	24	1-4,6	
06MT30/2	A2	446	03	ROS	101894	0654	EN	48 51.5 N	13 46.1 W	GPS	4490						
06MT30/2	A2	447	01	ROS	101894	1426	BE	48 39.1 N	14 21.4 W	GPS	4552						
06MT30/2	A2	447	01	ROS	101894	1549	BO	48 38.6 N	14 21.3 W	GPS	4552		4603	20	23	1-4,6,7,8,27,28	
06MT30/2	A2	447	01	ROS	101894	1733	EN	48 38.0 N	14 21.5 W	GPS	4552						
06MT30/2	A2	448	01	ROS	101894	2054	BE	48 44.2 N	14 55.6 W	GPS	4707						
06MT30/2	A2	448	01	ROS	101894	2222	BO	48 43.9 N	14 45.3 W	GPS	4707		4743		23	1-4,6,7,8,27,28	
06MT30/2	A2	448	01	ROS	101994	0011	EN	48 43.5 N	14 44.8 W	GPS	4707						
06MT30/2	A2	449	01	ROS	102094	0901	BE	48 21.1 N	17 20.4 W	GPS	4143						
06MT30/2	A2	449	01	ROS	102094	0950	BO	48 20.9 N	17 20.7 W	GPS	4143		2200		22	1-4,6,7,8,27,28	
06MT30/2	A2	449	01	ROS	102094	1051	EN	48 20.9 N	17 21.0 W	GPS	4143						
06MT30/2	A2	449	02	ROS	102094	1110	BE	48 20.9 N	17 21.1 W	GPS	4127						
06MT30/2	A2	449	02	ROS	102094	1222	BO	48 20.9 N	17 21.3 W	GPS	4127		4170		23	1-4,6,7,8,27,28	
06MT30/2	A2	449	02	ROS	102094	1348	EN	48 20.7 N	17 21.3 W	GPS	4127						
06MT30/2	A2	450	01	LVS	102094	2026	BO	48 13.0 N	18 26.0 W	GPS	4510		1700		10	1,12,13	
06MT30/2	A2	450	02	ROS	102094	2215	BE	48 12.5 N	18 25.6 W	GPS	4510						
06MT30/2	A2	450	02	ROS	102094	2322	BO	48 11.8 N	18 25.3 W	GPS	4510		4539		23	1-4,6,7,8,27,28	
06MT30/2	A2	450	02	ROS	102194	0018	EN	48 11.7 N	18 26.1 W	GPS	4510						
06MT30/2	A2	450	03	LVS	102194	0332	BO	48 12.1 N	18 26.3 W	GPS	4514		4391		10	1,12,13	
06MT30/2	A2	450	04	ROS	102194	0622	BE	48 12.5 N	18 26.2 W	GPS	4444						
06MT30/2	A2	450	04	ROS	102194	0720	BO	48 12.4 N	18 25.8 W	GPS	4444		1599		17	1-4,6,7,8,27,28	
06MT30/2	A2	450	04	ROS	102194	0808	EN	48 12.5 N	18 25.9 W	GPS	4444						
06MT30/2	A2	451	01	ROS	102194	1210	BE	48 06.3 N	19 10.0 W	GPS	4176						
06MT30/2	A2	451	01	ROS	102194	1237	BO	48 06.4 N	19 10.4 W	GPS	4176		1603		16	1-4,6,7,8,27,28	
06MT30/2	A2	451	01	ROS	102194	1318	EN	48 06.4 N	19 10.7 W	GPS	4176						
06MT30/2	A2	451	02	ROS	102194	1331	BE	48 06.6 N	19 10.4 W	GPS	4183						
06MT30/2	A2	451	02	ROS	102194	1441	BO	48 06.5 N	19 10.5 W	GPS	4183		4238		23	1-4,6,7,8,27,28	
06MT30/2	A2	451	02	ROS	102194	1610	EN	48 06.3 N	19 10.6 W	GPS	4183						
06MT30/2	A2	452	01	ROS	102394	0001	BE	47 53.1 N	20 55.3 W	GPS	4447						
06MT30/2	A2	452	01	ROS	102394	0120	BO	47 53.0 N	20 56.1 W	GPS	4447		4525	17	24	1-4,6,7,8,27,28	
06MT30/2	A2	452	01	ROS	102394	0301	EN	47 53.1 N	20 56.7 W	GPS	4447						
06MT30/2	A2	452	02	ROS	102394	0350	BE	47 52.9 N	20 55.8 W	GPS	4448						
06MT30/2	A2	452	02	ROS	102394	0520	BO	47 53.3 N	20 55.8 W	GPS	4448	4249	4500	20	19	1-4,6,7,8,27,28	

EXPO-CODE	WOCE WHP-ID	Stat. No.	Cast No.	Cast Type	Date	Time UTC	Code	Position Latitude	Longitude	Code	Bottom Depth	Meter Wheel	Max Pres	Bottom Dist.	No.of Btls	Parameters	Comments
06MT30/2	A2	452	02	ROS	102394	0640	EN	47 53.3 N	20 56.6 W	GPS	4448						
06MT30/2	A2	453	01	ROS	102394	1200	BE	47 42.2 N	22 05.7 W	GPS	4434						
06MT30/2	A2	453	01	ROS	102394	1310	BO	47 42.0 N	22 05.6 W	GPS	4434		4303		24	1-4,6,7,8,27,28	
06MT30/2	A2	453	01	ROS	102394	1429	EN	47 42.0 N	22 05.7 W	GPS	4434						
06MT30/2	A2	453	02	LVS	102394	1548	BO	47 42.3 N	22 05.2 W	GPS	4433		1800		10	1,12,13	
06MT30/2	A2	453	03	ROS	102394	1740	BE	47 42.4 N	22 05.7 W	GPS	4433						
06MT30/2	A2	453	03	ROS	102394	1918	BO	47 42.4 N	22 05.5 W	GPS	4433		4505	19	27	1-4,6,7,8,27,28	
06MT30/2	A2	453	03	ROS	102394	2050	EN	47 42.3 N	22 05.4 W	GPS	4433						
06MT30/2	A2	453	04	ROS	102394	2303	BE	47 42.2 N	22 05.5 W	GPS	4436						
06MT30/2	A2	453	04	ROS	102394	2343	BO	47 42.1 N	22 05.6 W	GPS	4436		2110		27	1-4,6,7,8,27,28	
06MT30/2	A2	453	04	ROS	102494	0050	EN	47 41.8 N	22 05.6 W	GPS	4436						
06MT30/2	A2	454	01	ROS	102494	0303	BE	47 32.4 N	22 27.4 W	GPS	4467						
06MT30/2	A2	454	01	ROS	102494	0340	BO	47 32.4 N	22 27.3 W	GPS	4467		1500		19	1-4,6	
06MT30/2	A2	454	01	ROS	102494	0440	EN	47 32.4 N	22 27.3 W	GPS	4467						
06MT30/2	A2	454	02	ROS	102494	0459	BE	47 32.6 N	22 27.4 W	GPS	4466						
06MT30/2	A2	454	02	ROS	102494	0618	BO	47 32.5 N	22 27.3 W	GPS	4466		4543		26	1-4,6	
06MT30/2	A2	454	02	ROS	102494	0802	EN	47 32.5 N	22 27.2 W	GPS	4466						
06MT30/2	A2	455	01	ROS	102494	1010	BE	47 36.3 N	22 48.9 W	GPS	4177						
06MT30/2	A2	455	01	ROS	102494	1051	BO	47 36.3 N	22 48.8 W	GPS	4177		1899		20	1-4,6,7,8,27,28	
06MT30/2	A2	455	01	ROS	102494	1201	EN	47 36.1 N	22 48.9 W	GPS	4177						
06MT30/2	A2	455	02	LVS	102494	1400	BO	47 35.8 N	22 48.7 W	GPS	4238		4210		10	1,12,13	
06MT30/2	A2	455	03	ROS	102494	1649	BE	47 36.2 N	22 49.1 W	GPS	4238						
06MT30/2	A2	455	03	ROS	102494	1805	BO	47 35.9 N	22 49.0 W	GPS	4238		4304		27	1-4,6,7,8,27,28	
06MT30/2	A2	455	03	ROS	102494	1952	EN	47 35.5 N	22 49.1 W	GPS	4238						
06MT30/2	A2	456	01	ROS	102494	2313	BE	47 29.3 N	23 33.3 W	GPS	3967						
06MT30/2	A2	456	01	ROS	102494	2344	BO	47 29.3 N	23 33.7 W	GPS	3967		1302		20	1-4,6	
06MT30/2	A2	456	01	ROS	102594	0051	EN	47 29.5 N	23 34.1 W	GPS	3967						
06MT30/2	A2	456	02	ROS	102594	0104	BE	47 29.5 N	23 34.1 W	GPS	3964						
06MT30/2	A2	456	02	ROS	102594	0210	BO	47 29.4 N	23 33.6 W	GPS	3964		4030	19	27	1-4,6	
06MT30/2	A2	456	02	ROS	102594	0346	EN	47 29.4 N	23 33.5 W	GPS	3964						
06MT30/2	A2	457	01	ROS	102594	0659	BE	47 22.9 N	24 15.8 W	GPS	3315						
06MT30/2	A2	457	01	ROS	102594	0724	BO	47 23.0 N	24 16.0 W	GPS	3315			866	11	1-4,6,7,8,27,28	
06MT30/2	A2	457	01	ROS	102594	0757	EN	47 23.1 N	24 15.9 W	GPS	3315						
06MT30/2	A2	457	02	ROS	102594	0823	BE	47 23.1 N	24 15.7 W	GPS	3317						
06MT30/2	A2	457	02	ROS	102594	0919	BO	47 23.0 N	24 15.1 W	GPS	3317		3312	23	28	1-4,6,7,8,27,28	
06MT30/2	A2	457	02	ROS	102594	1105	EN	47 23.1 N	24 17.0 W	GPS	3317						
06MT30/2	A2	458	01	ROS	102594	1523	BE	47 14.1 N	25 22.3 W	GPS	2886						
06MT30/2	A2	458	01	ROS	102594	1545	BO	47 13.9 N	25 22.3 W	GPS	2886			902	14	1-4,6,7,8,27,28	
06MT30/2	A2	458	01	ROS	102594	1627	EN	47 14.0 N	25 22.3 W	GPS	2886						

EXPO-CODE	WOCE WHP-ID	Stat. No.	Cast No.	Cast Type	Date	Time UTC	Code	Position Latitude	Longitude	Code	Bottom Depth	Meter Wheel	Max Pres	Bottom Dist.	No.of Btls	Parameters	Comments
06MT30/2	A2	458	02	LVS	102594	1755	BO	47 13.9 N	25 22.3 W	GPS	2894		2820		10	1,12,13	
06MT30/2	A2	458	03	ROS	102594	1947	BE	47 14.0 N	25 22.2 W	GPS	2863						
06MT30/2	A2	458	03	ROS	102594	2040	BO	47 14.1 N	25 22.2 W	GPS	2863		2868	20	27	1-4,6,7,8,27,28	
06MT30/2	A2	458	03	ROS	102594	2221	EN	47 13.5 N	25 23.1 W	GPS	2863						
06MT30/2	A2	459	01	ROS	102694	0144	BE	47 06.3 N	26 17.3 W	GPS	2430						
06MT30/2	A2	459	01	ROS	102694	0224	BO	47 06.3 N	26 17.2 W	GPS	2430		2373	12	28	1-4,6,7,8,27,28	
06MT30/2	A2	459	01	ROS	102694	0341	EN	47 06.4 N	26 17.2 W	GPS	2430						
06MT30/2	A2	460	01	ROS	102694	0517	BE	47 04.4 N	26 39.8 W	GPS	2716						
06MT30/2	A2	460	01	ROS	102694	0601	BO	47 04.5 N	26 39.5 W	GPS	2716		2717	19	28	1-4,6,7,8,27,28	
06MT30/2	A2	460	01	ROS	102694	0717	EN	47 04.5 N	26 39.4 W	GPS	2716						
06MT30/2	A2	461	01	ROS	102694	0853	BE	46 59.4 N	26 59.8 W	GPS	2120						
06MT30/2	A2	461	01	ROS	102694	0934	BO	46 59.3 N	26 59.8 W	GPS	2120		2123	21	27	1-4,6	
06MT30/2	A2	461	01	ROS	102694	1042	EN	46 58.8 N	27 00.0 W	GPS	2120						
06MT30/2	A2	462	01	ROS	102694	1232	BE	46 54.3 N	27 23.3 W	GPS	2770						
06MT30/2	A2	462	01	ROS	102694	1325	BO	46 53.9 N	27 23.3 W	GPS	2770		2803	17	27	1-4,6,7,8,27,28	
06MT30/2	A2	462	01	ROS	102694	1438	EN	46 53.9 N	27 23.5 W	GPS	2770						
06MT30/2	A2	463	01	ROS	102694	1624	BE	46 49.4 N	27 50.6 W	GPS	2440						
06MT30/2	A2	463	01	ROS	102694	1705	BO	46 49.3 N	27 50.4 W	GPS	2440		2456	18	28	1-4,6,7,8,27,28	
06MT30/2	A2	463	01	ROS	102694	1821	EN	46 49.4 N	27 50.6 W	GPS	2440						
06MT30/2	A2	464	01	ROS	102694	2018	BE	46 42.6 N	28 18.2 W	GPS	3450						
06MT30/2	A2	464	01	ROS	102694	2113	BO	46 42.6 N	28 18.1 W	GPS	3450		3464		28	1-4,6,7,8,27,28	
06MT30/2	A2	464	01	ROS	102694	2245	EN	46 42.7 N	28 18.0 W	GPS	3450						
06MT30/2	A2	465	01	ROS	102794	1911	BE	46 20.4 N	30 00.7 W	GPS	3125						
06MT30/2	A2	465	01	ROS	102794	2045	BO	46 20.5 N	30 00.8 W	GPS	3125		3114	19	27	1-4,6,7,8,27,28	
06MT30/2	A2	465	01	ROS	102794	2142	EN	46 20.5 N	30 00.8 W	GPS	3125						
06MT30/2	A2	466	01	ROS	102894	0026	BE	46 12.3 N	30 36.6 W	GPS	3625						
06MT30/2	A2	466	01	ROS	102894	0131	BO	46 12.3 N	30 36.8 W	GPS	3625		3643	18	27	1-4,6,7,8,27,28	
06MT30/2	A2	466	01	ROS	102894	0308	EN	46 12.3 N	30 37.0 W	GPS	3625						
06MT30/2	A2	467	01	ROS	102894	0542	BE	46 04.2 N	31 12.8 W	GPS	3347						
06MT30/2	A2	467	01	ROS	102894	0640	BO	46 04.1 N	31 12.8 W	GPS	3347		3361	19	27	1-4,6,7,8,27,28	
06MT30/2	A2	467	01	ROS	102894	0808	EN	46 04.2 N	31 12.9 W	GPS	3347						
06MT30/2	A2	468	01	ROS	102894	1323	BE	45 54.6 N	31 48.6 W	GPS	3601						
06MT30/2	A2	468	01	ROS	102894	1348	BO	45 54.4 N	31 48.6 W	GPS	3601		1401		24	1-4,6,7,8,27,28	
06MT30/2	A2	468	01	ROS	102894	1443	EN	45 54.6 N	31 48.7 W	GPS	3601						
06MT30/2	A2	468	02	LVS	102894	1637	BO	45 54.6 N	31 48.4 W	GPS	3658		3602		10	1,12,13	
06MT30/2	A2	468	03	ROS	102894	1857	BE	45 54.5 N	31 48.5 W	GPS	3639						
06MT30/2	A2	468	03	ROS	102894	1956	BO	45 54.5 N	31 48.6 W	GPS	3639		3695	18	28	1-4,6,7,8,27,28	
06MT30/2	A2	468	03	ROS	102894	2141	EN	45 54.4 N	31 48.4 W	GPS	3639						
06MT30/2	A2	469	01	ROS	102994	0741	BE	45 41.5 N	32 18.4 W	GPS	3588						

EXPO-CODE	WOCE WHP-ID	Stat. No.	Cast No.	Cast Type	Date	Time UTC	Code	Position Latitude	Longitude	Code	Bottom Depth	Meter Wheel	Max Pres	Bottom Dist.	No.of Btls	Parameters	Comments
06MT30/2	A2	469	01	ROS	102994	0809	BO	45 41.5 N	32 18.1 W	GPS	3588		1101		14	1-4,6,7,8,27,28	
06MT30/2	A2	469	01	ROS	102994	0904	EN	45 41.6 N	32 17.2 W	GPS	3588						
06MT30/2	A2	469	02	ROS	102994	0919	BE	45 41.6 N	32 17.2 W	GPS	3573						
06MT30/2	A2	469	02	ROS	102994	1005	BO	45 41.7 N	32 16.7 W	GPS	3573		3611	18	28	1-4,6,7,8,27,28	
06MT30/2	A2	469	02	ROS	102994	1150	EN	45 41.6 N	32 16.5 W	GPS	3573						
06MT30/2	A2	470	01	ROS	102994	1627	BE	46 31.6 N	32 45.5 W	GPS	3811						
06MT30/2	A2	470	01	ROS	102994	1659	BO	45 31.5 N	32 45.2 W	GPS	3811		1199		14	1-4,6,7,8,27,28	
06MT30/2	A2	470	01	ROS	102994	1759	EN	45 31.3 N	32 44.7 W	GPS	3811						
06MT30/2	A2	470	02	ROS	103094	0822	BE	45 31.4 N	32 44.8 W	GPS	3770						
06MT30/2	A2	470	02	ROS	103094	0931	BO	45 31.5 N	32 44.5 W	GPS	3770		3827	19	28	1-4,6,7,8,27,28	
06MT30/2	A2	470	02	ROS	103094	1108	EN	45 32.0 N	32 44.1 W	GPS	3770						
06MT30/2	A2	471	01	ROS	103094	1607	BE	45 19.5 N	33 18.2 W	GPS	3484						
06MT30/2	A2	471	01	ROS	103094	1635	BO	45 19.8 N	33 18.2 W	GPS	3484		1099		14	1-4,6,7,8,27,28	
06MT30/2	A2	471	01	ROS	103094	1730	EN	45 19.9 N	33 18.3 W	GPS	3484						
06MT30/2	A2	471	02	LVS	103094	1918	BO	45 20.0 N	33 18.5 W	GPS	3512		3459		10	1,12,13	
06MT30/2	A2	471	03	ROS	103094	2144	BE	45 20.1 N	33 18.4 W	GPS	3543						
06MT30/2	A2	471	03	ROS	103094	2252	BO	45 20.5 N	33 18.3 W	GPS	3543		3569	21	28	1-4,6,7,8,27,28	
06MT30/2	A2	471	03	ROS	103194	0038	EN	45 21.4 N	33 18.4 W	GPS	3543						
06MT30/2	A2	472	01	ROS	103194	0259	BE	45 12.6 N	33 45.8 W	GPS	3674						
06MT30/2	A2	472	01	ROS	103194	0328	BO	45 12.5 N	33 45.6 W	GPS	3674		1228		14	1-4,6	
06MT30/2	A2	472	01	ROS	103194	0425	EN	45 12.6 N	33 45.4 W	GPS	3674						
06MT30/2	A2	472	02	ROS	103194	0435	BE	45 12.5 N	33 45.3 W	GPS	3666						
06MT30/2	A2	472	02	ROS	103194	0548	BO	45 12.6 N	33 45.8 W	GPS	3666		3714		28	1-4,6,7,8,27,28	
06MT30/2	A2	472	02	ROS	103194	0743	EN	45 12.4 N	33 45.5 W	GPS	3666						
06MT30/2	A2	473	01	ROS	103194	1104	BE	45 01.4 N	34 25.7 W	GPS	3973						
06MT30/2	A2	473	01	ROS	103194	1138	BO	45 01.2 N	34 25.4 W	GPS	3973		1075		14	1-4,6,7,8,27,28	
06MT30/2	A2	473	01	ROS	103194	1227	EN	45 00.9 N	34 24.9 W	GPS	3973						
06MT30/2	A2	473	02	ROS	103194	1532	BE	45 01.6 N	34 25.7 W	GPS	3976						
06MT30/2	A2	473	02	ROS	103194	1645	BO	45 01.5 N	34 25.8 W	GPS	3976		4030	17	28	1-4,6,7,8,27,28	
06MT30/2	A2	473	02	ROS	103194	1824	EN	45 01.2 N	34 25.7 W	GPS	3976						
06MT30/2	A2	474	01	LVS	103194	2359	BO	44 50.4 N	35 04.1 W	GPS	4118		1600		10	1,12,13	
06MT30/2	A2	474	02	ROS	110194	0201	BE	44 50.5 N	35 04.8 W	GPS	4103						
06MT30/2	A2	474	02	ROS	110194	0322	BO	44 50.3 N	35 04.8 W	GPS	4103		4165	16	28	1-4,6,7,8,27,28	
06MT30/2	A2	474	02	ROS	110194	0510	EN	44 50.4 N	35 04.9 W	GPS	4103						
06MT30/2	A2	474	03	LVS	110194	0706	BO	44 49.7 N	35 04.5 W	GPS	4096		4036		10	1,12,13	
06MT30/2	A2	474	04	ROS	110194	0946	BE	44 50.2 N	35 04.2 W	GPS	4096						
06MT30/2	A2	474	04	ROS	110194	1017	BO	44 49.9 N	35 04.4 W	GPS	4096		1398		15	1-4,6,7,8,27,28	
06MT30/2	A2	474	04	ROS	110194	1118	EN	44 49.5 N	35 04.6 W	GPS	4096						
06MT30/2	A2	475	01	ROS	110294	1304	BE	44 34.1 N	36 05.3 W	GPS	4094						

EXPO-CODE	WOCE WHP-ID	Stat. No.	Cast No.	Cast Type	Date	Time UTC	Code	Position Latitude	Longitude	Code	Bottom Depth	Meter Wheel	Max Pres	Bottom Dist.	No.of Btls	Parameters	Comments
06MT30/2	A2	475	01	ROS	110294	1432	BO	44 34.5 N	36 05.6 W	GPS	4094		4160	10	28	1-4,6,7,8,27,28	
06MT30/2	A2	475	01	ROS	110294	1613	EN	44 34.9 N	36 06.0 W	GPS	4094						
06MT30/2	A2	476	01	ROS	110294	2100	BE	44 16.8 N	37 02.3 W	GPS	4054						
06MT30/2	A2	476	01	ROS	110294	2213	BO	44 16.9 N	37 02.6 W	GPS	4054		3300		28	1-4,6,7,8,27,28	
06MT30/2	A2	476	01	ROS	110294	2334	EN	44 16.8 N	37 02.5 W	GPS	4054						
06MT30/2	A2	476	02	ROS	110294	2353	BE	44 16.7 N	37 02.4 W	GPS	4060						
06MT30/2	A2	476	02	ROS	110394	0034	BO	44 16.8 N	37 02.5 W	GPS	4060		1298		16	1-4,6	
06MT30/2	A2	476	02	ROS	110394	0133	EN	44 16.8 N	37 02.5 W	GPS	4060						
06MT30/2	A2	476	03	ROS	110394	0149	BE	44 16.8 N	37 02.5 W	GPS	4054						
06MT30/2	A2	476	03	ROS	110394	0308	BO	44 16.9 N	37 02.6 W	GPS	4054		4105	12	28	1-4,6,7,8,27,28	
06MT30/2	A2	476	03	ROS	110394	0452	EN	44 16.6 N	37 02.3 W	GPS	4054						
06MT30/2	A2	477	01	ROS	110394	0926	BE	43 59.7 N	37 59.9 W	GPS	4306						
06MT30/2	A2	477	01	ROS	110394	1046	BO	43 59.7 N	37 59.8 W	GPS	4306		4383	19	28	1-4,6,7,8,27,28	
06MT30/2	A2	477	01	ROS	110394	1240	EN	43 59.7 N	38 00.0 W	GPS	4306						
06MT30/2	A2	478	01	ROS	110394	1537	BE	43 49.5 N	38 39.0 W	GPS	3233						
06MT30/2	A2	478	01	ROS	110394	1636	BO	43 49.4 N	38 38.9 W	GPS	3233		3394	16	28	1-4,6,7,8,27,28	
06MT30/2	A2	478	01	ROS	110394	1807	EN	43 49.4 N	38 38.7 W	GPS	3233						
06MT30/2	A2	479	01	ROS	110394	2114	BE	43 38.4 N	39 18.0 W	GPS	4542						
06MT30/2	A2	479	01	ROS	110394	2142	BO	43 38.3 N	39 17.5 W	GPS	4542		1501		14	1-4,6,7,8,27,28	
06MT30/2	A2	479	01	ROS	110394	2246	EN	43 38.4 N	39 16.4 W	GPS	4542						
06MT30/2	A2	479	02	LVS	110494	0108	BO	43 38.6 N	39 17.9 W	GPS	4558		4521		10	1,12,13	
06MT30/2	A2	479	03	ROS	110494	0407	BE	43 38.7 N	39 17.7 W	GPS	4529						
06MT30/2	A2	479	03	ROS	110494	0544	BO	43 38.2 N	39 16.9 W	GPS	4529		4598	18	28	1-4,6,7,8,27,28	
06MT30/2	A2	479	03	ROS	110494	0741	EN	43 38.0 N	39 15.9 W	GPS	4529						
06MT30/2	A2	480	01	ROS	110494	1738	BE	43 25.3 N	39 58.1 W	GPS	4808						
06MT30/2	A2	480	01	ROS	110494	1930	BO	43 25.0 N	39 58.8 W	GPS	4808		4900	20	28	1-4,6,7,8,27,28	
06MT30/2	A2	480	01	ROS	110494	2156	EN	43 24.7 N	39 59.9 W	GPS	4808						
06MT30/2	A2	481	01	ROS	110594	1125	BE	43 11.1 N	40 47.7 W	GPS	4766						
06MT30/2	A2	481	01	ROS	110594	1339	BO	43 11.6 N	40 48.3 W	GPS	4766		4854	12	28	1-4,6,7,8,27,28	
06MT30/2	A2	481	01	ROS	110594	1547	EN	43 12.7 N	40 48.7 W	GPS	4766						
06MT30/2	A2	482	01	ROS	110594	1958	BE	42 57.1 N	41 35.2 W	GPS	4815						
06MT30/2	A2	482	01	ROS	110594	2148	BO	42 57.5 N	41 35.7 W	GPS	4815		4900	25	28	1-4,6,7,8,27,28	
06MT30/2	A2	482	01	ROS	110594	2358	EN	42 58.0 N	41 36.4 W	GPS	4815						
06MT30/2	A2	483	01	LVS	110694	0529	BO	42 42.7 N	42 23.2 W	GPS	4793		2000		10	1,12,13	
06MT30/2	A2	483	02	ROS	110694	0818	BE	42 42.9 N	42 25.8 W	GPS	4851						
06MT30/2	A2	483	02	ROS	110694	1015	BO	42 42.4 N	42 22.5 W	GPS	4851		4925	19	28	1-4,6,7,8,27,28	
06MT30/2	A2	483	02	ROS	110694	1228	EN	42 41.7 N	42 19.3 W	GPS	4851						
06MT30/2	A2	483	03	LVS	110694	1420	BO	42 41.3 N	42 25.7 W	GPS	4844		4784		10	1,12,13	
06MT30/2	A2	483	04	ROS	110694	1844	BE	42 43.0 N	42 26.5 W	GPS	4713						

EXPO-CODE	WOCE WHP-ID	Stat. No.	Cast No.	Cast Type	Date	Time UTC	Code	Position Latitude	Longitude	Code	Bottom Depth	Meter Wheel	Max Pres	Bottom Dist.	No.of Btls	Parameters	Comments
06MT30/2	A2	483	04	ROS	110694	1917	BO	42 42.9 N	42 25.4 W	GPS	4713		1499		19	1-4,6,7,8,27,28	
06MT30/2	A2	483	04	ROS	110694	2015	EN	42 42.6 N	42 23.7 W	GPS	4713						
06MT30/2	A2	484	01	ROS	110794	0307	BE	42 28.3 N	43 16.1 W	GPS	4853						
06MT30/2	A2	484	01	ROS	110794	0444	BO	42 27.9 N	43 12.9 W	GPS	4853		4959	15	28	1-4,6,7,8,27,28	
06MT30/2	A2	484	01	ROS	110794	0710	EN	42 26.8 N	43 08.2 W	GPS	4853						
06MT30/2	A2	485	01	ROS	110794	1234	BE	42 13.1 N	44 08.7 W	GPS	4867						
06MT30/2	A2	485	01	ROS	110794	1437	BO	42 13.5 N	44 07.9 W	GPS	4867		4985	12	28	1-4,6,7,8,27,28	
06MT30/2	A2	485	01	ROS	110794	1647	EN	42 13.9 N	44 07.3 W	GPS	4867						
06MT30/2	A2	486	01	ROS	110794	2028	BE	41 59.6 N	45 00.0 W	GPS	4807						
06MT30/2	A2	486	01	ROS	110794	2232	BO	42 00.5 N	45 02.2 W	GPS	4807		4908	18	28	1-4,6,7,8,27,28	
06MT30/2	A2	486	01	ROS	110894	0050	EN	42 01.2 N	45 01.0 W	GPS	4807						
06MT30/2	A2	486	02	ROS	110894	0131	BE	41 59.7 N	45 00.4 W	GPS	4807						
06MT30/2	A2	486	02	ROS	110894	0228	BO	42 00.4 N	44 59.8 W	GPS	4807		1489		16	1-4,6,7,8,27,28	
06MT30/2	A2	486	02	ROS	110894	0324	EN	42 01.2 N	44 59.1 W	GPS	4807						
06MT30/2	A2	487	01	ROS	110994	1711	BE	43 05.1 N	48 26.8 W	GPS	2837						
06MT30/2	A2	487	01	ROS	110994	1835	BO	43 04.2 N	48 26.4 W	GPS	2837		2854	16	28	1-4,6,7,8,27,28	
06MT30/2	A2	487	01	ROS	110994	2006	EN	43 03.2 N	48 26.9 W	GPS	2837						
06MT30/2	A2	488	01	ROS	110994	2224	BE	43 08.9 N	48 44.0 W	GPS	2139						
06MT30/2	A2	488	01	ROS	110994	2342	BO	43 08.1 N	48 44.4 W	GPS	2139		2155	17	28	1-4,6,7,8,27,28	
06MT30/2	A2	488	01	ROS	111094	0059	EN	43 07.6 N	48 45.0 W	GPS	2139						

- **Summary of Sub-Sampling Schemes, Hydrographic Stations on M30/2**

	A	B	C	D	E	F	G	H	I	J	K	L	M	N	O	P	Q	R	S	T	U	V
122																						
1	Stat cast	Salz	Salz	O2	Nähr	CFCs	CCL4	3He	3He	Seeg	3H	tCO2	Alk	13C	14C	14C	139J	Chlphy	BIO	BIO-Nr	CTD	Kommentar
2		BSH						HeI	UB	3He				18O	LVS	AMS					ID	
3	436/1	36	24	24	24	28						3	3	3			0	3	1	24	DHI1	Kalibrierst CFC
4	436/2LVS																0				x	
5	436/3		24	24													0		25	48	DHI1	Kalibrierst
6	436/4			22													0		49	72	DHI2	Kalibrierst
7	437	11	7	7	7												0		73	78, 96	NB3	begin WOCE A2
8	438	11	9	10	10	7	7					8	8	8			0	8	79	88	NB3	
9	439/1																0				NB3, software	Cast aborted
10	439/2	11	11	11	11												0		90	100	NB3	
11	440	11	17	17	17	14	14	8		8	8	16	16	16			0	8	101	117	NB3	
12	441	17	21	21	21	7	7	10			10						0		118	138	NB3	
13	442	17	24	24	24	7	7										0		140	163	NB3	
14	443	29	24	24	24	14	14	14			14					6	0		164	187	NB3	
15	444	29	24	24	24												0		188	211	NB3	
16	445/1LVT		10	10	10										10		0				x	
17	445/2	44	22	22	22	22	22	12		22	12	18	18	18			6		212	234	NB3	
18	445/3LVT		10	10	10										10		0				x	
19	445/4	44	17	17	17	7	7	8		10	8	17	17	17			4	7	235	253		
20	446/1	53	15	15	15												0		254	269	DHI1	
21	446/2																0				software	abort
22	446/3	53	23	23	23												0		270	292	NB3	
23	447	51	20	20	20	18	18		5			20	20	20			5	2	293	312	NB3	
24	448	51	20	20	20	14	14	14	12		14	20	20		6	7	5		316	335	NB3	BIO 375,383
25	449/1	34	22	22	22	17	17	11			11	18	18	18	6	6	6	5	339	351	DHI1	
26	449/2	34	22	22	22	16	16					12	12	13			0		352	374	NB3	
27	450/1LVF		10	10	10			7			7				10		0				x	
28	450/2	42	20	20	20	20	20	9		8	9	13	13	13			0		384	403	NB3	
29	450/3LVT		10	10	10										10		0				x	
30	450/4	42	15	15	15	17	17	7		7	7	9	9	9			0	5	407	423	DHI1	
31	451/1	33	15	15	15	11	11		9								0	5	424	439	DHI1	
32	451/2	33	21	21	21	17	17		13								0		440	460	NB3	
33	452/1	39	18	18	18	12	12	9		9	9	15	15	15			0		463	480	DHI1	

	A	B	C	D	E	F	G	H	I	J	K	L	M	N	O	P	Q	R	S	T	U	V
122																						
34	452/2	39	18	16	16	14	14	13		7	13	10	10	10			0	3	487	504	NB3	Kalibrierst
35	453/1		24	24	24	28				16							0		509	532	NB3	Kalibrierst CFC
36	453/2LVF		10	10	10										10		0				x	
37	453/3	24	21	21	21	16	16	12		8	12	17	17				0		533	556	DHI1	
38	453/4	24	21	21	21	12	12	5			5	9	9				0	5	557	580	DHI1	
39	454/1	50	18	18	18												0		582	599	NB3	
40	454/2	50	21	21	21												7		601	624	DHI1	
41	455/1	38	191	19	19	18	18	9			9	14	14	14			0	5	626	644	NB3	
42	455/2LVT		10	10	10										10		5				x	
43	455/3	38	23	23	23	21	21	8		8	8	14	14	14			0	1	646	669	DHI1	
44	456/1	35	20	20	20												0		671	690	NB3	
45	456/2	35	24	23	23			11	10		11						0		691	714	DHI1	LDEO, UB, HD Intercal
46	457/1	8	10	10	10	8	8										0		715	724	NB3	
47	457/2	8	24	24	24	13	13	7		8	7						0		727	750	DHI1	
48	458/1	8	12	12	12	8	8	8		8	8	8	8		4		0	3	751	762	NB3	
49	458/2LVT		10	10	10										10		0				x	
50	458/3	55	22	22	22	19	19	11		8	11	13	13		2	6	0		765	787	DHI1	
51	459	55	24	22	24	7	7	9			9						11		789	812	DHI1	
52	460	45	24	22	21	16	16	7			7						0		813	836	DHI1	
53	461	45	21	21	21					8							0		837	860	DHI1	
54	462	49	22	22	22	17	17	12			12	22	22			6	0	4	861	883	DHI1	
55	463	49	23	22	22	7	7		6	8							0		885	908	DHI1	
56	464	60	22	22	22	22	22	8		16	8	23	23	23			0	3	909	932	DHI1	
57	465	60	23	23	23	14	14	12			12	23	23				0	3	933	955	DHI1	
58	466	152	21	21	21	20	20		8								0		956	978	DHI1	
59	467	152	22	22	22	14	14	7		16	7						0		979	1002	DHI1	
60	468/1	43	22	22	22	13	13	8			8	14	14	14		5	0	4	1003	1024	NB3	
61	468/2LVT		10	10	10										10		0				x	
62	468/3	43	21	21	21	20	20	9			9	16	16	16		1	7		1027	1050	DHI1	
63	469/1	30	12	12	12	12	12												1051	1064	NB3	
64	469/2	30	22	22	221	16	16		8										1065	1087	DHI1	
65	470/1	186	14	14	14	10	10	4		16	4	14	14					5	1089	1102	NB3	
66	470/2	186	22	22	22	18	18	8		16	8	23	23						1103	1126	DHI1	
67	471/1	195	14	14	14	10	10	8			8					4			1127	1140	NB3	
68	471/2LVT		10	10	10					16					10						x	Repro

	A	B	C	D	E	F	G	H	I	J	K	L	M	N	O	P	Q	R	S	T	U	V
122																						
69	471/3	195	23	23	23	24	24	10			10					2			1141	1164	DHI1	
70	472/1	194	12	12	12							12	12	12				3	1165	1178	NB3	
71	472/2	194	23	23	23	4	4					16	16	16					1179	1202	DHI1	
72	473/1	196	14	14	14	10	10	5			5								1203	1216	NB3	
73	473/2	196	23	23	23	21	21	13			13								1217	1240	DHI1	
74	474/1LVF		10	10	10										10						x	
75	474/2	1	23	23	23	18	18	9			9	16	16						1255	1278	DHI1	
76	474/3LVT		10	10	10										10						x	BIO+1279
77	474/4	1	15	15	15	10	10	7			7	14	14					6	1241	1254	NB3	
78	475/1	52	23	23	23	21	21					23	23	23			12	5	1296	1319	DHI1	
79	476/1	0	23	23	23	28		6	6	32									1320	1343	DHI1	Kal 3200m, Intercal HD, UB
80	476/2	52	16	16	16			7			7								1280	1295	NB3	
81	476/3	20	23	23	23	14	14	10			10								1344	1367	DHI1	
82	477/1	20	24	24	24	24	24	13			13	23	23					3	1368	1391	DHI1	
83	478	18	22	22	22	7	7												1392	1415	DHI1	
84	479/1	18	13	13	13	10	10	6			6	12	12			5		3	1416	1429	NB3	
85	479/2LVT		10	10	10										10						x	
86	479/3	10	23	23	23	21	21	12			12	14	14			1			1430	1453	DHI1	
87	480	10	23	23	23	23	23					23	23	23				2	1454	1477	DHI1	
88	481	4	24	24	24	24	24	15		24	15	24	24					3	1478	1501	DHI1	
89	482	4	24	24	24	25	25												1502	1525	DHI1	
90	483/1LVF		10	10	10										10						x	
91	483/2	15	24	24	24	25	25	10			10	16	16						1526	1549	DHI1	
92	483/3LVT		10	10	10										10						x	
93	483/4	15	16	16	16	17	17	9			9	14	14					3	1550	1565	DHI1	
94	484	26	23	23	23	24	24												1566	1589	DHI1	
95	485	26	22	22	22	25	25	12		16	12	22	22	22			10	2	1590	1613	DHI1	
96	486/1	56	24	24	24	19	19	12		11	12	15	15			6			1614	1637	DHI1	
97	486/2	56	16	16	16	10	10	8		5	8	16	16			5		5	1614	1653	NB3	
98	487	185	22	22	22	21	21	14			14	22	22	22		5		5	1654	1677	DHI1	
99	488	185	23	23	23	16	16	11			11	23	23					4	1678	1700	DHI1	End of section
100																						
101																						
102																						
103	**Total**	4266	1722	1737	1692	1062	978	474	77	311	468	694	694	359	158	65	78	123				**WOCE-A2**

- **Summary of Daily Station Activities M30/2**

15. Okt	16. Okt	17. Okt	18. Okt	19. Okt	19. Okt	21. Okt	22. Okt	23. Okt	24. Okt
436/1	437	444	446	**Sturm**	449/1	450/2	**Sturm**	452/1	454/1
DHI1	*NB3*	*NB3*	*NB3*	***W9–11***	*DHI1*	*NB3*	***WNW 9***	*DHI1*	*NB3*
436/3	438	445	447		449/2	450/4		452/2	454/2
NB3	*NB3*	*DHI1*	*NB3*		*NB3*	*DHI1*		*NB3*	*DHI1*
436/4	439		448			451/1		453/1	455/1
DHI2	*NB3*		*DHI1*			*DHI1*		*NB3*	*NB3*
	440					451/2		453/3	455/3
	NB3					*NB3*		*DHI1*	*DHI1*
	441							453/4	456/1
	NB3					**Sturm**		*DHI1*	*NB3*
	442					***W10-11***			
	NB3								
	443								
	NB3								

25. Okt	26. Okt	27. Okt	28. Okt	29. Okt	30. Okt	31. Okt	1. Nov	2. Nov	3. Nov
456/2	459	465	466	469/1	470/2	472/1	474/2	**Sturm**	477
DHI1	*DHI1*	*DHI1*	*DHI1*	*NB3*	*DHI1*	*NB3*	*DHI1*		*DHI1*
457/1	460		467	469/2	471/1	472/2	474/4	475	478
NB3	*DHI1*		*DHI1*	*DHI1*	*NB3*	*DHI1*	*NB3*	*DHI1*	*DHI1*
457/2	461		468/1	470/1	471/3	473/1		476/1	479/1
DHI1	*DHI1*		*NB3*	*NB3*	*DHI1*	*NB3*		*DHI1*	*NB3*
458/1	462		468/3			473/2		476/2	479/2
NB3	*DHI1*		*DHI1*			*DHI1*		*NB3*	*DHI1*
458/3	463								
DHI1	*DHI1*								
	464						**Sturm**		
	DHI1						***WNW 9***		

4. Nov	**5. Nov**	**6. Nov**	**7. Nov**	**8. Nov**	**9. Nov**	**10. Nov**	**11. Nov**	**12. Nov**
480	481	483/2	484	486/2	487			
DHI1	*DHI1*	*DHI1*	*DHI1*	*NB3*	*DHI1*			
Sturm	482/1		485		488			
NW 10	*DHI1*		*DHI1*		*DHI1*			
		483/4	486/1					
		DHI1	*DHI1*					
				Sturm				
				NNW9				
Sturm								
NW9								

7.1.3 Station List Leg M30/3 Section A1W

EXPO-CODE	WOCE WHP-ID	Stat. No.	Cast No.	Cast Type	Date	Time UTC	Code	Position Latitude	Longitude	Code	Bottom Depth	Meter Wheel	Max Pres	Bottom Dist.	No.of Btls	Parameters / Comments
06MT30/3	A1/W	489	1	ROS	111694	1619	BE	51 35.5 N	53 32.7 W	GPS	447					
06MT30/3	A1/W	489	1	ROS	111694	1642	BO	51 35.3 N	53 32.8 W	GPS	447	421	420	20	23	1-6, 10/Test "DHI1" CTD+ROS
06MT30/3	A1/W	489	1	ROS	111694	1714	EN	51 35.2 N	53 33.0 W	GPS	447					
06MT30/3	A1/W	489	2	ROS	111694	1737	BE	51 35.1 N	53 33.2 W	GPS	447					
06MT30/3	A1/W	489	2	ROS	111694	1802	BO	51 35.1 N	53 33.4 W	GPS	448	420	414		23	1-8, 10/Test "NB3" CTD+ROS
06MT30/3	A1/W	489	2	ROS	111694	1840	EN	51 35.2 N	53 33.5 W	GPS	447					
06MT30/3	A1/W	490	1	ROS	111894	0903	BE	54 45.4 N	54 29.3 W	GPS	250					
06MT30/3	A1/W	490	1	ROS	111894	0913	BO	54 45.2 N	54 29.4 W	GPS	250	227	221	20	5	1-8, 23
06MT30/3	A1/W	490	1	ROS	111894	0927	EN	54 45.0 N	54 29.5 W	GPS	250					
06MT30/3	A1/W	491	1	ROS	111894	1115	BE	54 57.3 N	54 17.2 W	GPS	380					
06MT30/3	A1/W	491	1	ROS	111894	1129	BO	54 57.3 N	54 17.1 W	GPS	380	351	351	14	6	1-6, 9, 10, 23
06MT30/3	A1/W	491	1	ROS	111894	1152	EN	54 57.2 N	54 16.8 W	GPS	379					
06MT30/3	A1/W	492	1	ROS	111894	1331	BE	55 06.6 N	54 08.3 W	GPS	959					
06MT30/3	A1/W	492	1	ROS	111894	1355	BO	55 06.5 N	54 07.9 W	GPS	943	907	911	16	13	1-10, 23
06MT30/3	A1/W	492	1	ROS	111894	1432	EN	55 06.3 N	54 07.7 W	GPS	930					
06MT30/3	A1/W	493	1	LVS	111894	1809	MR	55 15.9 N	53 57.6 W	GPS	2118	2041		40	10	1, 12, 13
06MT30/3	A1/W	493	2	ROS	111894	1949	BE	55 14.9 N	53 56.8 W	GPS	2063					
06MT30/3	A1/W	493	2	ROS	111894	2043	BO	55 14.4 N	53 56.7 W	GPS	2030	2017	2025	21	23	1-10, 23
06MT30/3	A1/W	493	2	ROS	111894	2148	EN	55 13.5 N	53 56.5 W	GPS	2037					
06MT30/3	A1/W	494	1	ROS	111994	0035	BE	55 25.2 N	53 49.6 W	GPS	2685					
06MT30/3	A1/W	494	1	ROS	111994	0132	BO	55 24.8 N	53 49.6 W	GPS	2686	2676	2701	16	24	1-10, 23
06MT30/3	A1/W	494	1	ROS	111994	0303	EN	55 24.2 N	53 49.6 W	GPS	2673					
06MT30/3	A1/W	495	1	LVS	111994	0545	MR	55 36.6 N	53 38.0 W	GPS	2930	2854		40	10	1, 12, 13
06MT30/3	A1/W	495	2	ROS	111994	0744	BE	55 36.7 N	53 37.2 W	GPS	2938					
06MT30/3	A1/W	495	2	ROS	111994	0848	BO	55 36.9 N	53 36.5 W	GPS	2940	2915	2936	18	23	1-10, 12, 23
06MT30/3	A1/W	495	2	ROS	111994	1011	EN	55 37.1 N	53 35.3 W	GPS	2933					
06MT30/3	A1/W	496	1	ROS	111994	1254	BE	55 50.8 N	53 23.3 W	GPS	3148					
06MT30/3	A1/W	496	1	ROS	111994	1356	BO	55 50.6 N	53 22.6 W	GPS	3144	3107	3140	9	24	1-10, 23/ROS quality test #1
06MT30/3	A1/W	496	1	ROS	111994	1515	EN	55 50.3 N	53 21.5 W	GPS	3143					
06MT30/3	A1/W	497	1	ROS	112094	2352	BE	59 44.9 N	49 09.5 W	GPS	3246					
06MT30/3	A1/W	497	1	ROS	112194	0101	BO	59 44.8 N	49 10.5 W	GPS	3242	3209	3227	40	24	1-10, 23
06MT30/3	A1/W	497	1	ROS	112194	0236	EN	59 44.8 N	49 11.5 W	GPS	3246					
06MT30/3	A1/W	498	1	ROS	112294	0943	BE	59 03.7 N	49 56.9 W	GPS	3489					
06MT30/3	A1/W	498	1	ROS	112294	1111	BO	59 03.2 N	49 58.2 W	GPS	3492	3473	3506	20	24	1-10, 12, 23
06MT30/3	A1/W	498	1	ROS	112294	1257	EN	59 02.7 N	49 59.7 W	GPS	3497					
06MT30/3	A1/W	498	2	LVS	112294	1430	MR	59 02.6 N	49 59.7 W	GPS	3496	3419		40	10	1, 12, 13
06MT30/3	A1/W	499	1	ROS	112294	1923	BE	59 28.1 N	49 28.1 W	GPS	3416					

EXPO-CODE	WOCE WHP-ID	Stat. No.	Cast No.	Cast Type	Date	Time UTC	Code	Position Latitude	Longitude	Code	Bottom Depth	Meter Wheel	Max Pres	Bottom Dist.	No.of Btls	Parameters / Comments
06MT30/3	A1/W	499	1	ROS	112294	2034	BO	59 29.0 N	49 27.2 W	GPS	3414	3402	3423	20	23	1-10, 23
06MT30/3	A1/W	499	1	ROS	112294	2204	EN	59 29.4 N	49 26.5 W	GPS	3415					
06MT30/3	A1/W	500	1	ROS	112394	0145	BE	59 59.1 N	48 54.0 W	GPS	3039					
06MT30/3	A1/W	500	1	ROS	112394	0248	BO	59 59.5 N	48 53.8 W	GPS	3035	3014	3031	30	23	1-10, 12, 23
06MT30/3	A1/W	500	1	ROS	112394	0418	EN	59 59.5 N	48 54.2 W	GPS	3043					
06MT30/3	A1/W	501	1	ROS	112394	0914	BE	60 10.6 N	48 41.0 W	GPS	2880					
06MT30/3	A1/W	501	1	ROS	112394	1023	BO	60 11.0 N	48 41.3 W	GPS	2886	2855	2899	17	24	1-10, 23
06MT30/3	A1/W	501	1	ROS	112394	1153	EN	60 11.9 N	48 42.1 W	GPS	2896					
06MT30/3	A1/W	502	1	ROS	112394	1352	BE	60 17.5 N	48 32.9 W	GPS	2767					
06MT30/3	A1/W	502	1	ROS	112394	1453	BO	60 18.0 N	48 34.2 W	GPS	2765	2742	2772	10	24	1-10, 12, 23
06MT30/3	A1/W	502	1	ROS	112394	1614	EN	60 18.4 N	48 35.6 W	GPS	2766					
06MT30/3	A1/W	503	1	LVS	112394	1709	MR	60 20.9 N	48 30.1 W	GPS	1574	1257		40	10	1, 12, 13
06MT30/3	A1/W	503	2	ROS	112394	1935	BE	60 20.8 N	48 31.3 W	GPS	1734					
06MT30/3	A1/W	503	2	ROS	112394	2030	BO	60 21.1 N	48 31.9 W	GPS	1666	1676	1692	29	17	1-10, 23
06MT30/3	A1/W	503	2	ROS	112394	1935	BE	60 20.8 N	48 31.3 W	GPS	1734					
06MT30/3	A1/W	504	1	ROS	112394	2313	BE	60 24.2 N	48 24.8 W	GPS	578					
06MT30/3	A1/W	504	1	ROS	112394	2335	BO	60 24.4 N	48 25.3 W	GPS	489	467	467	14	10	1-10, 23
06MT30/3	A1/W	504	1	ROS	112494	0006	EN	60 24.7 N	48 25.7 W	GPS	401					
06MT30/3	A1/W	505	1	ROS	112494	0214	BE	60 33.9 N	48 13.6 W	GPS	145					
06MT30/3	A1/W	505	1	ROS	112494	0227	BO	60 33.8 N	48 13.5 W	GPS	139	111	114	25	5	1-6, 9, 10, 12, 23
06MT30/3	A1/W	505	1	ROS	112494	0239	EN	60 33.9 N	48 13.4 W	GPS	130					

- **Station List Leg M30/3 Section A1E**

EXPO-CODE	WOCE WHP-ID	Stat. No.	Cast No.	Cast Type	Date	Time UTC	Code	Position Latitude	Longitude	Code	Bottom Depth	Meter Wheel	Max Pres	Bottom Dist.	No.of Btls	Parameters	Comments
06MT30/3	A1/E	506	1	ROS	112594	0004	BE	60 00.0 N	42 30.1 W	GPS	193						
06MT30/3	A1/E	506	1	ROS	112594	0019	BO	59 59.6 N	42 30.3 W	GPS	193	177	178	9	5	1-10, 23	
06MT30/3	A1/E	506	1	ROS	112594	0029	EN	59 49.5 N	42 30.5 W	GPS	192						
06MT30/3	A1/E	507	1	ROS	112594	0227	BE	59 57.6 N	42 10.1 W	GPS	507						
06MT30/3	A1/E	507	1	ROS	112594	0245	BO	59 57.4 N	42 10.0 W	GPS	500	474	474	17	8	1-10, 23	
06MT30/3	A1/E	507	1	ROS	112594	0302	EN	59 57.3 N	42 10.0 W	GPS	499						
06MT30/3	A1/E	508	1	ROS	112594	0424	BE	59 55.9 N	41 51.5 W	GPS	1827						
06MT30/3	A1/E	508	1	ROS	112594	0505	BO	59 55.2 N	41 51.6 W	GPS	1824	1789	1802	21	18	1-10, 23	
06MT30/3	A1/E	508	1	ROS	112594	0558	EN	59 54.5 N	41 52.1 W	GPS	1822						
06MT30/3	A1/E	509	1	ROS	112594	0823	BE	59 53.0 N	41 30.3 W	GPS	1897						
06MT30/3	A1/E	509	1	ROS	112594	0928	BO	59 52.5 N	41 29.8 W	GPS	1899	1852	1876	18	20	1-10, 23	
06MT30/3	A1/E	509	1	ROS	112594	1045	EN	59 51.6 N	41 29.2 W	GPS	1917						
06MT30/3	A1/E	510	1	ROS	112594	1304	BE	59 52.1 N	41 12.8 W	GPS	2031						
06MT30/3	A1/E	510	1	ROS	112594	1411	BO	59 52.0 N	41 13.4 W	GPS	2027	1992	2008	17	24	1-10, 23	
06MT30/3	A1/E	510	1	ROS	112594	1513	EN	59 51.8 N	41 13.8 W	GPS	2025						
06MT30/3	A1/E	511	1	ROS	112594	1746	BE	59 50.2 N	40 52.3 W	GPS	2339						
06MT30/3	A1/E	511	1	ROS	112594	1858	BO	59 50.9 N	40 53.5 W	GPS	2327	2394	2315	18	19	1-10 / Data flow interrupts	
06MT30/3	A1/E	511	1	ROS	112594	2019	EN	59 51.5 N	40 55.5 W	GPS	2282					during uptrace	
06MT30/3	A1/E	512	1	ROS	112894	0124	BE	59 45.1 N	40 02.9 W	GPS	2702						
06MT30/3	A1/E	512	1	ROS	112894	0229	BO	59 44.5 N	40 03.7 W	GPS	2710	2701	2690	20	24	1-10, 23	
06MT30/3	A1/E	512	1	ROS	112894	0338	EN	59 44.1 N	40 04.4 W	GPS	2711						
06MT30/3	A1/E	513	1	ROS	112894	0724	BE	59 38.8 N	38 55.4 W	GPS	2953						
06MT30/3	A1/E	513	1	ROS	112894	0833	BO	59 38.8 N	38 54.8 W	GPS	2955	2919	2936	19	24	1-10, 23	
06MT30/3	A1/E	513	1	ROS	112894	1021	BE	59 39.1 N	38 53.2 W	GPS	2958						
06MT30/3	A1/E	514	1	LVS	112894	1554	MR	59 31.2 N	37 38.4 W	GPS	3133	3051		40	10	1, 12, 13	
06MT30/3	A1/E	514	2	ROS	112894	1744	BE	59 31.1 N	37 38.3 W	GPS	3132						
06MT30/3	A1/E	514	2	ROS	112894	1850	BO	59 31.4 N	37 38.6 W	GPS	3130	3099	3134	18	24	1-10, 12, 23	
06MT30/3	A1/E	514	2	ROS	112894	2024	EN	59 32.1 N	37 39.5 W	GPS	3132						
06MT30/3	A1/E	515	1	ROS	112994	0109	BE	59 23.2 N	36 20.7 W	GPS	3120						
06MT30/3	A1/E	515	1	ROS	112994	0216	BO	59 23.5 N	36 22.0 W	GPS	3124	3101	3121	19	23	1-10, 23	
06MT30/3	A1/E	515	1	ROS	112994	0342	EN	59 23.6 N	36 22.5 W	GPS	3122						
06MT30/3	A1/E	516	1	ROS	112994	0758	BE	59 15.6 N	35 03.9 W	GPS	3057						
06MT30/3	A1/E	516	1	ROS	112994	0908	BO	59 15.4 N	35 04.9 W	GPS	3049	3005	3038	20	22	1-10, 23	
06MT30/3	A1/E	516	1	ROS	112994	1023	EN	59 15.1 N	35 06.1 W	GPS	3083						
06MT30/3	A1/E	517	1	ROS	112994	1500	BE	59 07.9 N	33 47.2 W	GPS	2286						
06MT30/3	A1/E	517	1	ROS	112994	1546	BO	59 07.9 N	33 47.3 W	GPS	2325	2249	2270	20	21	1-10, 23 / ROS Test # 2	
06MT30/3	A1/E	517	1	ROS	112994	1649	BE	59 07.7 N	33 46.7 W	GPS	2313						

EXPO-CODE	WOCE WHP-ID	Stat. No.	Cast No.	Cast Type	Date	Time UTC	Code	Position Latitude	Longitude	Code	Bottom Depth	Meter Wheel	Max Pres	Bottom Dist.	No.of Btls	Parameters	Comments
06MT30/3	A1/E	518	1	ROS	112994	1919	BE	59 03.2 N	33 02.2 W	GPS	2452						
06MT30/3	A1/E	518	1	ROS	112994	2041	BO	59 02.0 N	33 02.0 W	GPS	2449		2441	15	24	1-10, 23	
06MT30/3	A1/E	518	1	ROS	112994	2150	EN	59 02.5 N	33 01.9 W	GPS	2435						
06MT30/3	A1/E	519	1	ROS	113094	0039	BE	58 58.3 N	32 17.8 W	GPS	1623						
06MT30/3	A1/E	519	1	ROS	113094	0130	BO	58 58.3 N	32 18.1 W	GPS	1760	1760	1757	20	19	1-10, 23	
06MT30/3	A1/E	519	1	ROS	113094	0227	EN	58 58.4 N	32 18.8 W	GPS	1921						
06MT30/3	A1/E	520	1	ROS	113094	0503	BE	58 52.8 N	31 33.6 W	GPS	1503						
06MT30/3	A1/E	520	1	ROS	113094	0536	BO	58 52.8 N	31 33.8 W	GPS	1505	1478	1492	18	15	1-10, 23	
06MT30/3	A1/E	520	1	ROS	113094	0625	EN	58 52.8 N	31 34.4 W	GPS	1511						
06MT30/3	A1/E	521	1	ROS	113094	0906	BE	58 48.0 N	30 49.2 W	GPS	1189						
06MT30/3	A1/E	521	1	ROS	113094	0942	BO	58 47.7 N	30 48.4 W	GPS	1250	1234	1233	20	15	1-10, 23	
06MT30/3	A1/E	521	1	ROS	113094	1027	EN	58 47.6 N	30 47.8 W	GPS	1211						
06MT30/3	A1/E	522	1	ROS	113094	1305	BE	58 31.0 N	30 16.5 W	GPS	1748						
06MT30/3	A1/E	522	1	ROS	113094	1359	BO	58 30.5 N	30 16.4 W	GPS	1636	1670	1689	13	20	1-10, 23	
06MT30/3	A1/E	522	1	ROS	113094	1457	EN	58 30.5 N	30 16.9 W	GPS	1886						
06MT30/3	A1/E	523	1	ROS	113094	1755	BE	58 14.1 N	29 44.1 W	GPS	2296						
06MT30/3	A1/E	523	1	ROS	113094	1852	BO	58 14.4 N	29 43.6 W	GPS	2286	2255	2276	18	24	1-10, 23	
06MT30/3	A1/E	523	1	ROS	113094	2004	EN	58 15.1 N	29 42.9 W	GPS	2292						
06MT30/3	A1/E	524	1	ROS	113094	2338	BE	57 57.2 N	29 12.0 W	GPS	2232						
06MT30/3	A1/E	524	1	ROS	120194	0029	BO	57 57.7 N	29 11.3 W	GPS	2226	2239	2209	26	23	1-10, 23	
06MT30/3	A1/E	524	1	ROS	120194	0145	EN	57 58.1 N	29 10.5 W	GPS	2225						
06MT30/3	A1/E	525	1	ROS	120194	0642	BE	57 40.2 N	28 40.2 W	GPS	2470						
06MT30/3	A1/E	525	1	ROS	120194	0757	BO	57 40.7 N	28 40.0 W	GPS	2470	2439	2455	20	24	1-10, 23	
06MT30/3	A1/E	525	1	ROS	120194	0922	EN	57 40.9 N	28 39.5 W	GPS	2471						
06MT30/3	A1/E	526	1	LVS	120194	1044	MR	57 22.9 N	28 07.5 W	GPS	2655	2576		40	10	1, 12, 13	
06MT30/3	A1/E	526	2	ROS	120194	1641	BE	57 22.5 N	28 07.2 W	GPS	2662						
06MT30/3	A1/E	526	2	ROS	120194	1732	BO	57 22.4 N	28 08.0 W	GPS	2666	2623	2654	16	24	1-10, 23	
06MT30/3	A1/E	526	2	ROS	120194	1850	EN	57 22.2 N	28 07.6 W	GPS	2640						
06MT30/3	A1/E	527	1	ROS	120194	2215	BE	56 54.8 N	27 50.5 W	GPS							
06MT30/3	A1/E	527	1	ROS	120194	2332	BO	56 54.9 N	27 48.2 W	GPS	2933	2933	2867	40	22	1-10, 23/Data flow interrupts	
06MT30/3	A1/E	527	1	ROS	120294	0116	EN	56 54.7 N	27 45.3 W	GPS	2888					during uptrace	
06MT30/3	A1/E	528	1	MOR	120294	0455	BE	57 23.4 N	28 12.5 W	GPS						Dredging of Mooring "D2"	
06MT30/3	A1/E	528	1	MOR	120294	1500	EN	57 25.7 N	28 17.8 W	GPS						(failed)	
06MT30/3	A1/E	529	1	ROS	120394	0003	BE	56 27.3 N	27 29.8 W	GPS	2773						
06MT30/3	A1/E	529	1	ROS	120394	0103	BO	56 27.2 N	27 29.6 W	GPS	2766	2749	2778	17	24	1-10, 23	
06MT30/3	A1/E	529	1	ROS	120394	0218	EN	56 27.1 N	27 29.1 W	GPS	2769						
06MT30/3	A1/E	530	1	ROS	120394	0521	BE	55 59.4 N	27 08.8 W	GPS	2817						
06MT30/3	A1/E	530	1	ROS	120394	0624	BO	55 59.0 N	27 09.0 W	GPS	2796	2789	2784	26	22	1-10, 23	
06MT30/3	A1/E	530	1	ROS	120394	0750	EN	55 58.4 N	27 11.0 W	GPS	2802						

EXPO-CODE	WOCE WHP-ID	Stat. No.	Cast No.	Cast Type	Date	Time UTC	Code	Position Latitude	Longitude	Code	Bottom Depth	Meter Wheel	Max Pres	Bottom Dist.	No.of Btls	Parameters	Comments
06MT30/3	A1/E	531	1	ROS	120394	1047	BE	55 31.9 N	26 47.7 W	GPS	3208						
06MT30/3	A1/E	531	1	ROS	120394	1157	BO	55 31.8 N	26 48.1 W	GPS	3198	3185	3202	22	24	1-6, 9, 10, 23	
06MT30/3	A1/E	531	1	ROS	120394	1324	EN	55 31.4 N	26 48.5 W	GPS	3209						
06MT30/3	A1/E	532	1	ROS	120394	1626	BE	55 04.2 N	26 27.6 W	GPS	3380						
06MT30/3	A1/E	532	1	ROS	120394	1728	BO	55 04.3 N	26 28.1 W	GPS	3380	3346	3396	18	24	1-10, 23	
06MT30/3	A1/E	532	1	ROS	120394	1850	EN	55 04.3 N	26 29.3 W	GPS	3381						
06MT30/3	A1/E	533	1	ROS	120394	2203	BE	54 36.6 N	26 07.4 W	GPS	3427						
06MT30/3	A1/E	533	1	ROS	120394	2319	BO	54 35.9 N	26 07.8 W	GPS	3441	3491	3462	18	24	1-6, 9, 10, 23	
06MT30/3	A1/E	533	1	ROS	120494	0049	EN	54 35.1 N	26 08.3 W	GPS	3438						
06MT30/3	A1/E	534	1	ROS	120494	0322	BE	54 17.8 N	25 53.1 W	GPS	3132						
06MT30/3	A1/E	534	1	ROS	120494	0422	BO	54 17.6 N	25 52.5 W	GPS	3088	3053	3092	17	24	1-10, 23	
06MT30/3	A1/E	534	1	ROS	120494	0540	EN	54 17.2 N	25 52.1 W	GPS	3061						
06MT30/3	A1/E	535	1	ROS	120494	0802	BE	53 59.1 N	25 38.9 W	GPS	3385						
06MT30/3	A1/E	535	1	ROS	120494	0924	BO	53 58.1 N	25 38.0 W	GPS	3610	3517	3514	20	24	1-10, 23	
06MT30/3	A1/E	535	1	ROS	120494	1102	EN	53 57.3 N	25 36.8 W	GPS							
06MT30/3	A1/E	536	1	ROS	120494	1324	BE	53 40.4 N	25 24.8 W	GPS	3591						
06MT30/3	A1/E	536	1	ROS	120494	1437	BO	53 40.2 N	25 24.8 W	GPS	3598	3599	3627	17	22	1-10, 23	
06MT30/3	A1/E	536	1	ROS	120494	1614	EN	53 40.0 N	25 24.7 W	GPS	3599						
06MT30/3	A1/E	537	1	ROS	120494	1903	BE	53 27.8 N	24 41.1 W	GPS	3585						
06MT30/3	A1/E	537	1	ROS	120494	2026	BO	53 26.9 N	24 41.2 W	GPS	3564	3598	3590	20	24	1-10, 23	
06MT30/3	A1/E	537	1	ROS	120494	2210	EN	53 26.6 N	24 42.0 W	GPS	3533						
06MT30/3	A1/E	538	1	ROS	121294	0853	BE	53 10.2 N	23 31.3 W	GPS	3694						
06MT30/3	A1/E	538	1	ROS	121294	1011	BO	53 10.6 N	23 32.0 W	GPS	3695	3704	3735	17	23	1-10, 23	
06MT30/3	A1/E	538	1	ROS	121294	1143	EN	53 10.0 N	23 33.0 W	GPS	3690						
06MT30/3	A1/E	539	1	ROS	121294	1556	BE	52 52.1 N	22 23.0 W	GPS	4009						
06MT30/3	A1/E	539	1	ROS	121294	1707	BO	52 52.2 N	22 23.4 W	GPS	4014	4011	4072	18	24	1-10, 23	
06MT30/3	A1/E	539	1	ROS	121294	1851	EN	52 53.0 N	22 24.6 W	GPS	3990						
06MT30/3	A1/E	540	1	ROS	121294	2313	BE	52 33.8 N	21 14.0 W	GPS	3789						
06MT30/3	A1/E	540	1	ROS	121394	0029	BO	52 33.6 N	21 14.6 W	GPS	3786	3837	3816	15	24	1-8, 23	
06MT30/3	A1/E	540	1	ROS	121394	0158	EN	52 33.6 N	21 15.2 W	GPS	3791						
06MT30/3	A1/E	541	1	ROS	121394	0614	BE	52 19.9 N	20 00.1 W	GPS	3412						
06MT30/3	A1/E	541	1	ROS	121394	0728	BO	52 19.8 N	20 00.6 W	GPS	3277	3416	3454	17	24	1-10, 23	
06MT30/3	A1/E	541	1	ROS	121394	0854	EN	52 19.6 N	20 01.1 W	GPS	3316						
06MT30/3	A1/E	542	1	ROS	121394	1249	BE	52 20.1 N	18 52.0 W	GPS	4284						
06MT30/3	A1/E	542	1	ROS	121394	1419	BO	52 20.7 N	18 52.9 W	GPS	4227	4265	4300	16	22	1-10, 23	
06MT30/3	A1/E	542	1	ROS	121394	1600	EN	52 20.2 N	18 53.3 W	GPS	4255						
06MT30/3	A1/E	543	1	ROS	121394	1929	BE	52 19.8 N	17 49.9 W	GPS	4314						
06MT30/3	A1/E	543	1	ROS	121394	2048	BO	52 19.4 N	17 49.7 W	GPS	4313	4328	4395	11	24	1-10, 23	
06MT30/3	A1/E	543	1	ROS	121394	2232	EN	52 19.2 N	17 49.3 W	GPS	4319						

EXPO-CODE	WOCE WHP-ID	Stat. No.	Cast No.	Cast Type	Date	Time UTC	Code	Position Latitude	Longitude	Code	Bottom Depth	Meter Wheel	Max Pres	Bottom Dist.	No.of Btls	Parameters	Comments
06MT30/3	A1/E	544	1	ROS	121494	0120	BE	52 20.1 N	16 59.7 W	GPS	3916						
06MT30/3	A1/E	544	1	ROS	121494	0233	BO	52 20.0 N	16 59.4 W	GPS	3919	3932	3939	18	24	1-8 / ROS Test # 3	
06MT30/3	A1/E	544	1	ROS	121494	0413	EN	52 20.2 N	16 58.8 W	GPS	3917						
06MT30/3	A1/E	545	1	ROS	121494	0655	BE	52 19.9 N	16 11.9 W	GPS	3446						
06MT30/3	A1/E	545	1	ROS	121494	0805	BO	52 19.7 N	16 11.0 W	GPS	3452	3452	3488	20	24	1-10, 23	
06MT30/3	A1/E	545	1	ROS	121494	0935	EN	52 19.5 N	16 09.9 W	GPS	3449						
06MT30/3	A1/E	546	1	ROS	121494	1134	BE	52 20.0 N	15 46.9 W	GPS	3256						
06MT30/3	A1/E	546	1	ROS	121494	1241	BO	52 19.9 N	15 45.8 W	GPS	3248	3284	3282	20	24	1-10, 23	
06MT30/3	A1/E	546	1	ROS	121494	1403	EN	52 19.9 N	15 44.9 W	GPS	3239						
06MT30/3	A1/E	547	1	ROS	121494	1714	BE	52 20.0 N	15 30.0 W	GPS	2776						
06MT30/3	A1/E	547	1	ROS	121494	1810	BO	52 20.0 N	15 29.6 W	GPS	2736	2754	2784	19	24	1-10, 23	
06MT30/3	A1/E	547	1	ROS	121494	1926	EN	52 20.0 N	15 30.0 W	GPS	2751						
06MT30/3	A1/E	548	1	ROS	121594	0000	BE	52 19.9 N	15 12.9 W	GPS	1265						
06MT30/3	A1/E	548	1	ROS	121594	0031	BO	52 19.8 N	15 12.9 W	GPS	1262	1246	1254	20	14	1-10, 23	
06MT30/3	A1/E	548	1	ROS	121594	0105	EN	52 19.4 N	15 13.0 W	GPS	1266						
06MT30/3	A1/E	549	1	ROS	121594	0224	BE	52 19.9 N	14 55.8 W	GPS	839						
06MT30/3	A1/E	549	1	ROS	121594	0242	BO	52 20.0 N	14 55.5 W	GPS	837	819	819	21	9	1-6, 23	
06MT30/3	A1/E	549	1	ROS	121594	0307	EN	52 20.0 N	14 55.9 W	GPS	842						
06MT30/3	A1/E	550	1	ROS	121594	0424	BE	52 19.9 N	14 38.5 W	GPS	411						
06MT30/3	A1/E	550	1	ROS	121594	0433	BO	52 20.0 N	14 38.5 W	GPS	410	395	396		5	1-6, 23	
06MT30/3	A1/E	550	1	ROS	121594	0446	BE	52 20.0 N	14 38.5 W	GPS	410						
06MT30/3	A1/E	551	1	ROS	121594	0616	BE	52 20.0 N	14 15.4 W	GPS	336						
06MT30/3	A1/E	551	1	ROS	121594	0626	BE	52 20.0 N	14 15.5 W	GPS	337	317	318	19	4	1-6, 23	
06MT30/3	A1/E	551	1	ROS	121594	0636	BE	52 20.0 N	14 15.5 W	GPS	338						

7.2 List of moored instruments

7.2.1 Leg M30/1

Sediment trap mooring positions

Trap code	Coordinates		Depth
	N	W	(m)
IOS	49°00,00’	16°28,20’	4806
OMEX IV	48°59,51’	13°44,06’	4485
OMEX III	49°05,30’	13°23,40’	3670
OMEX II	49°11,47’	12°48,00’	1418

7.2.2 Leg M30/2

Current meter mooring positions

Trap code	Coordinates		Depth
	N	W	(m)
K1	46°21.70’	29°59.29’	3220
K2	45°56.66’	31°49.04’	3630
K3	45°20.36’	33°15.69’	3640

7.2.3 Leg M30/3

Current meter mooring

Code	Coordinates		Depth
	N	W	(m)
D2	57°24.7‘	28°13.5’	2587

7.3 List of Figures

Fig. (1) Track and Station map of Meteor leg M30/1
Fig. (2) Track and Station maps of Meteor legs M30/2 (WHP-A2) and M30/3 (WHP-A1)
Fig. (3a) Nitrate (including nitrite) profiles
Fig. (3b) Phosphate profiles
Fig. (3c) Silicate profiles
Fig. (4a) 24-hour running means of current meter data from OMEX 2 at 620 m from Jan - Sept 1994 (day Nos. 11 – 260).
Fig. (4b) 24-hour running means of current meter data from OMEX 2 at 1070 m from Jan - Sept 1994
Fig. (4c) 24-hour running means of current meter data from OMEX 3 at 580 m from Jan - Sept 1994 (Day Nos. 11 - 260).
Fig. (4d) 24-hour running means of current meter data from OMEX 3 at 1450 m from Jan - Sept 1994 (Day Nos. 11 - 260).
Fig. (4e) 24-hour running means of current meter data from OMEX 3 at 3280 m from Jan - Sept 1994 (Day Nos. 11 - 260).
Fig. (5) A rough estimate of seasonality in sedimentation of the mooring OMEX 3 between January and September 1994
Fig. (6) Chloroplastic pigments and heterotrophic activity within the uppermost centimetre of the sediments
Fig. (7a) Distribution of water samples along section WHP-A2
Fig. (7b) Salinity distribution from bottle samples along WHP-A2
Fig. (7c) Potential temperature along WHP-A2
Fig. (7d) Density σ_θ distribution along WHP-A2
Fig. (7e) Density σ_2 (reference 2000 dbar) distribution along section WHP-A2
Fig. (8a,b) Potential temperature (8a) and depth (8b) of the Labrador Sea Water core along 48 °N for 1982, 1993 and 1994
Fig. (8c,d) Salinity (8c) and density (8d) of the Labrador Sea Water core along 48°N for 1982, 1993 and 1994
Fig. (8e,f) Depth-averaged potential temperatures (top) and salinities (bottom) along 48°N for 1957-1994
Fig. (9a) Distribution of dissolved oxygen along section WHP-A2
Fig. (9b-d) Distributions of silicate (8b), nitrate (8c) and phosphate (8d) along section WHP-A2
Fig. (10) F 113 (upper part) and CCl4 distribution on A2. Values given in ppt.
Fig. (11) Selected tritium profiles for the Western Basin on section A2
Fig. (12) CTD-sections A1/West, (b) potential temperature (°C), (c) salinity, (d) density (σ_t)
Fig. (13) Pre and post cruise calibration
(a) Pressure at T = 10 °C (Oct 94)
(b) Pressure at T = 1.6 °C (Oct 94)
(c) Pressure at T = 8 - 9 °C (Nov 95)
Fig. (13d) Pre- and post-cruise calibration, Temperature
Fig. (14a) Salinity residuals, versus CTD salinity, M30/3
Fig. (14b) Salinity residuals,versus CTD stations,M30/3
Fig. (15) Oxygen residuals of final fit versus CTD stations

Fig. (16a) Distribution of water samples along WHP-A1
Fig (16b-c) Distribution of the concentrations of dissolved oxygen (16b) and silicate (16c) along WHP-A1
Fig. (16d-e) Distribution of nitrate (16d) and phosphate (16e) along WHP-A1
Fig. (17) Within 3 years the LSW in the Irminger Sea cooled down in the order of -0.23 °C. The 3-year cooling rate from the Iceland Basin and the Rockall Trough area is in the order of -0.1 °C.
Fig. (18) Within 3 years the density of the LSW core increased by 0.018 kg/m^3 in the Irminger Sea and by 0.012 kg/m^3 in the area east of the MAR.
Fig. (19) A mean deepening of the LSW core of about 250 dbar was found for the Irminger Sea and of more than 200 dbar for the Rockall Trough area. For the Iceland Basin a deepening of only 53 dbar was found.
Fig. (20) No striking change of the LSW core salinity appeared within the 3 years of observation.
Fig. (21) Positions of XBT profiles for "Meteor" cruise M30/3
Fig. (22) XBT sections (a) A1/West, (b) A1/East
Fig. (23) CTD and XCTD temperature profiles of the upper 150 dbar (a) at stat. # 542, (b) at stat. # 546
Fig. (24) CTD and XCTD temperature profiles of deeper layers (a) at stat. # 542, (b) at stat. # 546
Fig. (25) CTD and XCTD conductivity profiles of the upper 150 dbar (a) at stat. # 542, (b) at stat. # 546
Fig. (26) CTD and XCTD conductivity profiles of the deeper layers (a) at stat. # 542, (b) at stat. # 546
Fig. (27a,b) Results of oxygen measurements at calibration stations, (a) #496,(b) #517
Fig. (27c) Results of oxygen measurements at calibration stations, (c) #544
Fig. (28a) Quality control samples, (a) nitrate + nitrite and silicate
Fig. (28b) Quality control samples, phosphate
Fig. (29a,b) Distribution of tritium (A,B)along a section across the Labrador Sea (M30/3,WHP-A1W).
Fig. (29c,d) Distribution of $^3H/^3He$ age (C, D) along a section across the Labrador Sea (M30/3, WHP-A1W).
Fig. (30) CFC11 section (pmol/kg) of the northern part of the WHP-A1W Labrador Sea section
Fig. (31) CFC11 concentrations vs $\sigma_{1,5}$ for the stations in the Labrador Sea (•) and the central Irminger Sea (x). This density range characterizes the Labrador Sea Water (LSW)
Fig. (32) CFC11 section (pmol/kg) along section WHP-A1E
Fig. (33) Cumulated depth profiles of C_T^{ant} for the western (left) and eastern (right panel) basins of the North Atlantic Ocean along WHP-A2 in 1994
Fig (34) Profiles of total carbonate concentrations for selected stations (#515, #529, #541) of M30/3, section WHP-A1
Fig (35) One year of ALACE data in the Labrador Sea at 1500 m depth.

8 CONCLUDING REMARKS

The scientific complements of all three legs of this Meteor cruise takes pleasures in expressing their appreciation to Captains Kull and Bruns and their crews for the excellent and patient support and encouragement during our work at sea. FS Meteor proved again a very hospitable and productive floating laboratory. We also would like to thank the "Meteor Leitstelle", "Deutsche Forschungsgemeinschaft", the "Bundesministerium für Forschung und Technologie" and "Auswärtiges Amt" for the help, support and their contribution towards the success of this cruise. The support of many people in our home laboratories ensured our work at sea; they might not have liked to work in the North Atlantic in autumn at conditions we encountered but they nevertheless were essential to the outcome of this cruise.

All three chief scientists are pleased with the outcome of these German contributions to global programmes that after a long time of planning finally came to fruition in an international, productive and pleasant collaboration both at sea and ashore.

The goals of this cruise were supported by grants to individual research groups within the frame-work of the German contributions to OMEX, WOCE and JGOFS and by grants of the Deutsche Forschungsgemeinschaft (Ko900/3-1 and Ko900/4-1) for the cruise. This support is gratefully acknowledged.

9 REFERENCES

AMINOT, A., and KIRKWOOD, D.S. (1995):
ICES (fifth) Intercomparison Exercise for Nutrients in Seawater, ICES Copenhagen, (in press).

ATLAS, E.L., GORDON L.I., HAGER S.W., and P.K. PARK (1971):
A practical manual for use of the Technicon AutoAnalyser in seawater analyses, Revised Tech. Rep. 215, Ref. 71-22, Oregon State Univ., 47 pp.

BENDSCHNEIDER, K. and R.J. ROBINSON (1952):
A new spectrophotometric method for the determination of nitrite in seawater, J. Mar. Res., (11) 1, p. 87-96.

CULBERSON, D.H. (1991):
Dissolved Oxygen. In: WHP Operations and Methods, WHP Office Report WHPO 91-1, 15 pp.

DICKSON, R.R., J. MEINCKE, S.-A. MALMBERG and A.J. LEE (1988):
The "Great Salinity Anomaly" in the Northern North Atlantic 1968-1982. Prog. Oceanogr., 20, p. 103-151.

ELGIN, R. H. (1994):
An Evaluation of XCTD Performance with Design Improvements. Sippican, Inc., Marion, Mass., USA, unpublished, 6 pp.

GRASSHOFF, K., EHRHARDT, M., and K. KREMLING (1983):
Methods of Seawater Analysis, Verlag Chemie, Second Edition.

HANAWA, K., P. RUAL, R. BAILEY, A. SY and M. SZABADOS (1995):
A new depth-time equation for Sippican or TSK T-7, T-6 and T-4 expendable bathythermographs (XBT). Deep-Sea Res., 42, p. 1423-1451.

KIRKWOOD, D.S. (1995):
Nutrients: Practical notes on their determination in seawater, Techniques In Marine Environmental Science, (TIMES series), ICES, Copenhagen, (in press).

KIRKWOOD D. S. and A. R. FOLKARD (1986):
Results of the ICES salinity sample-bottle intercomparison. ICES C.M., 16 pp.

KIRKWOOD, D.S., A. AMINOT and M. PERTILLÖ (1991):
ICES (fourth) Intercomparison Exercise for Nutrients in Seawater, Cooperative Research Report No. 174. ICES Copenhagen, 83 pp.

KOLTERMANN, K.P. and A. SY (1994):
Western North Atlantic cools at intermediate depths. International WOCE Newsletter, 15, p. 5-6.

KÖRTZINGER, A., L. MINTROP, J.C. DUINKER (1996)
On the penetration depth and the inventory of anthropogenic CO_2 in the north Atlantic Ocean (submitted to JGR)

LAZIER, J. (1995):
The salinity decrease in the Labrador Sea over the past thirty years. In: Climate on decade-to-century time scales, National Academy of Sciences Press. Washington, D.C. (in press).

LAZIER, J., M. RHEIN, A. SY and J. MEINCKE (in preparation):
Surprisingly rapid renewal of Labrador Sea Water in the Irminger Sea.

MILLARD, R. C. (1993):
CTD oxygen calibration procedure. WHP Operations and Methods, WHP Office Report WHPO 91-1, Revision 1, 29 pp.

MURPHY, J. and J.P. RILEY (1962):
A modified single solution method for the determination of phosphate in natural waters, Anal. Chim. Acta, 27, p. 31-36.

MURRAY, C.N., J.P. RILEY and T.R.S. WILSON (1968):
The solubility of oxygen in Winkler reagents used for the determination of dissolved oxygen. Deep-Sea Res., 15, p. 237-238.

PINGREE, R.D. and B. LeCANN . (1989):
Celtic and Amorican slope and shelf residual currents. Prog. Oceanog. 23: 303-338.

PINGREE, R.D. and B. LeCANN (1990):
Structure, Strength and Seasonality of the slope currents in the Bay of Biscay region. J.mar.biol.Ass.U.K. 70: 857-885.

PFANNKUCHE, O. (1993):
Benthic response to the sedimentation of particulate organic matter at the BIOTRANS station, 47°N, 20°W. - Deep-Sea Res. II, 40: 135-149.

READ, J.F. and W.J. GOULD (1992):
Cooling and freshening of the subpolar North Atlantic Ocean since the 1960s. Nature, 360, 55-57.

SIPPICAN, Inc. (1992):
MK-12 Oceanographic Data Acquisition System, User's Manual. Sippican, Inc., Marion, Mass.

SIPPICAN, Inc. (1994):
XCTD: Expendable Conductivity, Temperature, Depth Profiling System. Document presented at Oceanology International 94, Brighton, 8-11 March 1994.

SY, A. (1991):
XBT measurements. In: WHP Operations and Methods, WHP Office Report WHPO 91-1, 19 pp.

SY, A. (1993):
Field Evaluation of XCTD Performance. WOCE Newsletter, No. 14, pp. 33-37.

SY, A. and H.-H. HINRICHSEN (1986):
The influence of long-term storage on the salinity of bottled seawater samples. Dt. Hydr. Z., 39, p. 35-40.

SY, A. and J.ULRICH (1994):
North Atlantic Ship-of-Opportunity XBT Programme 1990, Ber. BSH, 1, 134 pp.

TALLEY, L.D. and M.S. McCARTNEY (1982):
Distribution and circulation of Labrador Sea Water. J. of Physical Oceanography, 12, 1189-1205.

WOCE Operations Manual, WHP Operations and Methods (1994),
Part 3.1.3 : WHP Office Report WHPO91-1, WOCE Report No. 68/91, rev. 1

WOCE Operations Manual, WHP Operations and Methods (1994),
Part 3.1.2 : Requirements for WHP Data Reporting, Report WHPO90-1, WOCE Report No. 67/91, rev. 2

BSH, Hamburg
A. Sy
5 November 1996
To whom it may concern:
Cruise "Meteor" 30, leg 3, bottle data processing.

Because of the very limited resources it was necessary to deviate in some points from requirements outlined in WHPO 90-1. Otherwise different bottle data files ought to have been assembled according specific needs and specific computer software. Thus please, note the differences from WHP water sample requirements as described in WHPO 90-1 (section 3.3).

Data are reported in terms of corrected samples, i.e. mis- or double trips in the CTD rosette are corrected. No serious rosette problems occurred during this cruise.

Clearly bad (wrong) bottle trips have been removed completely. Bad single measurements have been removed and marked by 4. Samples drawn from leaking (malfunctioning) bottles are not reported except values seem to be more or less reasonable.

BIO denotes the Bedfort numbering system we used.

CTDRAW is not a real raw pressure. The values reported are calibrated in our acquisition data stream (transformation in physical units (dbar)) and stored in the bottle data file.
CTDRAW is corrected according laboratory calibration results (unloading curve) and pressure offset correction from beginning of profile.

CTDTMP is reported in ITS-90.

CTDSAL has been corrected with in-situ salinity correction.
Standard Conductivity used was C (15,35,0)=42.914.

OXYGEN has not been yet converted to UMOL/KG. They are reported as measured.

Finally: if you find errors of any kind, discrepancies in the data, etc, etc, please contact me. As anyone else I would like to work with the best available version of Meteor 30/3 data. Address information or inquiries should be sent to:

Alexander Sy
Bundesamt fuer Seeschiffahrt und Hydrographie
Bernhard-Nocht-Str. 78
D-22359 Hamburg
Germany

Tel: + 40 3190 3430 Fax: + 40 3190 5000 email: sy@hamburg.bsh.d400.deBSH, Hamburg

1998.09.21 SA

Meteor 30 leg 2 WHP-ID A02

Converted .sum file to our standard WOCE format.

.sum EXPOCODE was 06MT030/2 changed to 06MT30_2

changed WOCE SECT from A2 to A02

Sta. 436 (the first station) cast 1 and cast 3 - the latitude is 48 which puts the station one degree south of the rest of the track. I did not change.

Sta. 444 latitude for BE was 48 59.9, BO 49 59.8, and EN 48 59.8. Changed BO to 48 59.8 to agree with the others.

Converted .sea file to our standard WOCE format.

.sea EXPOCODE was 06MT30/2 changed to 06MT30_2

Dates on first header incorrect. Changed to agree with dates in .sum files.

Sta. 86, cast 2 had -9.00222 for some of the CFC-13 values.
Changed to -9.0000. Some of the valid values also had x.xx222.
I eliminated the fifth decimal place, but believe the 22 in the third and fourth decimal place is probably wrong.

The original file has a column with the heading BIO #. I don't know what that is, but I kept the information and put it just before the QUALT1 information.

File has CTDRAW for pressure.

Units for CFC-11, -12, -13, and CCL4 are PMOL/L in the original data.

Converted ctd data to .wct format.

The last 1 to 6 or 7 records for every ctd cast were duplicates, the first of these duplicates was usually a truncated record and the last was often combined with the originators first header record for the next station. I deleted these duplicate records.

These ctd casts contain parameters other than the CTDPRS, CTDTMP, CTDSAL, and CTDOXY. I retained all parameters.

Removed originators headers and replaced with the .wct headers.

1999.12.10
Cruise: M30/2 Expocode 06MT030_2
The cruise covers the sections A02.

The data reported here were aqcuired by:
Prof. Dr. Roether
Institut fuer Umweltphysik
Tracer Ozeanographie
University Bremen
P.O.Box 330 440
28334 Bremen
Tel. : +421 218 3511
Email: wroether@physik.uni-bremen.de

For questions about the data please contact:
Dr. Birgit Klein
Institut fuer Umweltphysik
Tracer Ozeanographie
University Bremen
P.O.Box 330 440
28334 Bremen
Tel. : +421 218 2931
Email: bklein@physik.uni-bremen.de

CFCs:
CFC11, CFC12, CFC113 and CCL4 have been measured on the cruise.
A capillary column (DBVRX, ID 0.45mm) was used in combination with a packed column (Carbograph 1AC 12 cm long, ID 0.87 mm). For stations 438-446 standard gas from Brookhaven (BNL: ALM-044933) was used. Contamination problems with the sample loops (0.5 ml and 2.0 ml) for the standards during these stations made it necessary to change the sample loops (0.5ml and 1.0 ml) and the standard. F11 and F113 for these stations showed originally large undersaturations. Because of the problems with the detector sensitivity stations 438-446 have been flagged questionable in an earlier version of the data submitted in (3/99). The CFC data for Sta. 438-446 have now been recalculated using a calibration curve with no contaminated sample loops which was performed directly after sta. 446.

For the latter part of the cruise (st. 447-488) a Bremer standard was used. Both standards have been calibrated against the SIO93 scale using standard gas from Ray Weiss for CFC-11 and CFC-12 and BNL standard for CFC-113 and CCl4. CFC measurements have been assigned individual errors. The overall performance is described below:

The CCl4 concentrations had to be corrected. CCl4 concentrations have been raised by 3% to account for insufficient extraction from the water sample.

Reproducibility:

F-11:	0.8 %	or	0.007 pmol/kg (whichever is greater)
F-12:	0.7 %	or	0,005 pmol/kg (whichever is greater)
F-113:	4.5 %	or	0.005 pmol/KG (whichever is greater)
CCl4:	1.0 %	or	0.010 pmol/kg (whichever is greater)

Precision:
F-11: 0.006 pmol/kg or a relative error of 0.2% referring to surface conc.
F12: 0.003 pmol/kg or a relative error of 0.2% referring to surface conc.
F-113: 0.002 pmol/kg or a relative error of 1.0 % referring to surface conc.
CCl4: 0.010 pmol/kg or a relative error of 0.3% referring to surface conc.

Mean water blank, detection limit:

F-11:	0,007 pmol/kg +/- 0.005
F-12:	0,006 pmol/kg +/- 0.003
F-113:	0,015 pmol/kg +/- 0.005
CCl4:	0,007 pmol/kg +/- 0.005

Air measurements:
ALE/GAGE values for 1994 (northern hemisphere) (SIO-1993 Scale):

F-11	F-12	F-113
265.3	521.6	83.3

Individual air measurements performed during the cruise (SIO 93 scale):

	Sta		F12 pptv	F11 pptv	F113 pptv	CCl4 pptv		ratio	qual
2	453	79	535.40	288.99	89.15	134.99	1.00	0.44	2211
3	453	80	529.60	282.34	88.18	131.86	1.00	0.44	1111
4	453	81	526.93	278.50	87.34	128.41	1.00	0.43	1111

Mean F12 = 528.27 std = 1.89 rel. error = 0.4
Mean F11 = 280.42 std = 2.72 rel. error = 1.0
Mean F113 = 88.22 std = 0.91 rel. error = 1.0
Mean CCl4 = 131.75 std = 3.29 rel. error = 2.5

	Sta		F12 pptv	F11 pptv	F113 pptv	CCl4 pptv		ratio	qual
6	458	4	528.72	278.48	90.21	136.96	1.00	0.30	1111
7	458	5	527.94	274.15	87.73	131.03	1.00	0.29	1111
8	458	6	528.43	273.90	86.62	128.63	1.00	0.29	1111

Mean F12 = 528.36 std = 0.39 rel. error = 0.1
Mean F11 = 275.51 std = 2.57 rel. error = 0.9
Mean F132 = 88.18 std = 1.84 rel. error = 2.1
Mean CCl4 = 133.89 std = 4.86 rel. error = 3.6

	Sta		F12 pptv	F11 pptv	F113 pptv	CCl4 pptv		ratio	qual
17	479	42	536.79	261.82	88.63	117.99	1.00	0.29	2221
18	479	43	530.45	260.70	86.40	114.19	1.00	0.29	1111
19	479	44	527.44	258.47	81.21	110.91	1.00	0.29	1111
20	479	45	529.94	258.98	83.29	113.35	1.00	0.29	1111
21	479	46	529.06	259.89	85.97	111.60	1.00	0.29	1111

Mean F12 = 529.22 std = 1.32 rel. error = 0.2
Mean F11 = 259.51 std = 0.99 rel. error = 0.4
Mean F132 = 84.22 std = 2.43 rel. error = 2.9
Mean CCl4 = 113.61 std = 2.78 rel. error = 2.4
quality flag 1= good measurement, 2=first measurement too high, 7= too high

Summary of air measurements (SIO93):

Stat:	F-11 pptV	F-12 pptv	F-113 pptv	CCl4 ptpv
453:	280.4(+/-2.7)	528.3(+/-1.9)	88.2(+/-0.9)	131.7(+/-3.3)
458:	275.5(+/-2.6)	528.4(+/-0.4)	88.2(+/-1.8)	133.9(+/-4.9)
479:	259.9(+/-1.0)	529.2(+/-1.3)	84.2(+/-2.4)	113.6(+/-2.8)

Helium and tritium measurements during this cruise have been performed from the lab in Heidelberg (R. Bayer).